

Investigation of Binder Aging and Mixture Performance in Service: Reclaimed Asphalt Pavement Mixtures

http://www.virginiadot.org/vtrc/main/online_reports/pdf/18-r26.pdf

STACEY D. DIEFENDERFER, Ph.D., P.E.
Senior Research Scientist

HARIKRISHNAN NAIR, Ph.D., P.E.
Senior Research Scientist

BENJAMIN F. BOWERS, Ph.D., P.E.
Research Scientist

Final Report VTRC 18-R26

Standard Title Page - Report on Federally Funded Project

1. Report No.: FHWA/VTRC 18-R26	2. Government Accession No.:	3. Recipient's Catalog No.:	
4. Title and Subtitle: Investigation of Binder Aging and Mixture Performance in Service: Reclaimed Asphalt Pavement Mixtures		5. Report Date: June 2018	
		6. Performing Organization Code:	
7. Author(s): Stacey D. Diefenderfer, Ph.D., P.E., Harikrishnan Nair, Ph.D., P.E., and Benjamin F. Bowers, Ph.D., P.E.		8. Performing Organization Report No.: VTRC 18-R26	
9. Performing Organization and Address: Virginia Transportation Research Council 530 Edgemont Road Charlottesville, VA 22903		10. Work Unit No. (TRAIS):	
		11. Contract or Grant No.: 101902	
12. Sponsoring Agencies' Name and Address: Virginia Department of Transportation Federal Highway Administration 1401 E. Broad Street 400 North 8th Street, Room 750 Richmond, VA 23219 Richmond, VA 23219-4825		13. Type of Report and Period Covered: Final	
		14. Sponsoring Agency Code:	
15. Supplementary Notes:			
16. Abstract: <p>In 2007, the Virginia Department of Transportation piloted a specification allowing up to 30% reclaimed asphalt pavement (RAP) in certain dense-graded asphalt surface mixtures while changing virgin binder grade requirements. The change affected only mixtures requiring an end binder grade of either PG 64-22 or PG 70-22. For mixtures specifying PG 64-22 binder, the virgin binder grade at RAP contents of 30% or less was no longer required to change. For mixtures specifying PG 70-22 binder, the virgin binder grade at RAP contents of 21% to 30% was no longer required to change from PG 64-22 to PG 64-28. Prior to this, both types of surface mixtures were allowed to contain only up to 20% RAP before binder grade adjustments were required. An initial laboratory study of mixtures produced under the pilot specification indicated that there were no significant differences for fatigue, rutting, and susceptibility to moisture between the higher content (21% to 30%) RAP mixtures and comparison mixtures (20% RAP or less).</p> <p>The current study evaluated the in-service performance of these mixtures after approximately 7 years and encompassed field visits and a laboratory investigation of a sample of 23 in-service pavements used in the initial laboratory evaluation. Cores were collected from each site and used to evaluate the binder and mixture properties. These data were compared to data from the original construction, when available, to assess the changes in the mixtures over time. Historical performance and maintenance data were also collected and evaluated to investigate the long-term performance characteristics of the sites.</p> <p>Laboratory testing, including dynamic modulus determination, repeated load permanent deformation analysis, and extracted binder grading and analysis, consistently showed no trends in the results with regard to RAP content. Overlay test results were influenced by more than just RAP (air-void content, etc.), and therefore no trend directly related to RAP content was shown. No trends in field performance could be determined because of the underlying structural conditions. Individual locations were found to show better or worse pavement performance, but this was attributed primarily to structural differences in the pavements and preexisting conditions. Surface deterioration observed in numerous test sections included fatigue cracking, longitudinal cracking, transverse cracking, raveling, and potholes. Binder analysis indicated that depth within a layer (in this case, top half versus bottom half) significantly affects binder properties, with stiffness decreasing with depth. However, increasing RAP contents appeared to mitigate the differences between the top half and bottom half of layers, possibly because of the preexisting aged composition of the RAP and its influence on the virgin binder properties.</p>			
17 Key Words: RAP, pavement performance, mixture performance, dynamic modulus, repeated load permanent deformation test, overlay test, performance grade, aging, GPC		18. Distribution Statement: No restrictions. This document is available to the public through NTIS, Springfield, VA 22161.	
19. Security Classif. (of this report): Unclassified	20. Security Classif. (of this page): Unclassified	21. No. of Pages: 152	22. Price:

FINAL REPORT

**INVESTIGATION OF BINDER AGING AND MIXTURE PERFORMANCE
IN SERVICE: RECLAIMED ASPHALT PAVEMENT MIXTURES**

**Stacey D. Diefenderfer, Ph.D., P.E.
Senior Research Scientist**

**Harikrishnan Nair, Ph.D., P.E.
Senior Research Scientist**

**Benjamin F. Bowers, Ph.D., P.E.
Research Scientist**

In Cooperation with the U.S. Department of Transportation
Federal Highway Administration

Virginia Transportation Research Council
(A partnership of the Virginia Department of Transportation
and the University of Virginia since 1948)

Charlottesville, Virginia

June 2018
VTRC 18-R26

DISCLAIMER

The contents of this report reflect the views of the authors, who are responsible for the facts and the accuracy of the data presented herein. The contents do not necessarily reflect the official views or policies of the Virginia Department of Transportation, the Commonwealth Transportation Board, or the Federal Highway Administration. This report does not constitute a standard, specification, or regulation. Any inclusion of manufacturer names, trade names, or trademarks is for identification purposes only and is not to be considered an endorsement.

Copyright 2018 by the Commonwealth of Virginia.
All rights reserved.

ABSTRACT

In 2007, the Virginia Department of Transportation piloted a specification allowing up to 30% reclaimed asphalt pavement (RAP) in certain dense-graded asphalt surface mixtures while changing virgin binder grade requirements. The change affected only mixtures requiring an end binder grade of either PG 64-22 or PG 70-22. For mixtures specifying PG 64-22 binder, the virgin binder grade at RAP contents of 30% or less was no longer required to change. For mixtures specifying PG 70-22 binder, the virgin binder grade at RAP contents of 21% to 30% was no longer required to change from PG 64-22 to PG 64-28. Prior to this, both types of surface mixtures were allowed to contain only up to 20% RAP before binder grade adjustments were required. An initial laboratory study of mixtures produced under the pilot specification indicated that there were no significant differences for fatigue, rutting, and susceptibility to moisture between the higher content (21% to 30%) RAP mixtures and comparison mixtures (20% RAP or less).

The current study evaluated the in-service performance of these mixtures after approximately 7 years and encompassed field visits and a laboratory investigation of a sample of 23 in-service pavements used in the initial laboratory evaluation. Cores were collected from each site and used to evaluate the binder and mixture properties. These data were compared to data from the original construction, when available, to assess the changes in the mixtures over time. Historical performance and maintenance data were also collected and evaluated to investigate the long-term performance characteristics of the sites.

Laboratory testing, including dynamic modulus determination, repeated load permanent deformation analysis, and extracted binder grading and analysis, consistently showed no trends in the results with regard to RAP content. Overlay test results were influenced by more than just RAP (air-void content, etc.), and therefore no trend directly related to RAP content was shown. No trends in field performance could be determined because of the underlying structural conditions. Individual locations were found to show better or worse pavement performance, but this was attributed primarily to structural differences in the pavements and preexisting conditions. Surface deterioration observed in numerous test sections included fatigue cracking, longitudinal cracking, transverse cracking, raveling, and potholes. Binder analysis indicated that depth within a layer (in this case, top half versus bottom half) significantly affects binder properties, with stiffness decreasing with depth. However, increasing RAP contents appeared to mitigate the differences between the top half and bottom half of layers, possibly because of the preexisting aged composition of the RAP and its influence on the virgin binder properties.

FINAL REPORT

INVESTIGATION OF BINDER AGING AND MIXTURE PERFORMANCE IN SERVICE: RECLAIMED ASPHALT PAVEMENT MIXTURES

Stacey D. Diefenderfer, Ph.D., P.E.
Senior Research Scientist

Harikrishnan Nair, Ph.D., P.E.
Senior Research Scientist

Benjamin F. Bowers, Ph.D., P.E.
Research Scientist

INTRODUCTION

As of 2013, approximately 85% of Virginia's interstates and 97% of Virginia's primary routes consisted of an asphalt surface (Virginia Department of Transportation [VDOT], 2013). This equates to approximately 8,700 directional miles (approximately 25,720 lane-miles) of asphalt-surfaced pavement for interstate and primary routes that require ongoing maintenance. VDOT awarded 483 contracts in calendar year 2013 that included approximately 6.1 million tons of various asphalt mixtures with a materials value of approximately \$515 million. This represents a significant investment in asphalt paving.

Since 2007, VDOT has allowed the production and placement of dense-graded asphalt mixtures having up to 30% reclaimed asphalt pavement (RAP) with no change in binder grade. This allowance affected only mixtures requiring an end binder grade of either PG 64-22 or PG 70-22. For mixtures specifying PG 64-22 binder, the virgin binder grade at RAP contents of 30% or less was no longer required to change. For mixtures specifying PG 70-22 binder, the virgin binder grade at RAP contents of 21% to 30% was no longer required to change from PG 64-22 to PG 64-28. Prior to this, both types of surface mixtures were allowed to contain only up to 20% RAP before binder grade adjustments were required. An initial study of these mixtures with a higher RAP content (Maupin et al., 2008) indicated that in the laboratory, there were no significant differences between the higher RAP content (21% to 30%) mixtures and the comparison mixtures (20% RAP or less) with regard to fatigue, rutting, and susceptibility to moisture. In addition, there were no construction problems attributed to the use of the mixtures with the higher RAP content. During the study, binder was recovered from mixtures sampled during construction and graded to determine the effect of adding higher percentages of RAP, and it was found that in nearly all cases, the increased RAP content resulted in a combined binder grade that increased one high temperature grade over that of the virgin binder grade. Since the 2008 work, the use of these mixtures with a higher RAP content has continued to increase, and more recently, interest in incorporating even higher percentages of RAP into mixtures has increased.

Unfortunately, there is still not a great understanding of the impact of mixing aged binder from the RAP with virgin binder. In practice, the presence or absence of RAP and its impact on the long-term binder properties is generally ignored, with the exception of the assumption that the RAP will stiffen the mixture and may be used to “bump” the binder grade during production. Work conducted by Apeagyei et al. (2011) on plant mixtures indicated that some mixtures for which RAP contents greater than 20% were used in order to stiffen the mixture from the base binder grade of PG 64-22 to PG 70-22 may not be stiffening from the RAP. In addition, there are no detailed field studies indicating how the presence of RAP affects binder grade and performance over the service life of the mixture. In fact, few studies have been performed to assess changes in virgin binder properties over the service life of the mixture or to relate such changes to the actual mixture performance (Al-Azri et al., 2006; Al-Khateeb et al., 2005; Glover et al., 2008; Woo et al., 2008).

The increasing use of RAP in mixtures and this lack of documented performance indicate a need to examine mixtures produced with various RAP contents to assess their long-term performance and the benefits of allowing varying percentages of RAP.

PURPOSE AND SCOPE

The purpose of the study was to address a number of questions about the long-term properties of asphalt binders and their impact on pavement performance. The influence of RAP on binder grade was a primary consideration. The study addressed the question of how RAP content influences binder grade and mixture performance by looking at the following:

- Is there any difference in the performance of asphalt mixtures containing varying percentages of RAP after 7 to 8 years of service life?
- What is the effect of 7 to 8 years of service on the binder grade of the mixtures and how is this affected by varying percentages of RAP?
- Does depth within the surface layer affect the aging of the binder?

The study scope encompassed field visits and a laboratory investigation of a sample of in-service pavements constructed with varying binders and RAP contents. These pavements included the trial sections evaluated during construction in 2007 by Maupin et al. (2008) and the comparison sites from that study. Site visits were conducted and visual assessments were performed at 23 locations. Cores were collected from each site and used to evaluate the mixture properties, including the binder characteristics. These data were compared to data from the original construction when available to assess the changes in the mixtures over time. Historical performance and maintenance data were also collected and evaluated to investigate the long-term performance characteristics of the sites.

METHODS

Literature Review

A literature review was conducted by searching various databases related to transportation engineering such as Transport Research International Documentation (TRID), the Catalog of Transportation Libraries (TLCat), the Catalog of Worldwide Libraries (WorldCat), and the Transportation Research Board Research in Progress (RiP) and Research Needs Statements (RNS) databases.

Site Evaluation

Locations

Twenty-three sites were evaluated in this study. These included 12 sites paved with mixtures having RAP contents of 21% to 30% (shown in Table 1) that were considered “higher RAP” mixtures and 11 sites paved with mixtures containing RAP contents of 20% or less that were considered the comparison group (shown in Table 2). Figure 1 shows the geographical spread of the site locations.

The designation of 21% RAP contents not being included in the comparison group of projects, despite the minimal change in RAP content, was based on the specification used at the time of construction that determined that RAP contents exceeding 20% were considered “high RAP.”

Table 1. Sites Evaluated With Mixtures Containing RAP Contents of 21% to 30%

Site	Route	County	Year	NMAS	Binder	% RAP	Contractor
A	SR 6	Goochland	2007	12.5 mm	PG 64-22	25	Branscome Richmond
B	SR 6	Goochland	2007	19.0 mm	PG 64-22	30	Branscome Richmond
C	CR 703	Dinwiddie	2007	12.5 mm	PG 64-22	25	B.P. Short & Son Paving Co., Inc.
D	SR 40	Dinwiddie	2007	12.5 mm	PG 64-22	25	B.P. Short & Son Paving Co., Inc.
F	SR 24	Appomattox	2007	9.5 mm	PG 64-22	25	Marvin V. Templeton and Sons
J	CR 611	Surry	2007	12.5 mm	PG 64-22	25	B.P. Short & Son Paving Co., Inc.
O	US 29	Pittsylvania	2007	12.5 mm	PG 64-22	21	W-L Construction and Paving
P	CR 988	Pittsylvania	2007	12.5 mm	PG 64-22	21	W-L Construction and Paving
R	US 221	Floyd	2007	12.5 mm	PG 64-22	30	Adams Construction Co.
S	US 58	Carroll	2007	12.5 mm	PG 64-22	30	Adams Construction Co.
U	US 29	Nelson	2007	12.5 mm	PG 64-22	25	Marvin V. Templeton & Sons
X	I-664	Chesapeake	2007	12.5 mm	PG 64-22	30	Branscome, Inc.

NMAS = nominal maximum aggregate size; RAP = reclaimed asphalt pavement; SR = State Route; CR = County Route; US = US Route; I = interstate; PG = performance grade.

Table 2. Comparison Sites With Mixtures Containing RAP Contents of 20% or Less

Site	Route	County	Year	NMAS	Binder	% RAP	Contractor
E	I-64	Louisa	2006	9.5 mm	PG 70-22	0	Mega Construction
H, I	SR 211	Rappahannock	2006	9.5 mm	PG 64-22	20	Superior Paving Corp.
K, L	US 220	Highland	2006	12.5 mm	PG 64-22	10	B&S Contracting, Inc.
M, N	SR 143	York	2006	9.5 mm	PG 64-22	20	Branscome, Inc.
Q	US 11	Montgomery	2006	9.5 mm	PG 70-22	15	Adams Construction Co.
T	SR 671	South Hampton	2006	9.5 mm	PG 64-22	10	Rose Brothers Paving Company, Inc.
V	I-64	Louisa	2007	9.5 mm	PG 70-22	0	S.L. Williamson Company, Inc.
W	US 301	Caroline	2007	12.5 mm	PG 70-22	20	Branscome Richmond

NMAS = nominal maximum aggregate size; RAP = reclaimed asphalt pavement; SR = State Route; CR = County Route; US = US Route; I = interstate; PG = performance grade.



Figure 1. Site Locations

Mix designs were compiled and are presented in Appendix A. A brief summary of the designs is provided in Table 3. Mixtures A and B contained a single production surface mixture sampled at two locations along the same site. Mixture B (IM) is the intermediate layer located in section B. Mixtures C/D, O/P, and R/S were each sampled from two unique sites, although the mix designs were the same. Mixtures H/I, K/L, and M/N were produced as both hot mix asphalt (HMA) and warm mix asphalt (WMA); both types of mixtures were evaluated. Mixtures H and K were produced as WMA using Sasobit as an additive; Mixture M was produced as a WMA using the Evotherm DAT additive system.

Table 3. Mix Design Summary

Section	Mix Design	NMAS	Binder	Design AC	RAP Content
A	4047-739	12.5 mm	PG 64-22	5.6%	25%
B	4047-739	12.5 mm	PG 64-22	5.6%	25%
B (IM)	4047-738	19.0 mm	PG 64-22	5.0%	30%
C, D	4015-722	12.5 mm	PG 64-22	5.5%	25%
E	4047-200608	9.5 mm	PG 70-22	5.6%	0%
F	3014-2007-15	9.5 mm	PG 64-22	5.5%	25%
H, I	7008-200615	9.5 mm	PG 64-22	5.5%	20%
J	4015-07-19	12.5 mm	PG 64-22	5.8%	25%
K, L	8012-612	12.5 mm	PG 64-22	5.2%	10%
M, N	5011-06-10	9.5 mm	PG 64-22	5.7%	20%
O, P	3007-2007-18	12.5 mm	PG 64-22	5.9%	21%
Q	2025-200531	9.5 mm	PG 70-22	5.7%	15%
R, S	2065-2007-4	12.5 mm	PG 64-22	5.5%	30%
T	5024-200605	9.5 mm	PG 64-22	5.5%	10%
U	3005-2007-06	12.5 mm	PG 64-22	5.7%	25%
V	7017-2007-10	9.5 mm	PG 70-22	5.7%	0%
W	4051-720	12.5 mm	PG 70-22	5.4%	20%
X	5029-2007-04	12.5 mm	PG 64-22	5.4%	30%

NMAS = nominal maximum aggregate size; AC = asphalt content; RAP = reclaimed asphalt pavement.

Coring

Ten cores 6 in (150 mm) in diameter were taken from each pavement site for evaluation. Core locations were randomized along the length and width of the pavement site.

Visual Survey

A visual survey was conducted at each pavement section in accordance with the guidelines for distress identification by Miller and Bellinger (2003) in order to provide specific measurements of distresses. Condition indices were not calculated from the visual distress surveys conducted. The survey distances varied depending on the length of the pavement section and the traffic control setup, vehicle traffic volumes, and roadway geometry for safety purposes. The minimum survey distance was 1,000 ft, and the maximum was 3,500 ft. Most surveys were conducted on sections of 1,000 or 1,500 ft.

Pavement Management System (PMS) Data

Distress data for comparison and RAP sites were extracted from VDOT's Pavement Management System (PMS). VDOT's Maintenance Division acquires and maintains the results of an annual condition survey of all interstates, all primaries, and approximately 20% of secondary pavements. For the survey, detailed distress data for each 0.1 mile of right-lane or principal-direction pavement surface are collected and summarized. Condition is reported on a scale from 0 to 100, heavily distressed to new or like new, respectively. The overall section rating, the Critical Condition Index, is the lower of two ratings that summarize the load related and non-load related distresses for a pavement. In addition to other possibilities, a Critical Condition Index of 60 will typically trigger a maintenance action for the existing surface.

Laboratory Materials Evaluation

Core Air Voids

Air-void contents were determined in accordance with AASHTO T 269, Percent Air Voids in Compacted Dense and Open Asphalt Mixtures (American Association of State Highway and Transportation Officials [AASHTO], 2014).

Permeability

Permeability testing on cores collected from each site was performed in accordance with Virginia Test Method (VTM) 120, Method of Test for Measurement of Permeability of Bituminous Paving Mixtures Using a Flexible Wall Permeameter (VDOT, 2014).

Dynamic Modulus

Dynamic modulus tests were performed with an Asphalt Mixture Performance Tester generally in accordance with AASHTO T 342, Standard Method of Test for Determining Dynamic Modulus of Hot-Mix Asphalt Concrete Mixtures (AASHTO, 2014). Tests were performed on specimens 38 mm in diameter by 110 mm tall cored horizontally from field cores, as described in Bowers, et al., 2015a. Three testing temperatures (4.4°C, 21.1°C, and 37.8°C) and six testing frequencies from 0.1 to 25 Hz were used. Tests were conducted starting from the coldest to the warmest temperatures. In addition, at each test temperature, the tests were performed starting from the highest to the lowest frequency. Load levels were selected in such a way that at each temperature-frequency combination, the applied strain was in the range of 75 to 125 macrostrain. All tests were conducted in the uniaxial mode without confinement. Stress versus strain values were captured continuously and used to calculate dynamic modulus. The results at each temperature-frequency combination for each mixture type are reported for three replicate specimens.

Repeated Load Permanent Deformation

The repeated load permanent deformation (RLPD) test (also known as the flow number test) is used to evaluate the rutting resistance of asphalt mixtures. An Asphalt Mixture Performance Tester with a 15 kN loading capacity was used to conduct the tests. Tests were performed on specimens 38 mm in diameter by 110 mm tall cored horizontally from field cores. All RLPD testing was conducted on specimens previously tested for dynamic modulus. Tests were conducted at 54°C based on LTPPBIND software that represents the 50% reliability maximum high pavement temperature at locations in central Virginia. A repeated haversine axial compressive load pulse of 0.1 s every 1.0 s was applied to the specimens. The tests were performed in the confined mode using a confining stress of 10 psi (68.9 kPa) and a deviator stress of 70 psi (483 kPa). The tests were continued for 10,000 cycles or a permanent strain of 10%, whichever came first. During the test, permanent strain (ϵ_p) versus the number of loading cycles was recorded automatically, and the results were used to estimate the flow number. The flow number was determined numerically as the cycle number at which the strain rate is at a minimum based on the Francken model.

In addition to calculations of the flow number, the slope and intercepts of the secondary portion of the cycle versus permanent strain curve was estimated in log-log space by the application of a power-law function (Eq. 1):

$$\varepsilon_p = aN^b \quad [\text{Eq. 1}]$$

where

ε_p = permanent strain
a = intercept in log-log space
N = cycle number
b = slope in log-log space.

The slope of this line is indicative of the plastic strain rate of the mixture. A higher slope relative to other mixtures indicates a mixture that is likely more susceptible to rutting. The intercept of the line is indicative of the plastic strain at cycle $N = 1$ (Khosravifar et al., 2015; Von Quintus et al., 2012).

Texas Overlay Test

The Texas overlay test was performed to assess the susceptibility of each mixture to cracking. Testing was performed on field cores 150 mm in diameter and of varying thicknesses using a universal testing machine with a loading capacity of 25 to 100 kN generally in accordance with TX-248-F, Test Procedure for Overlay Test (Texas Department of Transportation, 2009). Testing was performed at a temperature of $25 \pm 0.5^\circ\text{C}$. Loading was applied for a total of 1,200 cycles or until a reduction of 93% or more of the maximum load was reached.

Binder Extraction and Recovery

Extraction of binder from cores was performed in accordance with AASHTO T 164, Quantitative Extraction of Asphalt Binder From Hot Mix Asphalt (HMA), Method A (AASHTO, 2014) using n-propyl bromide as the solvent. Binder was recovered from the solvent in accordance with the Rotavap recovery procedure specified in AASHTO T 319, Quantitative Extraction and Recovery of Asphalt Binder From Asphalt Mixtures (AASHTO, 2014).

Binder Testing

Binder grading was performed in accordance with AASHTO M 320, Performance-Graded Asphalt Binder (AASHTO, 2014). In addition, shear modulus mastercurves were generated for the recovered binders. Nine test temperatures from 5 to 85°C and 10 test frequencies from 0.01 to 25 Hz were used to generate data for mastercurve construction. Mastercurves were constructed using least squares optimization of the Christensen-Anderson model (Christensen and Anderson, 1992) (Eqs. 2 and 3):

$$G^*(\omega) = G_g \cdot \left(1 + \frac{\omega_c}{\omega}\right)^{-\left(\frac{R}{\log 2}\right)} \quad [\text{Eq. 2}]$$

$$\delta(\omega) = \frac{90}{\left[1 + \left(\frac{\omega}{\omega_c}\right)^{\frac{\log 2}{R}}\right]} \quad [\text{Eq. 3}]$$

where

$G^*(\omega)$ = complex shear modulus, kPa

$\delta(\omega)$ = phase angle, rad

G_g = glassy modulus, kPa

ω_c = crossover frequency

ω = reduced frequency

R = rheological index.

4): Temperature shift factors were fitted to the Williams-Landel-Ferry (WLF) equation (Eq.

$$\log a_T = \frac{-C_1 (T - T_R)}{C_2 + T - T_R} \quad [\text{Eq. 4}]$$

where

a_T = shift function

C_1 and C_2 = empirical constants

T = test temperature, °C

T_R = reference temperature, °C.

Gel Permeation Chromatography

Gel permeation chromatography (GPC) was performed to analyze the molecular weight distribution of the asphalt binder after the recovery process. Testing was performed using an EcoSEC GPC by Tosoh Biosciences, which had a guard column, one TSKgel SuperHZ2500 column with a mean pore size of 30 Å, two TSKgel SuperHZ3000 columns with a mean pore size of 75 Å, and one TSKgel SuperHZ4000 column with a mean pore size of 200 Å in series. Columns were calibrated using polystyrene standards. The elution solvent was tetrahydrofuran stabilized with butylated hydroxytoluene.

Analysis of the data consisted of calculating the percentage of large molecules present within the molecular weight distribution of the binder. This process involves taking the area of the first 5/13 s of the chromatogram and dividing it by the total area beneath the chromatogram. This ratio, converted to a percentage, relates to the stiffness of the binder and its oxidative properties (Bowers et al., 2014; Bowers et al., 2015b; Doh et al., 2008; Kim et al., 2006, Lee et al., 2006; Zhao et al., 2014). A higher percentage of large molecular sizes (LMS) equates to a stiffer binder.

RESULTS AND DISCUSSION

Literature Review

RAP is commonly used in varying percentages in asphalt mixtures because of its economic and environmental benefits. In the past, RAP was successfully used under the Marshall mix design method (Decker, 1997; Kandhal, 1997); however, during the initial adoption of the Superpave mix design method, the use of RAP initially decreased because the design method was based on virgin mixtures. Over time, the use of RAP in Superpave mixtures grew as additional guidance on its incorporation was developed (McDaniel and Anderson, 2001; McDaniel and Shah, 2003; National Cooperative Highway Research Program, 2001; West et al., 2013), although there are often still concerns expressed about potential impacts on performance.

A 2007 survey of state agencies showed that average allowable RAP contents in asphalt mixtures ranged from 10% to 20%, with the average amount actually used being 12%. Uncertainty with regard to the long-term performance of asphalt pavements containing RAP materials was the primary reason reported for this limited use (Copeland, 2011). A more recent survey of the states indicated that not only has the tonnage of RAP used increased but the average RAP content of asphalt mixtures has also increased to approximately 17% (Hansen and Newcomb, 2011). However, with increased RAP use, concerns have increased about the potential impact of RAP contents on mixture performance and service life.

Although numerous field sections have been placed around the United States to evaluate Superpave mixtures with RAP contents greater than 20% to 25%, very little has been published on the topic of their long-term field performance. In addition, the number of studies evaluating even pre-Superpave mixtures containing RAP is limited. In 2009, the National Center for Asphalt Technology (NCAT) (West et al., 2011) examined the Specific Pavement Studies 5 (SPS5) information in the database of the Long-Term Pavement Performance program (LTPP). SPS5 consisted of 50 mm and 125 mm overlays constructed from virgin and 30% RAP mixtures. The NCAT study found that the 30% RAP overlays performed as well as the virgin overlays in terms of the international roughness index, rutting, block cracking, and raveling. NCAT has also evaluated HMA with a higher RAP content on the pavement test track in several studies (West et al., 2012; Willis et al., 2012). In 2006, four surface mixtures containing 45% RAP with various asphalt binders (PG 52-28, PG 67-22, PG 76-22, and PG 76-22 with Sasobit) were constructed over a perpetual asphalt pavement foundation to assess surface performance. After 20 million equivalent single-axle loads, less texture change and cracking were measured in the sections produced with softer virgin asphalt grades. In 2009, a structural pavement study was conducted on the test track to compare a control virgin HMA test section to HMA and WMA sections containing 50% RAP. The RAP and virgin structural sections were designed and constructed to have equivalent binder contents, and all other properties were held within normal production tolerances. The structural sections containing 50% RAP withstood 10 million equivalent single-axle loads of trafficking, and their performance was equivalent to that of the control with regard to both cracking and rutting.

Anderson and Daniel (2013) examined case studies of roadway sections from across the United States constructed from 1977 to 1999 that contained 20% to 72% RAP. The analysis

used approximately 10 years of in-service pavement condition data to evaluate the performance of the sections versus that of the virgin control sections. Although there were differences in performance, namely, the RAP sections were less crack resistant, of lower ride quality, and more rut resistant than the control sections, these differences were in many cases not statistically significant. None of the distress factors was severe enough to be detrimental to the expected life spans of the RAP sections, which were typically less than 5% different than that of the virgin sections.

Site Evaluation

Visual Survey

Visual survey data were compiled and evaluated for all sites. Table 4 presents a summary of the cracking and raveling data for sites with mixtures having $\leq 20\%$ RAP and sites with mixtures having 21% to 30% RAP. Distresses were classified as low, medium, or high, and quantitative measures are presented for each classification. In addition, the number of sites exhibiting each distress severity and the percentage of sites exhibiting each distress severity are shown.

Statistical analysis was performed using two-sample, two-tailed unequal variance *t*-tests with a level of significance of $\alpha = 0.05$ to assess the differences in quantified distresses between the sites with mixtures having $\leq 20\%$ RAP and those with mixtures having 21% to 30% RAP, as shown in Table 5. Tests were performed by comparing the pools of data for each severity. In addition, data for all severities for each distress were compared. The results indicated that all sites performed similarly based on the visual assessment.

In addition, statistical analysis using two-tailed paired *t*-tests was performed to compare total percentages of lane area or length observed for each distress level across all sites; the results are shown in Table 6. The results again indicated no significant difference between sites with mixtures having $\leq 20\%$ RAP and sites with mixtures having $>20\%$ RAP.

The visual survey and coring results showed several distress types in both categories of sections. Examples of these distresses follow. It should be noted that terminology differs between cracking as determined in the visual survey and as described here. The visual survey does not distinguish the origin of cracking, such as top-down or bottom-up, particularly as this distinction requires some knowledge of the structural condition of the pavement or some level of forensic investigation, such as coring to determine the crack origin. Cracking is described here in terms of origin where applicable to enable further an understanding of the mechanisms involved and to distinguish between cracking that may be due to material properties and that which is structurally related and thus not a direct measure of material properties or performance. For example, top-down cracking is dependent on surface layer material properties, as it originates at the surface. However, bottom-up cracking originates in the lower pavement layers because of insufficient structural capacity for the applied loading and propagates upward; these cracks are indicative of the surface material's strength being exceeded but are driven by structural incapacity, and it is improper to attribute this directly to a lack of performance of the surface material.

Table 4. Summary of Visual Survey Cracking and Raveling Data

≤20% RAP				21% to 30% RAP			
Site	Low Severity	Medium Severity	High Severity	Site	Low Severity	Medium Severity	High Severity
Fatigue Cracking, ft²							
E	1,240	600	5,800	A	3,608	1,650	249
H	0	433	0	B	18,040	4,530	500
I	0	998	0	C	2,017	0	0
K	0	119	0	D	1,736	0	0
L	0	8	0	F	0	0	0
M	0	0	0	J	112	0	0
N	0	0	0	O	0	0	0
Q	0	988.2	0	P	0	9.2	0
T	0	502.2	0	R	0	319	0
V	0	0	0	S	0	101.1	0
W	0	20.9	0	U	0	0	0
				X	0	0	0
Total	1,240	3,669.3	5,800	Total	25,513	6,609.3	749
No. Sites	1	8	1	No. Sites	5	5	2
% Sites	9%	73%	9%	% Sites	42%	42%	17%
Longitudinal Cracking, Wheelpath, ft							
E	0	0	0	A	0	0	0
H	0	962	0	B	40	0	0
I	0	3,000	0	C	22	0	0
K	184	0	0	D	49	0	0
L	67	72	0	F	0	0	0
M	0	0	0	J	39	232	0
N	0	0	0	O	1816	197.2	0
Q	0	3.4	0	P	122.6	52.7	0
T	136.3	211.7	0	R	0	1208	0
V	0	0	0	S	25.2	8034	0
W	0	450.2	0	U	6.2	0	0
				X	0	0	0
Total	387.3	4,699.3	0	Total	2,120	9,723.9	0
No. Sites	2	5	0	No. Sites	6	3	0
% Sites	18%	45%	0%	% Sites	50%	25%	0%
Longitudinal Cracking, Non-wheelpath, ft							
E	0	0	44	A	0	1,000	1,000
H	0	1,000	0	B	130	110	250
I	0	25	0	C	16	0	0
K	0	1,686	0	D	0	0	0
L	0	1,112	0	F	0	406	0
M	0	1,231.9	0	J	184	92	0
N	0	1,000	0	O	0	0	0
Q	0	0	0	P	0	0	0
T	0	343.3	0	R	0	39	0
V	0	0	0	S	115.7	480.8	0
W	0	202.3	0	U	0	0	0
				X	0	0	0
Total	0	6,600.5	44	Total	445.7	2,127.8	1,250
No. Sites	0	4	1	No. Sites	4	6	2
% Sites	0%	36%	9%	% Sites	33%	50%	17%
Transverse Cracking, Unsealed, ft							
E	0	33	0	A	0	0	0
H	0	21	0	B	0	0	0
I	0	0	0	C	9.5	0	0
K	27	19	0	D	0	0	0
L	0	17	0	F	0	161	0
M	0	0	0	J	0	0	0
N	168	204	228	O	0	0	0
Q	0	12	0	P	0	148	50
T	5	7	0	R	0	20	0
V	147	36	0	S	12	34	0
W	0	6	0	U	31	24	0
				X	0	0	0
Total	347	355	228	Total	52.5	387	50

No. Sites	4	9	1	No. Sites	3	5	1
% Sites	36%	82%	9%	% Sites	25%	42%	8%
Raveling, ft²							
E	0	0	0	A	0	0	0
H	0	0	0	B	720	860	0
I	0	0	0	C	0	0	0
K	0	0	0	D	66	0	0
L	0	0	0	F	0	0	0
M	0	172.4	0	J	0	0	0
N	0	0	0	O	0	0	0
Q	0	5	0	P	0	0	0
T	0	0	0	R	0	117	0
V	0	0	0	S	0	0	0
W	0	230	0	U	0	0	0
				X	0	0	0
Total	0	407.4	0	Total	786	977	0
No. Sites	0	2	0	No. Sites	2	2	0
% Sites	0%	18%	0%	% Sites	17%	17%	0%

No sealed longitudinal cracking, bleeding, or reflection cracking was observed.

Table 5. *p*-Value Results From Two-Sample, Two-Tailed *t*-Tests Performed on Pooled Visual Survey Data

Distress	Low Severity	Medium Severity	High Severity	All Severities
Fatigue	0.2034	0.6003	0.4000	0.2900
Longitudinal, Wheelpath	0.3673	0.6016	-	0.4823
Longitudinal, Non-wheelpath	0.0770	0.0587	0.2588	0.2860
Transverse, Unsealed	0.1857	0.9993	0.4503	0.2431
Raveling	0.2964	0.5669	-	0.2577

p-values less than or equal to 0.05 indicate significant differences between datasets for sites with mixtures having RAP contents ≤ 20% and those with mixtures having RAP contents of 21% to 30%. - = no test performed as all data points were zero.

Table 6. *p*-Value Results From Paired, Two-Tailed *t*-Tests Performed on Paired Percentage by Severity Level

Distress	Severity	Percentage RAP		<i>p</i> -value
		≤20% RAP ^a	21%-30% RAP ^b	
Fatigue Cracking ^c	Low	0.9%	12.1%	0.6193
	Medium	2.7%	3.1%	
	High	4.2%	0.4%	
Longitudinal Cracking, Wheelpath ^d	Low	3.4%	12.0%	0.2090
	Medium	40.6%	55.2%	
	High	0.0%	0.0%	
Longitudinal Cracking, Non-wheelpath ^d	Low	0.0%	2.5%	0.5462
	Medium	57.4%	12.1%	
	High	0.4%	7.1%	
Transverse Cracking, Unsealed ^d	Low	3.0%	0.3%	0.0792
	Medium	3.1%	2.2%	
	High	2.0%	0.3%	
Raveling ^c	Low	0.0%	4.5%	0.2366
	Medium	3.5%	5.6%	
	High	0.0%	0.0%	

p-values less than or equal to 0.05 indicate significant differences between comparison and RAP datasets; RAP = reclaimed asphalt pavement.

^a For sites with ≤20% RAP, the number of sites evaluated was 11, the total length evaluated was 11,500 ft, and the total lane area evaluated was 138,000 ft².

^b For sites with 21%-30% RAP, the number of sites evaluated was 12, the total length evaluated was 17,600 ft, and the total lane area evaluated was 211,200 ft².

^c Percentage = quantity/total lane area evaluated.

^d Percentage = quantity/total length evaluated.

The purpose of discussing the general conditions observed in the sections is to note that all sections are undergoing various types of deterioration. Most of the deterioration observed was not directly influenced by the surface material properties; in fact, most appeared to be related to structural deficiencies within the underlying layers. Distresses such as fatigue cracking, delamination, and moisture damage in underlying layers will eventually result in cracking that is apparent on the surface of a pavement. However, this should not be attributed to poor performance of the surface material.

High severity fatigue cracking was observed at several locations in Section A (25% RAP), located along SR 6 in Goochland County, as shown in Figure 2. In addition, several new asphalt patches were observed. A detailed forensic evaluation was not performed to evaluate cracking causes although it appeared that since most of the cracks were located along the wheelpath, pavement structural issues were a contributing factor. The presence of moisture in the fatigued areas supports the inference of structural issues.

Top-down cracking was observed in a number of sections, as validated by cores. Top-down cracking was included in the visual survey under the longitudinal wheelpath cracking category. Sites H and I (20% RAP) located along US 211 in Rappahannock County were found to have top-down cracking, as shown in Figure 3. Site R (30% RAP) located on US 221 in Floyd County exhibited cracking in the right wheelpath within the surface layer. Sites O (21% RAP) and U (25% RAP) located along US 29 in Nelson and Pittsylvania counties, respectively, were found to be in generally excellent condition, although cracking was observed. Full-depth cores indicated that most of the cracks were within the surface layer originating from the top.



Figure 2. Cracking and Patches on Section A, SR 6 in Goochland County



Figure 3. Cores From Sites H and I (SR 211 in Rappahannock County) Showed That Cracking Was Initiating From the Top Down

Raveling was also observed among the sites. A core from Site C (25% RAP), located along CR 703 in Dinwiddie County, displayed mixture raveling, as shown in Figure 4, although this was not seen in the visual survey. Medium severity raveling, as shown in Figure 5, was observed in Site Q (15% RAP) located along US 11 in Montgomery County. Visual survey data indicated that Sites B and D exhibited low severity raveling and Sites B, M, R, and W displayed medium severity raveling.



Figure 4. Mixture Raveling in a Core From Site C, CR 703 in Dinwiddie County



Figure 5. Raveling Observed in Site Q, US 11 in Montgomery County

Delamination was also found in a number of sites during coring. In addition to raveling, Site Q (15% RAP) located on US 11 in Montgomery County was found to have debonded layers when cored, as shown in Figure 6. Cores from section R (30% RAP), located on US 221 in Floyd County, were also debonded, as shown in Figure 7. Construction records reported that shoving and cracking were “prevalent” throughout the mat and the longitudinal edges appeared to move “inches per roller pass.” Although Site S (30% RAP), located on US 58 in Carroll County, was in reasonably good condition based on the visual survey, full-depth cores revealed debonded layers, as shown in Figure 8.



Figure 6. Cores Indicated Debonding and Stripping in Site Q (US 11 in Montgomery County)



Figure 7. Delaminated Pavement Layers Found in Site R (US 221 in Floyd County)



Figure 8. Debonding Shown in a Core From Site S (US 58 in Carroll County)

Moisture damage was also observed in cores. Cores from Site F (25% RAP), located on SR 24 in Appomattox County, showed evidence of moisture damage and several full-depth cracks, as shown in Figure 9. Site Q (15% RAP) located on US 11 in Montgomery County was found to have moisture damage in addition to the debonding previously mentioned, as shown in Figure 6. Fines pumping through cracks on the surface were seen in Site T (10% RAP) located on SR 671 in South Hampton County; cores indicated moisture damage, as shown in Figure 10.



Figure 9. Full depth Crack Seen in Site F, SR 24 in Appomattox County



Figure 10. Pumping of Fines and Moisture Damage in a Core From Site T (SR 671 in South Hampton County)

Pavement Management System Data

Distress data were extracted from VDOT's Pavement Management System (PMS) for both sites with mixtures having $\leq 20\%$ RAP and those having 21% to 30% RAP; the data are summarized in Tables 7 and 8. For some sites, exact mile points were not available, and hence PMS data are not shown. Complete details are provided in Appendix B. All sites showed low rut depths of less than 0.16 in with the exception of Site A/B, which had a rut depth of 0.23 in. Most of the pavements were in acceptable ride condition. Very low truck traffic was found for all sites except I-664. With the exception of secondary pavements, most sites had automated distress data available beginning in 2007. Some of the predominant failure mechanisms observed in comparison sites were stripping of underlying layers, debonding, longitudinal cracking, and joint failures, which are not directly attributable to the surface mixture performance.

Table 7. 2014 PMS Distress Data for Sites With Mixtures Having RAP Contents of 20% or Less

Site	Route	County	% RAP	CCI	IRI, in/mile	Rut Depth, in	Traffic, AADTT
E	I-64	Louisa	0	-	-	-	-
H, I	SR 211	Rappahannock	20	27	60	0.11	54
K, L	US 220	Highland	10	40	78	0.09	17
M, N	SR 143	York	20	46	106	0.08	82
Q	US 11	Montgomery	15	78	90	0.13	81
T	SR 671	South Hampton	10	-	-	-	-
V	I-64	Louisa	0	-	-	-	-
W	US 301	Caroline	20	-	-	-	-

PMS = VDOT's Pavement Management System; RAP = reclaimed asphalt pavement; CCI = Critical Condition Index; IRI = International Roughness Index; AADTT = average annual daily truck traffic; - = data not available.

Table 8. 2014 PMS Distress Data for Sites With Mixtures Having RAP Contents of 21% to 30%

Site	Route	County	% RAP	CCI	IRI, in/mile	Rut Depth, in	Traffic, AADTT
A, B	SR 6	Goochland	25	75	109	0.23	121
C ^a	CR 703	Dinwiddie	25	95	128	0.15	48
D	SR 40	Dinwiddie	25	82	90	0.12	67
F	SR 24	Appomattox	25	95	75	0.09	189
J	CR 611	Surry	25	-	-	-	-
O	US 29	Pittsylvania	21	86	75	0.15	889
P	CR 988	Pittsylvania	21	-	-	-	-
R	US 221	Floyd	30	61	114	0.11	60
S	US 58	Carroll	30	66	113	0.14	57
U	US 29	Nelson	25	93	73	0.16	806
X	I-664	Chesapeake	30	89	81	0.16	2163

PMS = VDOT's Pavement Management System; RAP = reclaimed asphalt pavement; CCI = Critical Condition Index; IRI = International Roughness Index; AADTT = average annual daily truck traffic; - = data not available.

^a Only 2010 data were available.

Laboratory Materials Evaluation

Core Air Voids

Air voids were measured for all undamaged cores. The results are shown in Tables 9 and 10. Individual measurements were variable, as typically expected. Average air-void contents for each section ranged from 4.6% to 8.9%.

Table 9. Air-void Content and Permeability Test Results for Cores From Sections With Mixtures Having RAP Contents of 20% or Less

Site	% RAP	Property	1	2	3	4	5	6	7	8	9	10	Average
E	0	VTM, %	11.9	10.5	8.1	6.4	6.2	8.1	6.3	5.7	6.2	6.8	7.6
		Permeability x 10 ⁻⁵ cm/sec	117.4	66.9	17.3	0.7	0.5	18.6	0.7	0.0	0.3	1.9	22.4
H	20	VTM, %	6.8	7.4	6.5	-	3.6	5.6	6.8	7.0	3.6	4.9	5.8
		Permeability x 10 ⁻⁵ cm/sec	3.1	3.9	0.9	NA	0.0	0.5	1.4	3.0	0.0	0.1	1.4
I	20	VTM, %	6.4	5.3	6.0	5.7	5.8	6.0	5.8	5.8	7.0	7.6	6.1
		Permeability x 10 ⁻⁵ cm/sec	55.3	0.2	4.2	0.6	2.7	3.4	2.2	1.4	1.3	0.9	7.2
K	10	VTM, %	6.5	4.7	4.1	6.8	4.0	5.6	8.8	8.2	6.2	5.3	6.0
		Permeability x 10 ⁻⁵ cm/sec	0.0	0.0	0.0	22.9	0.0	0.0	3.6	4.1	0.2	1.0	3.2
L	10	VTM, %	7.5	4.6	5.0	7.3	6.3	4.6	7.9	6.6	6.5	6.0	6.2
		Permeability x 10 ⁻⁵ cm/sec	48.9	0.0	0.0	33.4	20.3	0.5	49.0	20.7	547.8	0.3	72.1
M	20	VTM, %	5.5	-	7.7	5.7	6.3	10.0	7.6	7.9	7.7	8.4	7.4
		Permeability x 10 ⁻⁵ cm/sec	0.0	NA	1.5	0.0	0.0	6.2	1.3	2.4	1.4	3.3	1.8
N	20	VTM, %	7.4	10.6	-	8.4	9.5	10.1	8.9	7.6	7.9	8.1	8.7
		Permeability x 10 ⁻⁵ cm/sec	68.6	499.7	NA	98.3	194.9	462.2	143.1	72.1	86.2	135.0	195.6
Q	15	VTM, %	6.1	8.2	-	9.9	9.0	11.4	8.6	7.1	8.4	9.5	8.7
		Permeability x 10 ⁻⁵ cm/sec	8.9	48.1	NA	292.2	157.5	606.2	84.7	14.4	59.5	182.8	161.6
T	10	VTM, %	6.1	5.6	7.2	6.4	7.7	5.8	7.1	6.5	6.3	3.8	6.3
		Permeability x 10 ⁻⁵ cm/sec	4.5	4.2	9.5	5.8	10.2	5.1	7.8	4.9	5.7	0.0	5.8
V	0	VTM, %	8.1	9.6	-	8.8	8.6	8.3	10.0	7.6	7.0	6.9	8.3
		Permeability x 10 ⁻⁵ cm/sec	17.1	85.2	NA	29.2	10.2	30.4	93.6	13.0	5.9	11.6	32.9
W	20	VTM, %	10.0	8.6	9.6	12.8	7.5	6.0	5.7	3.2	3.9	4.3	7.2
		Permeability x 10 ⁻⁵ cm/sec	NA	0.8	2.3	370.8	1.7	0.0	0.0	0.0	0.0	0.0	41.7

RAP = reclaimed asphalt pavement; VTM = voids in total mix; NA = testing not performed; - = core was broken or damaged.

Table 10. Air-void Content and Permeability Test Results for Cores From Sections With Mixtures Having RAP Contents of 21%-30%

Site	% RAP	Property	1	2	3	4	5	6	7	8	9	10	Average
A ^a	25	VTM, %	4.4	7.3	4.8	6.5	6.4	5.2	6.8	5.7	6.2	6.7	6.0
		Permeability x 10 ⁻⁵ cm/sec	0.0	8.7	0.8	8.6	3.8	0.6	22.7	9.7	0.5	0.5	5.6
B ^b	25	VTM, %	7.9	8.9	6.8	5.5	8.4	9.6	10.6	11.1	8.6	12.0	8.9
		Permeability x 10 ⁻⁵ cm/sec	NA	14.9	0.0	0.0	13.8	17.8	29.7	80.3	22.3	93.1	30.2
B (IM)	30	VTM, %	6.9	6.3	5.4	4.5	6.9	8.9	7.5	8.2	6.9	6.8	6.8
		Permeability x 10 ⁻⁵ cm/sec	NA	0.0	0.0	0.0	4.1	17.9	8.5	13.1	5.6	3.6	5.9
C	25	VTM, %	6.0	10.6	2.1	2.7	3.6	3.9	2.9	4.0	4.3	5.7	4.6
		Permeability x 10 ⁻⁵ cm/sec	0.0	9.0	12.4	20.3	28.8	9.4	97.5	6.0	23.4	137.7	34.5
D	25	VTM, %	8.0	7.5	8.3	6.7	8.2	7.7	10.3	8.4	7.3	11.5	8.4
		Permeability x 10 ⁻⁵ cm/sec	3.0	0.0	4.3	0.0	5.0	0.0	23.5	4.3	0.0	57.4	9.8
F	25	VTM, %	6.8	4.1	8.4	-	4.8	3.7	4.5	4.0	4.5	4.6	5.0
		Permeability x 10 ⁻⁵ cm/sec	0.3	0.0	0.7	NA	0.0	0.0	0.0	0.0	0.0	0.0	0.1
J	25	VTM, %	6.4	7.3	10.5	7.8	10.3	8.6	8.2	8.5	8.9	8.3	8.5
		Permeability x 10 ⁻⁵ cm/sec	1.0	0.0	48.2	24.6	NA	24.8	15.4	65.7	55.3	0.0	26.1
O	21	VTM, %	7.8	6.0	6.0	6.5	8.7	7.8	7.1	-	7.9	6.2	7.1
		Permeability x 10 ⁻⁵ cm/sec	4.39	0	0	0	9.76	4.59	2.86	NA	5.39	0	3.0
P	21	VTM, %	7.3	-	7.1	6.5	9.8	7.7	6.1	7.7	6.2	6.8	7.3
		Permeability x 10 ⁻⁵ cm/sec	2.3	NA	1.9	0.6	32.9	5.7	0.0	4.7	0.0	1.0	5.4
R	30	VTM, %	8.0	-	9.1	7.0	8.3	9.4	10.3	9.3	8.4	8.6	8.7
		Permeability x 10 ⁻⁵ cm/sec	12.0	NA	44.0	10.8	15.1	77.9	143.3	57.6	18.5	19.0	44.2
S	30	VTM, %	6.6	-	10.7	6.3	9.1	8.4	9.2	9.4	7.5	9.0	8.5
		Permeability x 10 ⁻⁵ cm/sec	0.0	NA	384.2	0.0	182.5	44.5	205.9	210.9	12.1	167.7	134.2
U	25	VTM, %	8.1	7.1	7.8	5.6	6.1	5.3	7.8	5.1	5.3	6.8	6.5
		Permeability x 10 ⁻⁵ cm/sec	2.3	3.1	0.3	0.0	0.0	0.0	1.6	0.0	0.0	0.0	0.7
X	30	VTM, %	6.4	6.0	5.1	6.0	5.5	4.6	5.5	4.9	4.5	4.8	5.3
		Permeability x 10 ⁻⁵ cm/sec	NA	1.6	0.8	3.1	5.1	0.4	1.6	0.9	0.0	0.0	1.5

RAP = reclaimed asphalt pavement; VTM = voids in total mix; IM = intermediate mix; NA = testing not performed; - = core was broken or damaged.

^a All mixtures are surface mixtures unless noted.

^b Sections A and B were composed of a single contiguous surface mixture.

Permeability

Permeability was measured for all undamaged cores. A summary of permeability results is presented in Tables 9 and 10. Section 211.03 of VDOT's *Road and Bridge Specifications* (VDOT, 2007) requires a maximum design permeability of 150×10^{-5} cm/sec at 7.5% air voids for mixtures. All mixtures except that from Site N met this criterion despite the variability in air-void contents, indicating that permeability should not be a concern.

Dynamic Modulus

Dynamic modulus test results are presented in Appendix C. Because of insufficient core thickness, dynamic modulus testing was not performed on specimens from Sites A, F, H, I, and Q. Tables 11 and 12 show summaries of the test results for evaluated mixtures having RAP contents of 20% or less and those having RAP contents of 21% to 30%, respectively.

To identify any trends in modulus associated with RAP content, the dynamic modulus values at all temperatures and three frequencies, 0.1 Hz, 1.0 Hz, and 10 Hz, were graphed for all mixtures. The selected frequencies were chosen because they would provide results that spanned the range of frequencies tested. Figures 11 through 13 show the results; all mixtures were ordered by increasing RAP content and virgin binder grade. The results indicated that neither RAP content nor virgin binder grade appears to have meaningful or trending influences on the measured modulus.

This visual assessment was further investigated using *t*-tests to evaluate significant differences between individual mixture test results at each temperature and frequency combination. The two-tailed *t*-test was employed assuming unequal variance for analysis. The results indicated that there were differences at a level of significance of $\alpha = 0.05$ between datasets for individual mixtures; however, there were no consistent trends in the significant differences that indicated any dependence on mixture properties. Table 13 presents an example of the analysis results for all mixtures at a temperature of 21.1°C (70°F) and test frequencies of 1 Hz and 5 Hz. Complete results are shown in Appendix D.

Statistical comparisons of the modulus values were performed to determine if there were significant differences between mixtures with RAP contents less than or equal to 20% and those with RAP contents of 21% to 30%. No significant differences were found using the two-tailed *t*-test assuming unequal variance at a level of significance of $\alpha = 0.05$ for any combination of temperature and frequency.

Table 11. Dynamic Modulus Test Results for Mixtures Having RAP Contents 20% or Less

Temp., °C	Frequency, Hz	E	V	K	L	T	M	N	W
		9.5 mm	9.5 mm	12.5 mm	12.5 mm	9.5 mm	9.5 mm	9.5 mm	12.5 mm
		PG 70-22	PG 70-22	PG 64-22	PG 64-22	PG 64-22	PG 64-22	PG 64-22	PG 70-22
		0% RAP	0% RAP	10% RAP	10% RAP	10% RAP	20% RAP	20% RAP	20% RAP
37.8	0.1	166,387	94,328	101,231	123,587	60,836	62,042	50,098	64,493
	0.5	309,027	179,460	194,829	220,022	122,107	116,771	96,425	127,188
	1	391,408	232,640	252,544	275,427	160,919	150,345	125,487	169,539
	5	645,611	413,261	443,960	451,889	296,457	263,362	223,469	320,292
	10	777,886	514,981	550,418	544,230	374,995	326,264	279,060	412,149
	25	968,175	666,690	705,898	661,662	492,113	418,586	360,503	550,418
21.1	0.1	773,341	521,942	574,688	573,527	368,178	327,129	280,976	375,309
	0.5	1,100,933	802,929	863,845	813,758	584,429	495,879	426,642	630,576
	1	1,255,205	940,521	1,005,256	922,440	693,715	578,519	497,931	762,657
	5	1,644,582	1,317,861	1,383,611	1,208,744	1,010,115	797,995	690,127	1,150,149
	10	1,817,661	1,491,568	1,559,107	1,332,606	1,164,145	899,824	778,626	1,334,540
	25	2,041,309	1,723,676	1,781,111	1,491,471	1,377,351	1,036,410	896,966	1,590,097
4.4	0.1	2,163,769	1,787,010	1,865,523	1,541,944	1,457,774	1,047,058	943,554	1,568,583
	0.5	2,509,829	2,173,100	2,237,255	1,793,246	1,813,479	1,266,577	1,131,342	2,009,159
	1	2,657,574	2,337,524	2,398,150	1,894,096	1,973,455	1,364,092	1,212,165	2,200,367
	5	2,988,067	2,702,633	2,763,548	2,125,721	2,348,088	1,583,556	1,404,301	2,643,215
	10	3,120,389	2,850,378	2,913,421	2,214,339	2,508,500	1,675,124	1,485,113	2,827,268
	25	3,280,124	3,035,204	3,100,036	2,316,736	2,710,682	1,788,460	1,583,953	3,053,914

RAP = reclaimed asphalt pavement; temp. = temperature.

Table 12. Dynamic Modulus Test Results for Mixtures Having RAP Contents From 21%-30%

Temp., °C	Frequency, Hz	O	P	B	C	D	J	U	R	S	X	
		9.5 mm	9.5 mm	12.5 mm	12.5 mm	12.5 mm	9.5 mm	9.5 mm	9.5 mm	9.5 mm	12.5 mm	
		PG 64-22	PG 64-22	PG 64-22	PG 64-22	PG 64-22	PG 64-22	PG 64-22	PG 64-22	PG 64-22	PG 64-22	PG 64-22
		21% RAP	21% RAP	25% RAP	25% RAP	25% RAP	25% RAP	25% RAP	25% RAP	30% RAP	30% RAP	30% RAP
37.8	0.1	103,243	98,331	41,940	93,675	71,924	75,555	39,871	128,706	99,133	150,172	
	0.5	193,770	188,481	84,678	171,352	141,426	150,462	77,300	241,343	193,384	270,350	
	1	249,271	242,020	116,209	216,503	187,195	197,831	103,755	304,918	251,350	341,274	
	5	432,792	414,179	236,702	362,111	343,063	352,006	200,200	500,912	440,915	564,245	
	10	534,947	507,632	315,844	440,915	433,808	436,322	260,826	602,922	544,907	683,224	
	25	681,242	644,112	430,810	549,499	564,390	558,830	348,622	747,089	695,794	849,631	
21.1	0.1	536,301	533,352	267,014	439,077	417,564	431,294	246,467	647,110	556,365	684,868	
	0.5	802,155	782,140	476,255	645,805	658,810	652,766	415,678	909,435	829,326	981,567	
	1	930,175	902,618	589,046	746,509	777,015	760,868	504,683	1,030,976	958,361	1,121,770	
	5	1,275,123	1,221,991	921,134	1,023,821	1,107,846	1,056,600	766,524	1,338,408	1,291,802	1,488,764	
	10	1,433,069	1,369,059	1,082,416	1,151,551	1,262,311	1,194,627	893,771	1,475,614	1,441,095	1,653,188	
	25	1,644,099	1,566,987	1,306,113	1,326,998	1,471,021	1,379,550	1,069,750	1,568,293	1,638,684	1,868,327	
4.4	0.1	1,720,486	1,697,715	1,281,408	1,403,627	1,521,736	1,446,364	1,068,203	1,779,371	1,743,861	1,949,887	
	0.5	2,056,731	2,012,930	1,666,193	1,696,216	1,875,144	1,747,753	1,372,975	2,049,866	2,051,848	2,291,886	
	1	2,202,978	2,149,314	1,838,788	1,824,671	2,026,612	1,880,269	1,509,214	2,164,059	2,179,699	2,436,730	
	5	2,534,002	2,457,374	2,241,074	2,125,963	2,373,204	2,190,601	1,833,808	2,424,499	2,469,339	2,761,856	
	10	2,670,434	2,586,409	2,407,481	2,254,708	2,517,226	2,320,507	1,971,546	2,532,890	2,588,923	2,893,212	
	25	2,836,406	2,745,467	2,276,947	2,431,750	2,692,722	2,481,015	2,143,851	2,670,289	2,735,411	3,076,588	

RAP = reclaimed asphalt pavement; temp. = temperature.

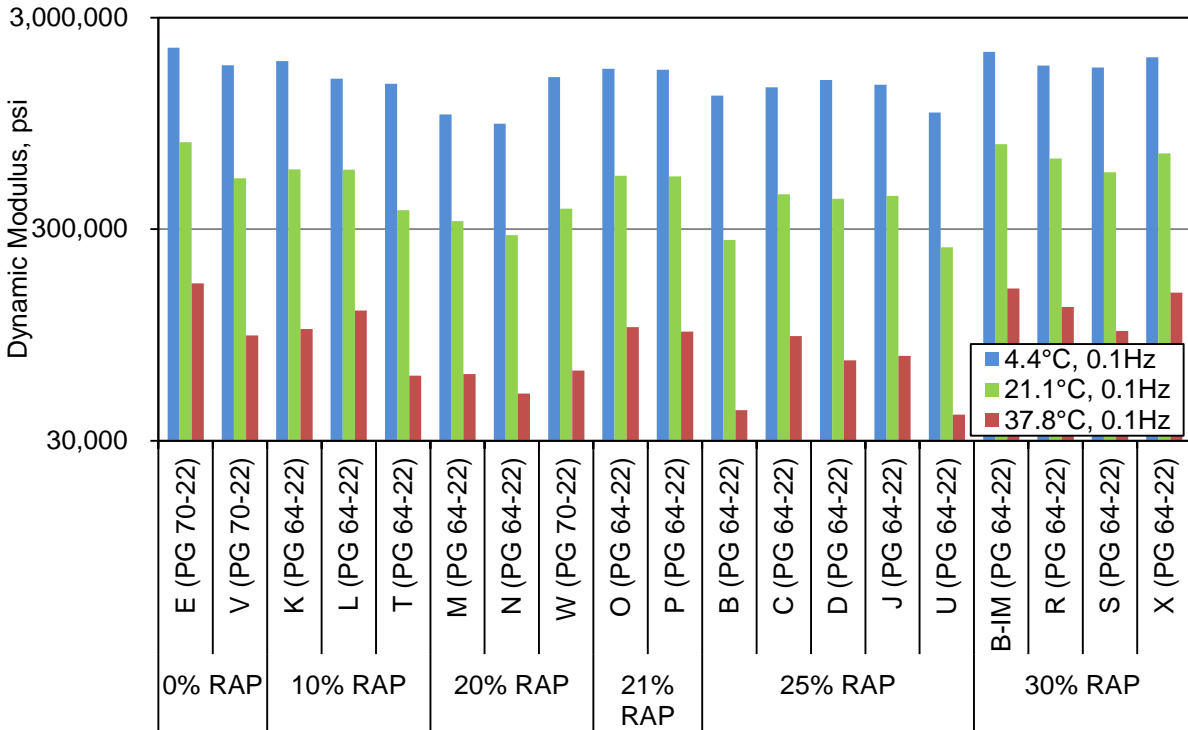


Figure 11. Dynamic Modulus Values at All Test Temperatures and 0.1 Hz Frequency for All Tested Cores. RAP = reclaimed asphalt pavement.

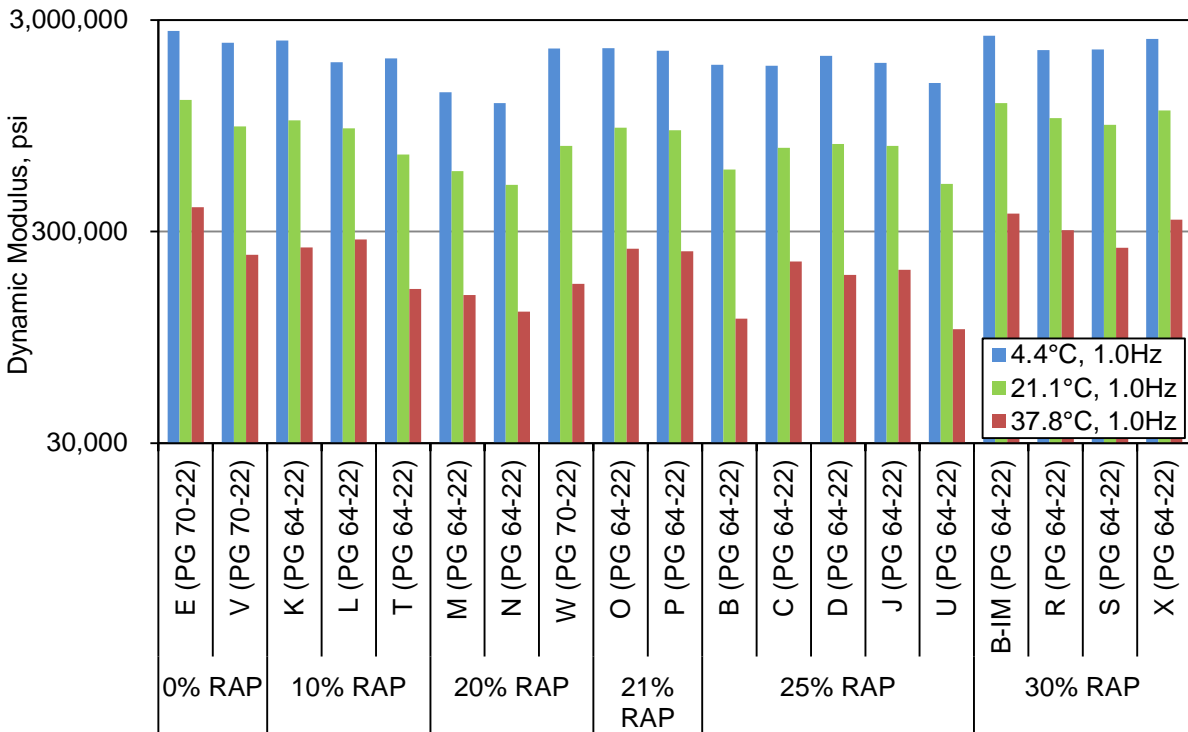


Figure 12. Dynamic Modulus Values at All Test Temperatures and 1.0 Hz Frequency for All Tested Cores. RAP = reclaimed asphalt pavement.

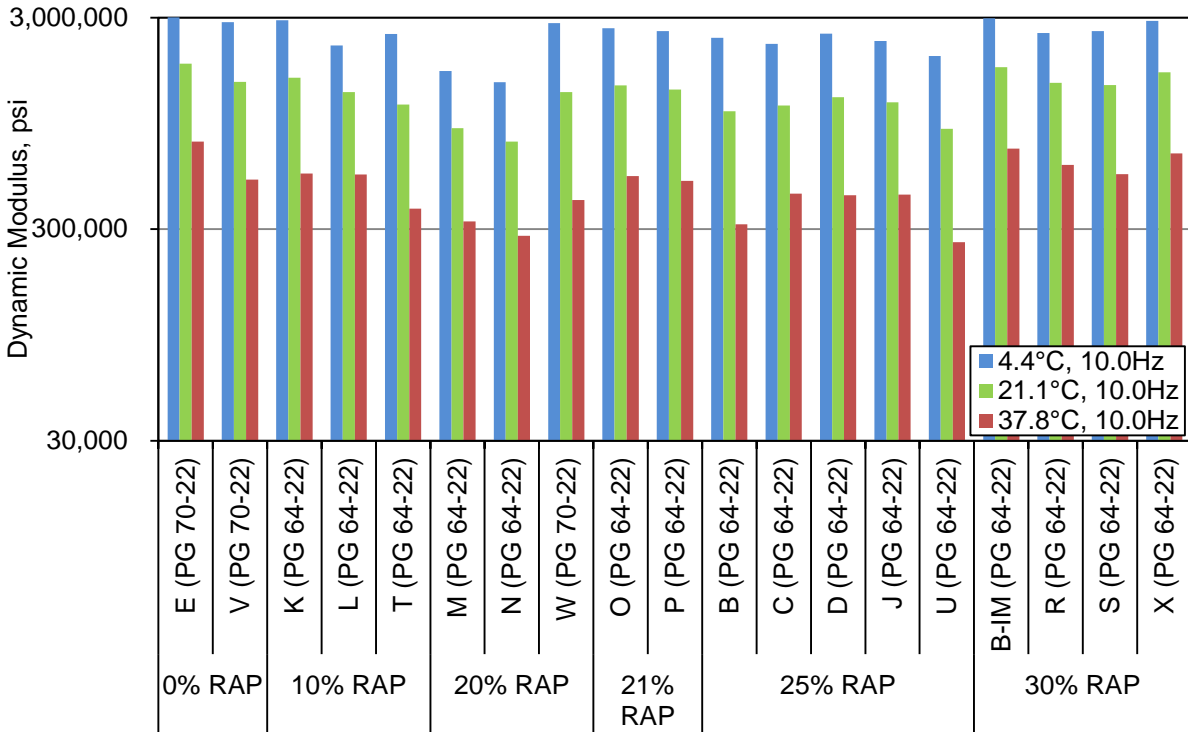


Figure 13. Dynamic Modulus Values at All Test Temperatures and 10.0 Hz Frequency for All Tested Cores. RAP = reclaimed asphalt pavement.

Table 13. *t*-test Comparisons of Mixtures at 21.1°C (70°F) and 1 Hz (lower left half of table) and 5 Hz (upper right half of table)

Section (% RAP)	E (0%)	V (0%)	K (10%)	L (10%)	T (10%)	M (20%)	N (20%)	W (20%)	O (21%)	P (21%)	B (25%)	C (25%)	D (25%)	J (25%)	U (25%)	B-IM (30%)	R (30%)	S (30%)	X (30%)
E (0%)		0.0331	0.3005	0.0259	0.0241	0.0238	0.0103	0.0081	0.0314	0.0379	0.7502	0.0791	0.0087	0.0100	0.0088	0.0035	0.0734	0.0424	0.4695
V (0%)	0.0325		0.7562	0.8089	0.1668	0.3797	0.0417	0.1069	0.9007	0.7171	0.0976	0.3719	0.1194	0.0210	0.0045	0.0030	0.1336	0.7024	0.3342
K (10%)	0.3315	0.7800		0.6989	0.2249	0.5284	0.2858	0.3114	0.7273	0.6454	0.3849	0.3558	0.3349	0.3073	0.1089	0.1417	0.9007	0.8203	0.6416
L (10%)	0.0179	0.3215	0.4937		0.1521	0.5420	0.0883	0.1571	0.9362	0.8618	0.0791	0.4140	0.1822	0.0960	0.0187	0.0134	0.2083	0.6248	0.3007
T (10%)	0.0396	0.1854	0.2097	0.2676		0.2427	0.6443	0.5803	0.1421	0.1891	0.0290	0.7997	0.5082	0.5622	0.2607	0.4061	0.1132	0.1658	0.0846
M (20%)	0.0212	0.2654	0.4607	0.9084	0.2976		0.2258	0.3245	0.5188	0.7491	0.0578	0.5608	0.3785	0.2556	0.0903	0.0508	0.1386	0.3076	0.2130
N (20%)	0.0066	0.0476	0.2265	0.1729	0.8611	0.1931		0.8455	0.1022	0.2106	0.0310	0.9976	0.7135	0.7909	0.0864	0.0700	0.0172	0.0415	0.1132
W (20%)	0.0123	0.1760	0.3781	0.6473	0.4006	0.6970	0.3266		0.1596	0.2810	0.0246	0.9361	0.8888	0.9830	0.0634	0.1127	0.0419	0.0909	0.1138
O (21%)	0.0251	0.6420	0.6589	0.5860	0.1778	0.4810	0.0766	0.3322		0.8165	0.0862	0.3990	0.1846	0.1144	0.0236	0.0194	0.2792	0.7294	0.3191
P (21%)	0.0272	0.4240	0.5286	0.9216	0.2521	0.8326	0.1848	0.6027	0.6846		0.0792	0.4740	0.3220	0.2416	0.0441	0.0515	0.2777	0.5954	0.2765
B (25%)	0.5749	0.0459	0.4400	0.0278	0.0510	0.0301	0.0080	0.0183	0.0409	0.0425		0.0924	0.0271	0.0332	0.0185	0.0138	0.1992	0.1147	0.6320
C (25%)	0.0813	0.2890	0.2835	0.4745	0.9568	0.4986	0.9641	0.6154	0.3494	0.4511	0.1015		0.8795	0.9410	0.2906	0.4541	0.2332	0.3382	0.1692
D (25%)	0.0079	0.1016	0.3106	0.4290	0.5335	0.4522	0.4913	0.7334	0.2000	0.4094	0.0113	0.7329		0.8446	0.0542	0.0888	0.0441	0.0993	0.1237
J (25%)	0.0051	0.0109	0.2485	0.2034	0.7401	0.2179	0.7678	0.3989	0.0811	0.2179	0.0056	0.8897	0.6092		0.0148	0.0340	0.0052	0.0125	0.1219
U (25%)	0.0043	0.0004	0.0931	0.0272	0.2500	0.0676	0.0773	0.0382	0.0152	0.0352	0.0042	0.3384	0.0413	0.0104		0.1712	0.0030	0.0020	0.0500
B-IM (30%)	0.0027	0.0024	0.1472	0.0545	0.5503	0.0747	0.2101	0.0956	0.0235	0.0689	0.0028	0.6709	0.1270	0.0936	0.0508		0.0013	0.0029	0.0565
R (30%)	0.0413	0.6614	0.8465	0.2555	0.1798	0.2300	0.0519	0.1460	0.4967	0.3451	0.0590	0.2657	0.0870	0.0091	0.0001	0.0024		0.1735	0.5962
S (30%)	0.0242	0.6432	0.7002	0.4370	0.1956	0.3420	0.0483	0.2318	0.8569	0.5517	0.0339	0.3227	0.1305	0.0171	0.0012	0.0033	0.3976		0.3739
X (30%)	0.4275	0.3783	0.7030	0.2019	0.0817	0.1874	0.0853	0.1432	0.2992	0.2243	0.6191	0.1502	0.1127	0.0949	0.0392	0.0556	0.4280	0.3239	

Shaded bold cells indicate significant differences in modulus values between sites at a level of significance of $\alpha = 0.05$.

Repeated Load Permanent Deformation

RLPD tests were performed on eight mixtures using small-scale specimens. The number of mixtures was limited by the availability of cores of suitable thickness with which to prepare test specimens. A common method for analyzing RLPD data is to evaluate the flow number (F_N), which occurs between the linear secondary and the tertiary phase of cycles, versus the accumulated strain.

Figure 14 shows averaged test results for each of the eight mixtures tested. None of the specimens tested ever reached tertiary flow; thus the F_N could not be recorded. This is likely due to the fact that the specimens were tested in a confined setting, which would reduce the tendency for the mixture to flow after 10,000 cycles. In addition, there were no instances of rutting observed in the field sites, indicating that the mixtures are not rut susceptible and supporting the lack of tertiary flow. An alternative method for evaluating these mixtures is to regress a power-law function onto the specimen's secondary portion. This allows for a slope and an intercept to be estimated, which can be in turn be used as a rutting indicator for mixture comparisons.

Figure 15 shows the average secondary portion slope and intercept of the replicates for each mixture tested. Mixtures are grouped in accordance with their RAP content. The secondary portion was defined as the linear portion after the primary stage was completed, visually established as 1,000 cycles, to the completion of the test, as no tertiary flow occurred.

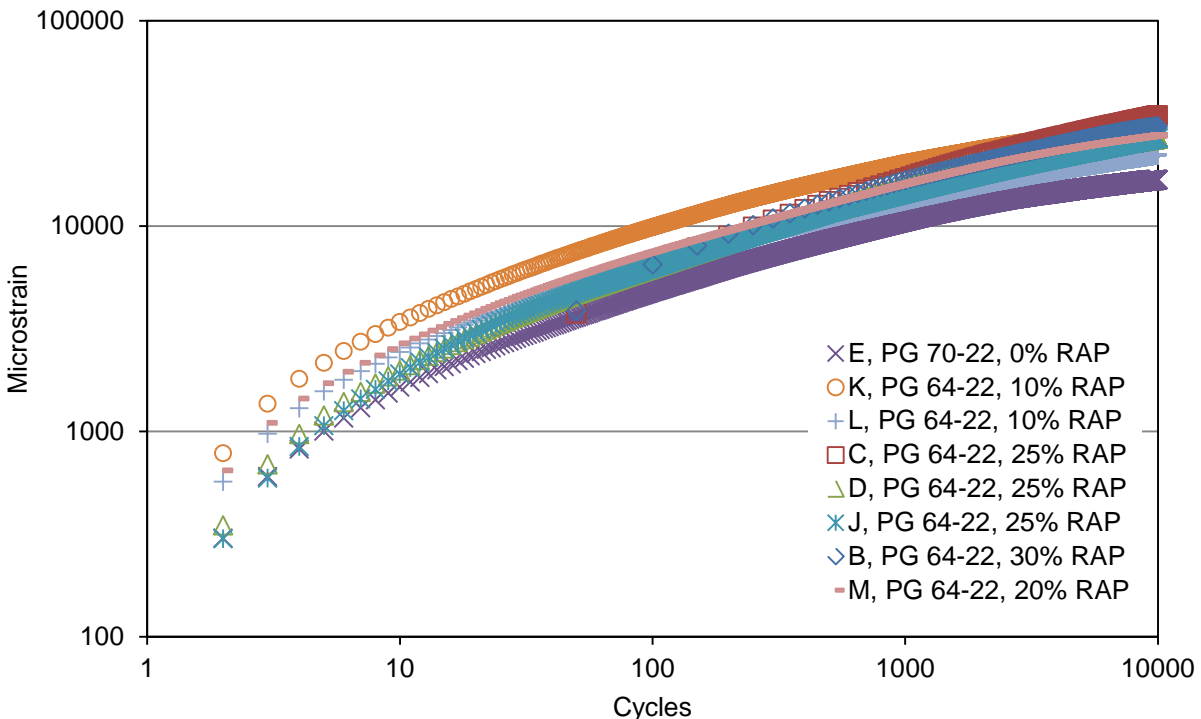


Figure 14. Average RLPD Data for Each Mixture Tested. RLPD = repeated load permanent deformation; RAP = reclaimed asphalt pavement.

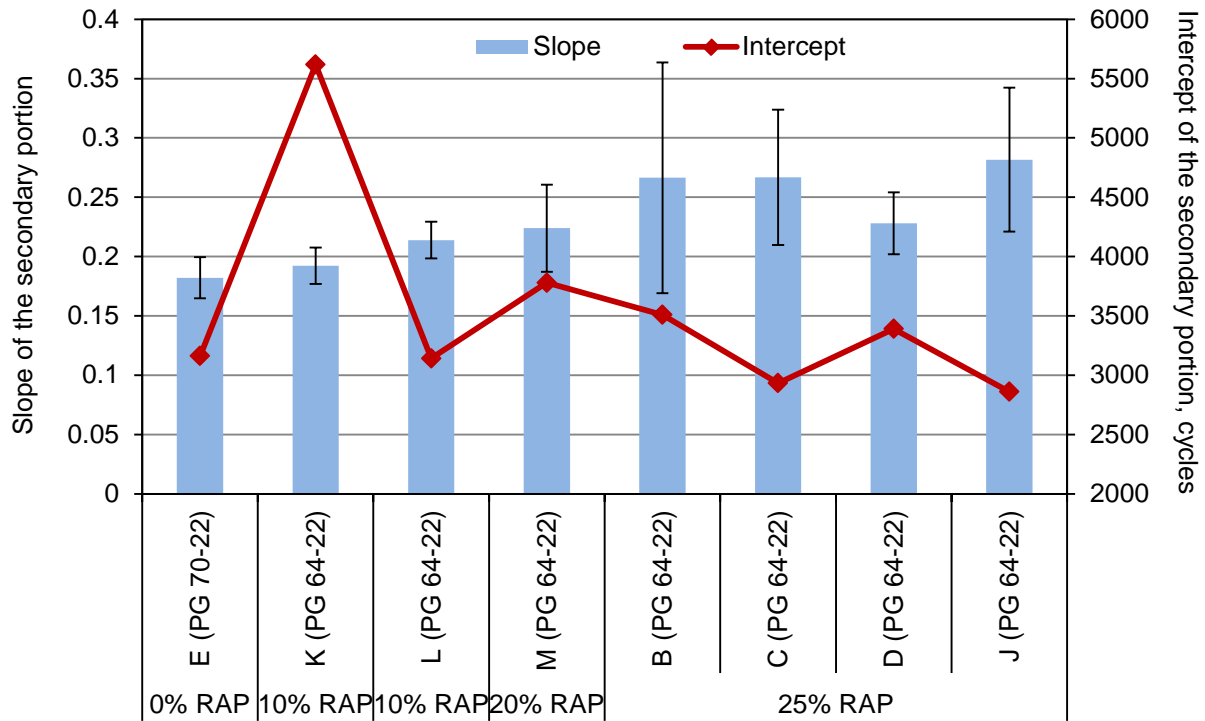


Figure 15. Average Slope and Intercept of Each Mixture, Grouped by RAP Content. Error bars indicate 1 standard deviation.

The trend represented in Figure 15 is that the average slope generally increases as RAP contents are increased. This would be indicative of a higher potential for plastic deformation or rutting. One might expect that the intercept would be lower for these mixtures if the secondary slope is indeed higher versus the lower-RAP mixtures; however, this also does not seem to be the case. Compared to the field performance of the mixtures, which does not indicate any tendencies toward excessive rutting, the trends are interesting.

There are a few potential reasons for the contradiction in performance with the test result indication that the higher RAP samples may be more susceptible to rutting. The specifications under which these mixtures were designed and produced allowed mixtures specified to incorporate PG 70-22 binder, but which containing 21% or more RAP, to use a PG 64-22 virgin asphalt base binder in lieu of the required PG 70-22 binder as long as the resultant combined binder met the requirements for a PG 70-22 binder. In addition, it was assumed that all of the RAP binder was available to contribute to the total asphalt content of the mixture. However, it has been found that these assumptions do not always result in a mixture with a performance comparable to that of mixtures designed with 20% RAP or less and PG 70-22 virgin binder. Apeageyi et al. (2011) reported an increase in rutting F_N because of a PG grade reduction of the virgin binder. They noted that increasing RAP contents resulted in a notable reduction in the effective binder content of the mixture. A lower effective binder content could yield a less rut-resistant asphalt mixture because of a lack of binder to glue the aggregates together.

In addition, a lack of complete blending between the virgin and RAP binders can affect rutting resistance. This could explain why the recovered binder grades for the higher RAP mixtures were of equal or greater stiffness than those of the lower-RAP mixtures. The recovery

process forces blending to occur, resulting in a well-blended composite material that does not necessarily exist under actual production and service conditions. Theoretically, in practice the softer binder could be forming a mid-grade composite through blending with the RAP (e.g., a grade between the recovered grade and the initial virgin binder grade) but not completely blending with the RAP binder. If this is the case, there could be pockets of softer composite binder and pockets of stiff binder and/or RAP binder, leading to a decrease in rut resistance.

An alternate reason for the contradictions in test results to conventionally expected performance is that there could be error introduced into the RLPD test results when used with the small-scale test geometry. Although the use of the small-scale geometry has been validated for dynamic modulus testing (Bowers et al., 2015a; Li and Gibson, 2013), there is no literature reporting the use of small-scale specimens for RLPD testing. There is a possibility that the RLPD strain parameters used in the test, although appropriate for larger specimen sizes, may be inducing damage in the mixture past the threshold of desired behavior.

Texas Overlay Test

The Texas overlay test was conducted on 13 of the mixtures. Replicate tests were performed on each mixture, and the number of replicates ranged from four to six. The target coefficient of variation (COV) between cores was less than 30%, which was found to be difficult to achieve in many cases, most likely because of specimen variability. There are many approaches to reducing the data in an effort to narrow the COV and exclude outliers. One approach is to remove the samples with the highest and lowest number of cycles to failure, assuming at least five replicates are available. An alternative approach is to remove the data points that appear to be outliers by a test of reasonableness. This second approach was used in this study. Figure 16 shows the data prior to the removal of believed outlier specimens, and Figure 17 shows the data after outliers were removed. On the primary (left) y-axis is the number of cycles to failure, as represented by the blue bars with error bars representing ± 1 standard deviation, and the secondary (right) y-axis represents the COV as represented by the line.

It is worth noting that the COV was reduced after the removal of outlier data; however, Mixtures P and X still maintained COV values higher than the 30% recommended by the test method. For both mixtures, this was partially attributed to the low number of cycles to failure. There was no evidence of a conclusive trend between RAP content and cracking susceptibility as measured by the overlay test.

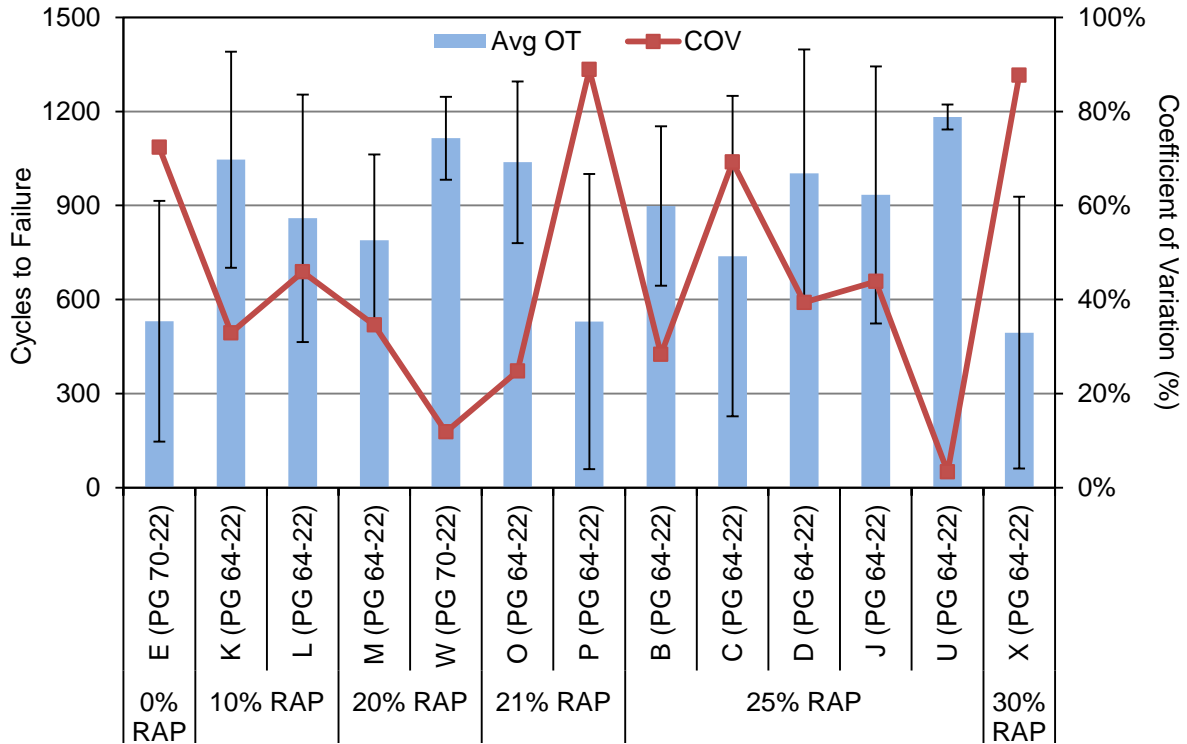


Figure 16. Overlay Test Results Prior to Removal of Outlier Data. Error bars indicate 1 standard deviation. OT = overlay test; COV = coefficient of variation; RAP = reclaimed asphalt pavement.

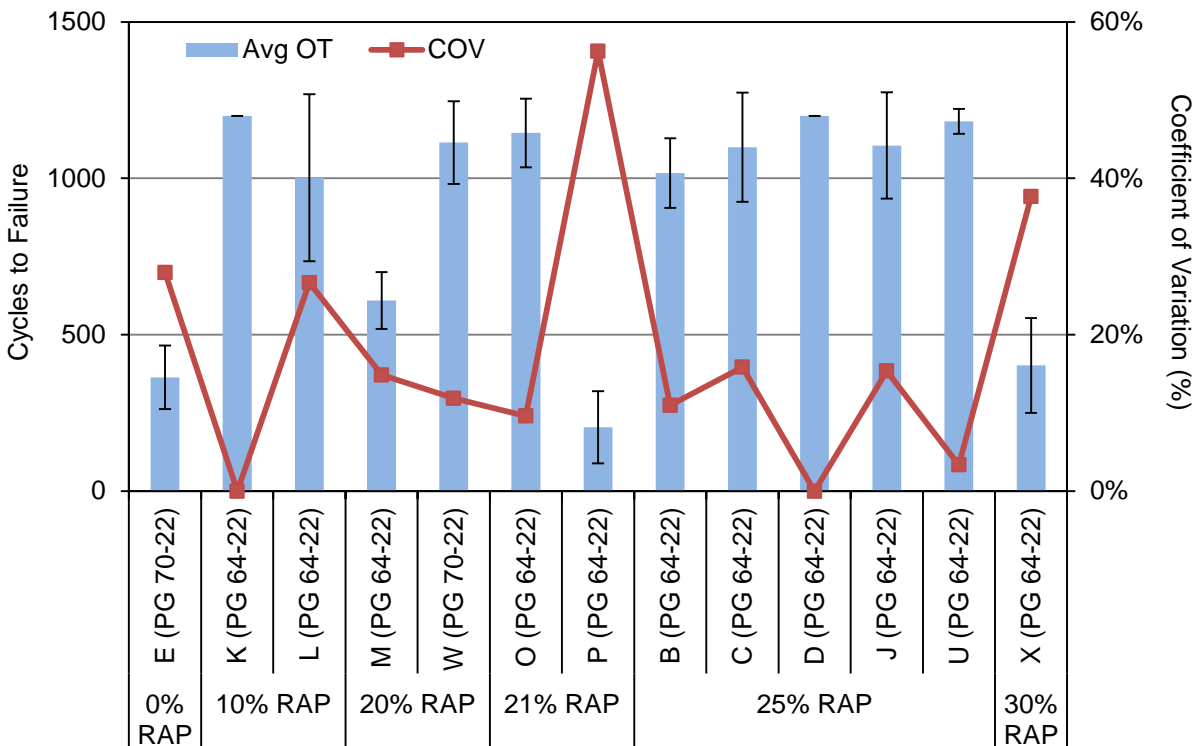


Figure 17. Overlay Test Results After Removal of Outlier Data. Error bars indicate 1 standard deviation. OT = overlay test; COV = coefficient of variation; RAP = reclaimed asphalt pavement.

Binder Testing

Performance Grading

A summary of the detailed results of binder grading is shown in Appendix F. Table 14 summarizes the performance grade for binder from each site. Of interest, most of the binders graded as a PG 82-XX binder, with the exception of two full surface and two bottom-half specimens that graded as a PG 76-XX binder and one top-half specimen that graded as a PG 88-XX binder. The top-half specimen from Site B did not meet the PG criteria as specified in AASHTO M 320, as the failure temperatures exceeded the limits of the specification.

Table 14. Summary of Performance Grading Results for Extracted and Recovered Binders

Site	Location Within Layer ^a	% RAP	Performance Grade	Failure Temperature, °C			
				High	Intermediate	Stiffness	M-value
A	Bottom	25	82-16	78.47	26.5	-22.6	-21.7
A	Top	25	82-16	82.81	29.67	-20.5	-18.5
B	Bottom	25	82-10	89.42	34.62	-16.2	-14.7
B	Top	25	NA ^b	103.9	40.43	-14.4	-4.9
B	Intermediate ^c	30	76-16	79.68	27.12	-22.0	-21.6
C	Full	25	82-10	87.21	30.9	-19.8	-15.6
D	Full	25	82-16	84.55	29.74	-21.0	-19.3
E	Full	0	82-10	89.29	35.2	-16.0	-14.6
F	Full	25	82-16	80.35	27.1	-22.9	-18.6
F	Full	25	82-10	84.77	27.76	-22.2	-15.2
H	Bottom	20	76-16	81.15	28.46	-22.1	-18.5
H	Top	20	82-16	83.52	29.22	-21.3	-17.2
I	Bottom	20	82-16	86.38	31.57	-19.6	-16.5
I	Top	20	88-10	88.71	33.06	-18.5	-14.3
J	Full	25	82-10	84.27	31.7	-20.8	-15.6
K	Full	10	76-16	82.89	31.6	-20.7	-16.6
L	Full	10	82-10	84.84	33.26	-18.7	-12.0
M	Full	20	82-16	83.03	28.37	-24.0	-18.7
N	Bottom	20	82-16	88.79	31.84	-19.0	-16.0
N	Top	20	82-16	88.94	29.26	-22.4	-17.7
O	Full	21	82-10	89.00	36.6	-17.8	-10.7
P	Full	21	82-10	84.29	32.58	-20.3	-13.0
Q	Bottom	15	76-10	84.76	29.15	-24.9	-15.6
Q	Top	15	82-10	92.33	34.64	-23.0	-11.8
R	Bottom	30	82-10	83.88	31.85	-21.4	-14.0
R	Top	30	82-10	85.65	32.06	-21.2	-13.2
S	Bottom	30	82-16	84.27	29.08	-20.5	-16.5
S	Top	30	82-10	88.33	34.52	-19.4	-12.0
U	Full	25	76-16	77.79	27.33	-23.2	-18.5
V	Bottom	0	82-16	84.26	30.31	-19.3	-18.8
V	Top	0	82-10	92.06	36.42	-15.9	-13.2
W	Full	20	82-16	82.72	30.73	-20.9	-17.6
X	Full	30	82-16	86.25	30.81	-19.8	-17.1

Note: Sections A and B contain a contiguous surface mixture.

^a All cores are surface layer cores unless otherwise noted. Selected cores were split into a top half and a bottom half for evaluation.

^b Did not meet requirements for standard performance grade in accordance with AASHTO M 320.

^c Intermediate = core taken from intermediate layer.

Table 15 shows the comparison of failure temperatures for binder extracted from the top half and the bottom half of cores. The results indicated that in nearly every case, the binder recovered from the top half of the core was stiffer than that obtained from the bottom half. This was expected, as the surface of the cores undergoes ultraviolet exposure; in addition, the rate of diffusion of oxygen would be expected to be higher at the upper portion of the core, leading to increased aging, as compared to the lower portion (Glover et al., 2014). In addition, the difference in failure temperature between the top half and bottom half of cores generally decreased with increasing RAP content, with the exception of Core B. Figure 18 shows that the trends are generally the same for all failure temperatures. The influence of factors such as core air-void contents was not evaluated, as multiple cores were combined to acquire sufficient recovered binder for grading.

Table 16 presents the results of binder grading performed during this study on recovered binder from cores at 6 to 7 years of service as compared to the binder grading performed on virgin binders, RAP stockpile samples, and loose mixtures sampled during construction in 2006 and 2007. Table 16 indicates that all mixtures, regardless of RAP content, gained one to two high-temperature performance grades over the in-service period evaluated. Low-temperature grades were similarly affected, with only one site (Site W) found to retain the as-constructed low-temperature grade in-service. The results for Sites Q and R, wherein cores were split into a top half and a bottom half for evaluation, indicated that the increase in grade temperature was influenced by proximity to the surface of the pavement. Figure 19 shows the indication that the mixtures containing less RAP aged over the 6-year period to a greater extent than those containing higher RAP contents; Sites V and Q (top half) had the highest true grade results and the lowest RAP contents, whereas the sites with mixtures having 25% to 30% RAP resulted in lower differences in failure temperatures.

Table 15. Comparison of Failure Temperatures for Binder Extracted From the Top Half and Bottom Half of Cores

Failure Temperatures	Half	Site									
		V	Q	H	I	N	A	B	F	R	S
		0% RAP	15% RAP	20% RAP	20% RAP	20% RAP	25% RAP	25% RAP	25% RAP	30% RAP	30% RAP
RTFO failure temperature, °C	Top	92.1	92.3	83.5	88.7	88.9	82.8	103.9	84.8	85.7	88.3
	Bottom	84.3	84.8	81.2	86.4	86.8	78.5	89.4	80.4	83.9	84.3
Difference		7.8	7.6	2.4	2.3	2.1	4.3	14.5	4.4	1.8	4.1
PAV failure temperature, °C	Top	36.4	34.6	29.2	33.1	29.3	29.7	40.4	27.8	32.1	34.5
	Bottom	30.3	29.2	28.5	31.6	31.8	26.5	34.6	27.1	31.9	29.1
Difference		6.1	5.5	0.8	1.5	-2.6	3.2	5.8	0.7	0.2	5.4
Stiffness failure temperature, °C	Top	-15.9	-23.0	-21.3	-18.5	-22.4	-20.5	-14.4	-22.2	-21.2	-19.4
	Bottom	-19.3	-24.9	-22.1	-19.6	-19.0	-22.6	-16.2	-22.9	-21.4	-20.5
Difference		3.5	1.9	0.8	1.0	-3.5	2.1	1.8	0.7	0.2	1.1
M-value failure temperature, °C	Top	-13.2	-11.8	-17.2	-14.3	-17.7	-18.5	-4.9	-15.2	-13.2	-12.0
	Bottom	-18.8	-15.6	-18.5	-16.5	-16.0	-21.7	-14.7	-18.6	-14.0	-16.5
Difference (Top – Bottom)		5.6	3.8	1.3	2.2	-1.7	3.2	9.8	3.4	0.9	4.5

RAP = reclaimed asphalt pavement; RTFO = rolling thin film oven; PAV = pressure aging vessel.

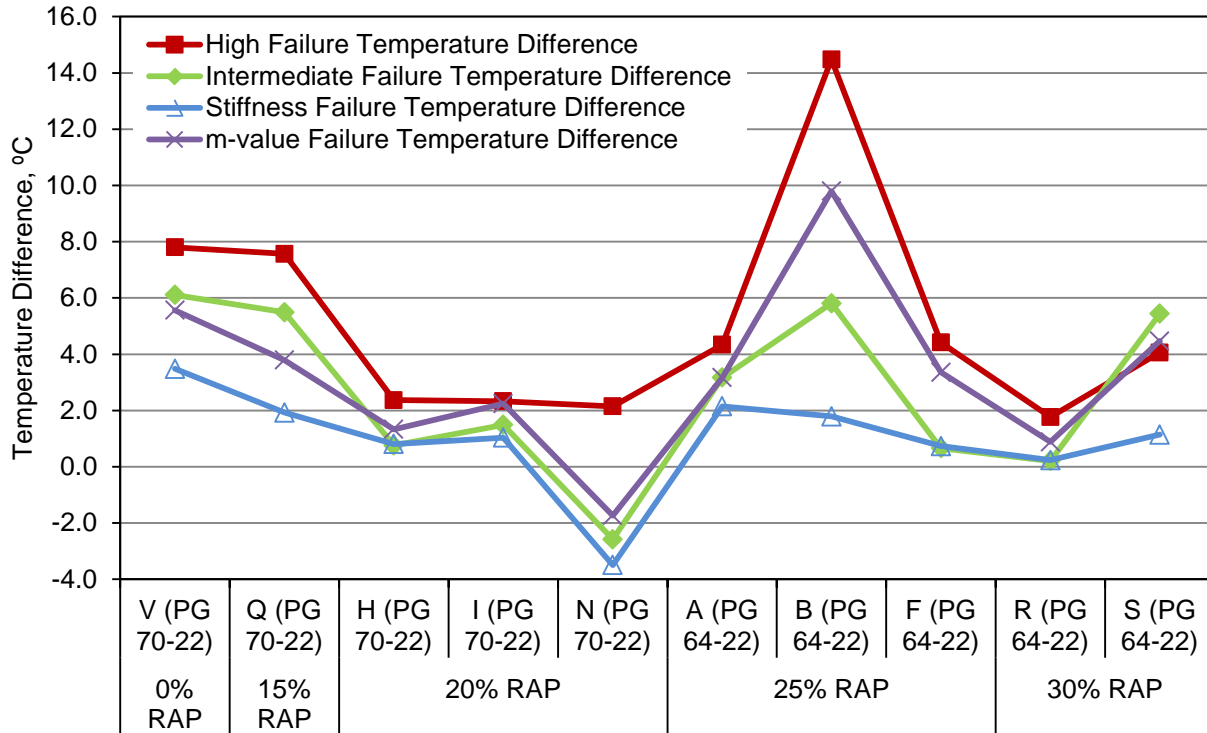


Figure 18. Difference in Failure Temperatures for Binder Extracted From Top Half and Bottom Half of Cores. Difference is expressed as top half failure temperature – bottom half failure temperature. RAP = reclaimed asphalt pavement.

The observed trends of increased aging, as measured by changes in failure temperatures, in mixtures having lower percentages of RAP may support the hypothesis that since RAP has already undergone significant aging (assuming the RAP source is from milled pavement and not from plant waste), it will not continue to stiffen and further age extensively.

Increased scrutiny of the role that aging plays in mixture performance, especially as related to binder aging, has led to the development of additional parameters proposed to be indicative of cracking potential. One of these parameters, ΔT_{cr} , was suggested by Anderson et al. (2011) as an index to predict the thermal cracking potential of binders. ΔT_{cr} is the difference in critical temperature determined using the bending beam rheometer (BBR) stiffness and that determined using the BBR m-value. As binders age, the difference between the critical temperatures is known to increase, as the aging process affects the stiffness and relaxation properties differently. Minimum thresholds for ΔT_{cr} of -2.5 and -5.0 representing the cracking warning and cracking limit, respectively, have been suggested (Anderson et al., 2011; Rowe, 2011). The cracking warning is intended to indicate an accelerated risk of cracking wherein preventative action should be taken. The cracking limit indicates that the materials need immediate remediation to prevent cracking. ΔT_{cr} has been further investigated and was found to be related to more universal cracking. Reinke et al. (2016) evaluated ΔT_{cr} relative to performance data for two sets of pavement sites and found only moderate correlation to thermal cracking ($R^2 = 0.62$ and $R^2 = 0.46$, respectively, for each site) but a much greater correlation to fatigue or total cracking ($R^2 = 0.95$ and $R^2 = 0.97$, respectively, for each site).

Table 16. Comparison of Performance Grading Results From Samples Collected at Construction and After 6 Years in Service

Site	RAP	Virgin Binder (At Construction)		Abscon Recovery (At Construction)				Rotavap Recovery (6-7 Years In-Service)	
		Performance Grade	True Grade	RAP Stockpile		Loose Mix		Cores	
				Performance Grade	True Grade	Performance Grade	True Grade	Performance Grade	True Grade
V	0%	PG 70-22	PG 72-23	NA	NA	PG 70-22	PG 73-25	PG 82-10	PG 92-13
Q ^a	15%	PG 70-22	PG 71-24	PG 82-22	PG 85-27	PG 70-22	PG 73-23	Top: PG 82-10	PG 92-11
		PG 70-22	PG 71-23	PG 82-22	PG 85-27	PG 76-22	PG 76-22	Bottom: PG 82-10	PG 84-15
W	20%	PG 70-22	PG 72-24	PG 82-16	PG 94-16	PG 76-16	PG 79-16	PG 82-16	PG 82-17
O ^a	21%	PG 64-22	PG 65-24	PG 82-10	PG 95-14	PG 76-16	PG 77-21	PG 82-10	PG 89-10
		PG 64-22	PG 66-24	PG 82-10	PG 95-14	PG 70-22	PG 72-22		
		PG 64-22	PG 66-25	PG 82-10	PG 95-14	PG 70-22	PG 74-22		
D	25%	PG 64-22	PG 67-24	PG 82-10	PG 88-13	PG 76-22	PG 76-22	PG 82-16	PG 84-19
F	25%	PG 64-22	PG 66-24	PG 82-16	PG 90-18	PG 70-22	PG 71-22	PG 82-10	PG 84-15
J	25%	PG 64-22	PG 67-24	PG 82-10	PG 96-13	PG 70-22	PG 71-23	PG 82-10	PG 84-15
U ^a	25%	PG 64-22	PG 65-24	PG 82-16	PG 94-17	PG 70-22	PG 73-23	PG 76-16	PG 77-18
		PG 64-22	PG 64-24	PG 82-16	PG 94-17	PG 64-22	PG 69-25		
		PG 64-22	PG 65-24	PG 82-16	PG 94-17	PG 70-22	PG 74-22		
R	30%	PG 64-22	PG 64-24	PG 82-28	PG 83-18	PG 76-16	PG 76-20	Top: PG 82-10	PG 85-13
								Bottom: PG 82-10	PG 83-14
X	30%	PG 64-22	PG 67-26	PG 82-16	PG 93-17	PG 76-22	PG 76-25	PG 82-16	PG 86-17

RAP = reclaimed asphalt pavement.

^a Several samples were collected over multiple days of construction.

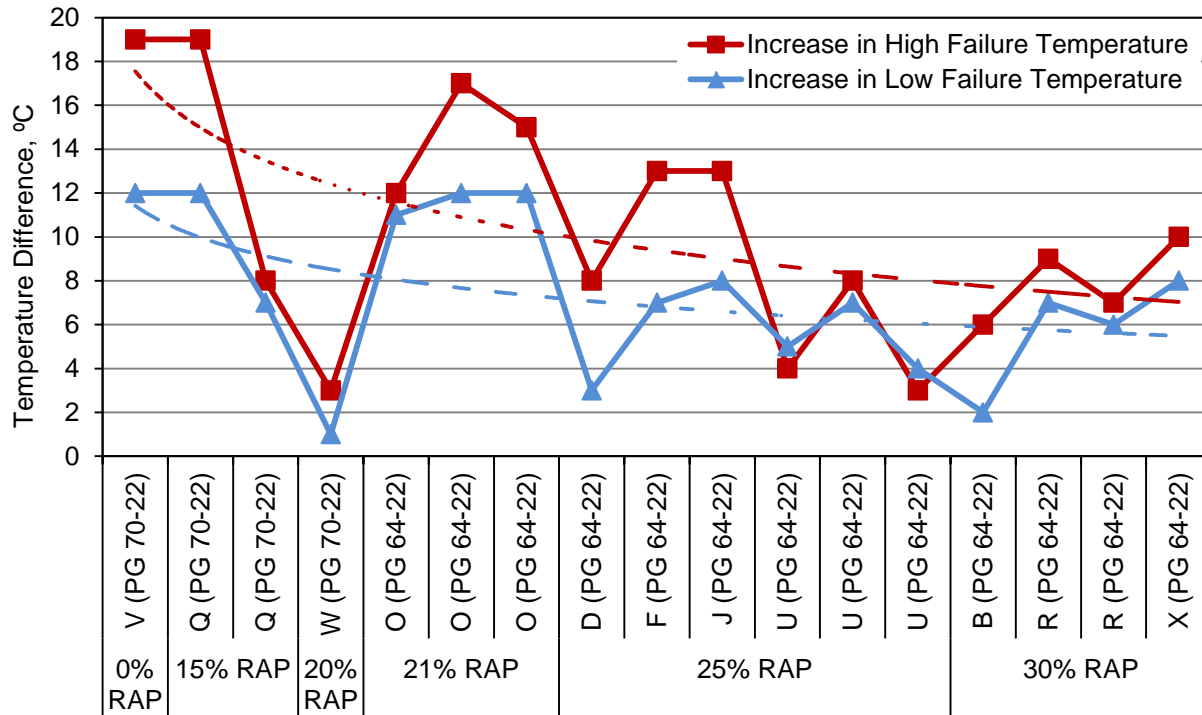


Figure 19. Increase in High and Low Failure Temperatures With RAP Content. RAP = reclaimed asphalt pavement.

ΔT_{cr} was determined for each of the recovered binders, and the results are presented in Tables 17 through 19. Table 17 shows the results for binders recovered from the entire core, and Tables 18 and 19 present the results for binder recovered from cores that were split into the top and bottom layers prior to recovery. An examination of the results provided several interesting observations. Table 17 indicates that values of ΔT_{cr} exceeding the cracking warning and cracking limit were found across the range of RAP contents. Only three mixtures, having 0% RAP, 25% RAP, and 30% RAP (an intermediate mixture), had values that stayed below the cracking warning value after their time in service. The values for mixtures having 10% RAP, 21% RAP, and 25% RAP were all found to exceed the cracking limit value.

Tables 18 and 19 indicate that values of ΔT_{cr} were reduced as the binder was located farther from the surface, supporting the role that aging plays in changing binder properties. As indicated in Table 18, only one binder did not exceed the cracking warning and five exceeded the cracking limit. Table 19 indicates that even at the increased depth from the surface, only three binders did not exceed the cracking warning and two exceeded the cracking limit. The variation of difference in ΔT_{cr} between the top half and bottom half of cores was also striking, ranging from approximately 0.5 to 8.0°C, demonstrating that aging is a unique process for every binder.

The relationships among ΔT_{cr} , RAP content, continuous low temperature grade, and the stiffness and m-value failure temperatures were further examined using correlation analysis. This analysis indicated a minimal correlation between ΔT_{cr} and RAP content with a coefficient of -0.1554. Critical cracking temperature was found only moderately correlated with the continuous low temperature grade and with the m-value failure temperature, having correlation coefficients of 0.6988 and 0.7007, respectively. There was no correlation with the stiffness

failure temperature, indicated by a correlation coefficient of 0.1604. The outcomes of this analysis suggest that although there are concerns about the cracking potential of the binders, these concerns are independent of the RAP content of the mixture.

Table 17. Critical Cracking Temperature for Binders Recovered From Cores

Section	RAP Content	Continuous Grade	Stiffness Failure Temperature, °C	M-value Failure Temperature, °C	ΔT_{cr}
E	0%	89-14	-16.0	-14.6	-1.4
K	10%	82-16	-20.7	-16.6	<i>-4.1</i>
L	10%	84-12	-18.7	-12.0	-6.7
M	20%	83-18	-24.0	-18.7	-5.2
W	20%	82-17	-20.9	-17.6	<i>-3.3</i>
O	21%	89-10	-17.8	-10.7	-7.1
P	21%	84-13	-20.3	-13.0	-7.2
C	25%	87-15	-19.8	-15.6	<i>-4.2</i>
D	25%	84-19	-21.0	-19.3	<i>-1.7</i>
J	25%	84-15	-20.8	-15.6	-5.2
U	25%	77-18	-23.2	-18.5	<i>-4.7</i>
B-IM	30%	79-21	-22.0	-21.6	<i>-0.4</i>
X	30%	86-17	-19.8	-17.1	<i>-2.8</i>

Values of ΔT_{cr} exceeding the cracking warning value of -2.5 are italicized, and values exceeding the cracking limit of -5.0 are in bold type. RAP = reclaimed asphalt pavement; IM = intermediate mix.

Table 18. Critical Cracking Temperature for Binders Recovered From Top Half of Cores

Section	RAP Content	Continuous Grade	Stiffness Failure Temperature, °C	M-value Failure Temperature, °C	ΔT_{cr}
V	0%	92-13	-15.9	-13.2	<i>-2.7</i>
Q	15%	92-11	-23.0	-11.8	-11.2
H	20%	83-17	-21.3	-17.2	<i>-4.1</i>
I	20%	88-14	-18.5	-14.3	<i>-4.3</i>
N	20%	88-17	-22.4	-17.7	<i>-4.7</i>
A	25%	82-18	-20.5	-18.5	<i>-2.0</i>
B	25%	103-4	-14.4	-4.9	-9.5
F	25%	84-15	-22.2	-15.2	-7.0
R	30%	85-13	-21.2	-13.2	-8.0
S	30%	88-12	-19.4	-12.0	-7.4

Values of ΔT_{cr} exceeding the cracking warning value of -2.5 are italicized, and values exceeding the cracking limit of -5.0 are in bold type. RAP = reclaimed asphalt pavement.

Table 19. Critical Cracking Temperature for Binders Recovered From Bottom Half of Cores

Section	RAP Content	Continuous Grade	Stiffness Failure Temperature, °C	M-value Failure Temperature, °C	ΔT_{cr}
V	0%	84-18	-19.3	-18.8	-0.6
Q	15%	84-15	-24.9	-15.6	-9.4
H	20%	81-18	-22.1	-18.5	-3.6
I	20%	86-16	-19.6	-16.5	-3.0
N	20%	88-16	-19.0	-16.0	-3.0
A	25%	78-21	-22.6	-21.7	-1.0
B	25%	89-14	-16.2	-14.7	-1.5
F	25%	80-18	-22.9	-18.6	-4.3
R	30%	83-14	-21.4	-14.0	-7.4
S	30%	84-16	-20.5	-16.5	-4.1

Values of ΔT_{cr} exceeding the cracking warning value of -2.5 are italicized, and values exceeding the cracking limit of -5.0 are in bold type. RAP = reclaimed asphalt pavement.

Shear Modulus Mastercurves

Binder testing was also performed on extracted and recovered binders to collect shear modulus and phase angle data; summaries of the data collected are presented in Appendix G. Figure 20 shows an example of a shifted mastercurve.

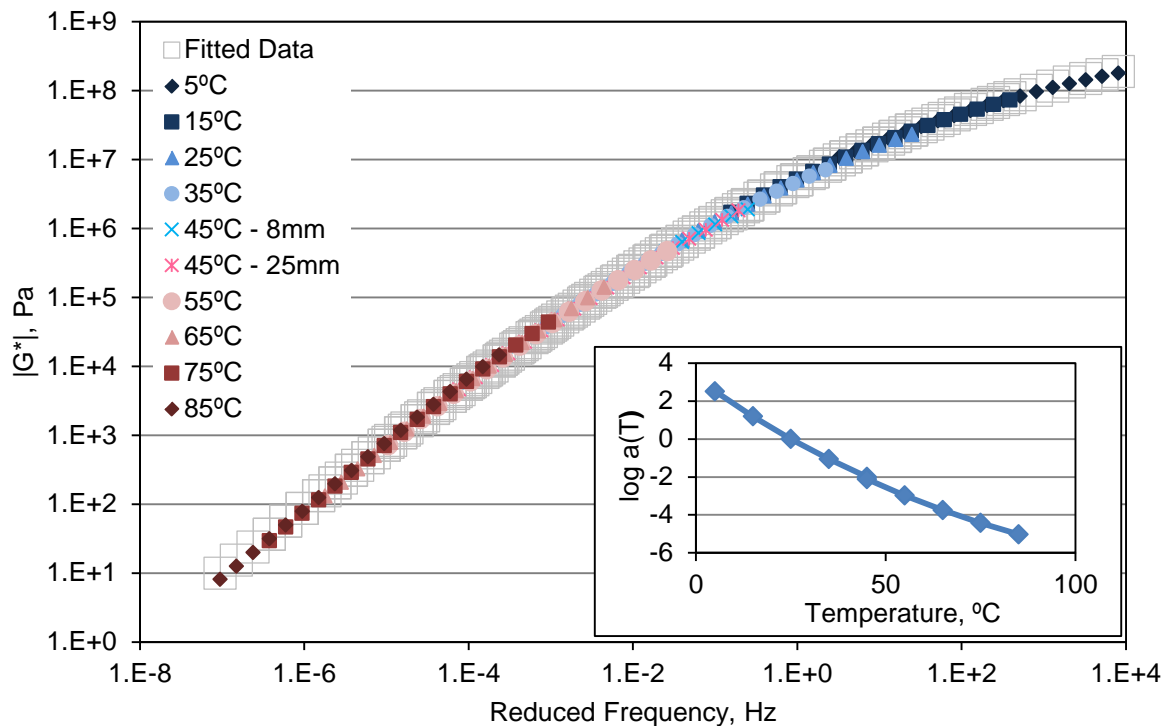


Figure 20. Example of Shifted Mastercurve Showing Measured and Fitted Data and Shift Factors

Analysis of the differences in measured modulus values between the top half and bottom half of cores was performed by plotting the log (G^*) for the top half versus the bottom half measured modulus values at each temperature frequency combination, as shown in Figure 21. Fitting trendlines to the data indicated that the difference in the modulus between the top half and bottom half of the cores was consistent irrespective of RAP content.

Evaluation of the modulus and phase angle data was performed in Black Space, wherein the complex modulus is plotted versus the phase angle to compare changes in each. It is claimed that the use of Black Space diagrams can offer clear illustrations of aging impacts (see Rowe discussion in Anderson et al., 2011). Figure 22 shows the Black Space plots for extracted binder from mixtures with varying RAP contents at temperatures from 5 to 45°C at a test frequency of 0.09959 rad/sec (0.01585 Hz) using an 8 mm plate size. Similar plots can be generated for all frequencies tested. Generally the figure shows the increase in stiffness and decrease in phase angle exhibited by the binders with decreasing test temperature. The patterning of response is generally similar at each temperature and can be seen in the callout for results at 25°C. As shown, neither the phase angle nor stiffness follows any trends with RAP content; this is likely influenced by the various base binders used in the mixtures and the varying stiffness of each RAP source. Considering that the shown data are at intermediate binder temperatures, wherein dynamic shear rheometer data are typically related to fatigue (the intermediate temperature $G^*\sin\delta$ measurement), these results are supportive of the visual survey and PMS indications that the 21% to 30% RAP mixtures are generally not any more likely to undergo premature fatigue cracking than the mixtures containing lesser amounts of RAP.

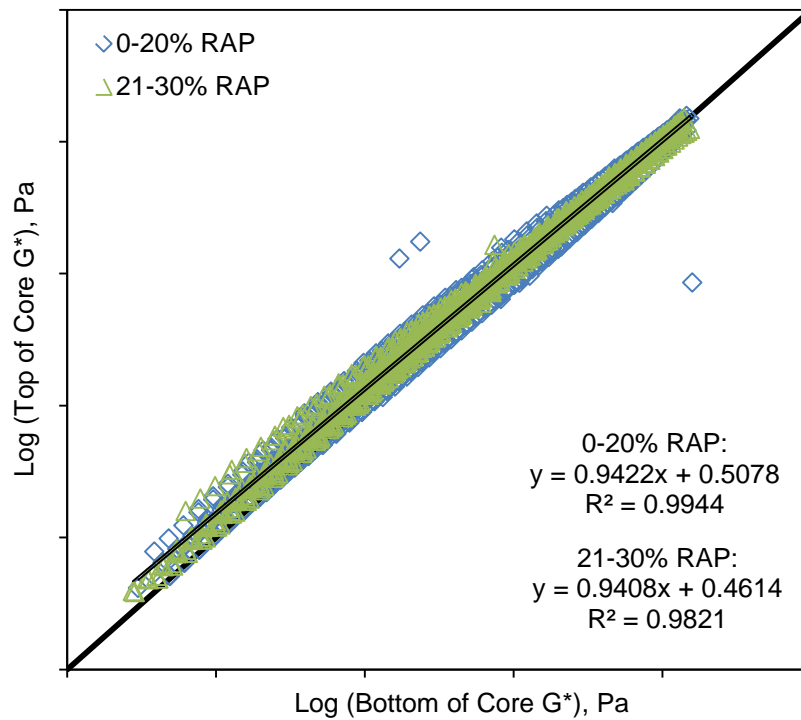


Figure 21. Plot of Log (G^*) for Top of Cores Versus Bottom of Cores

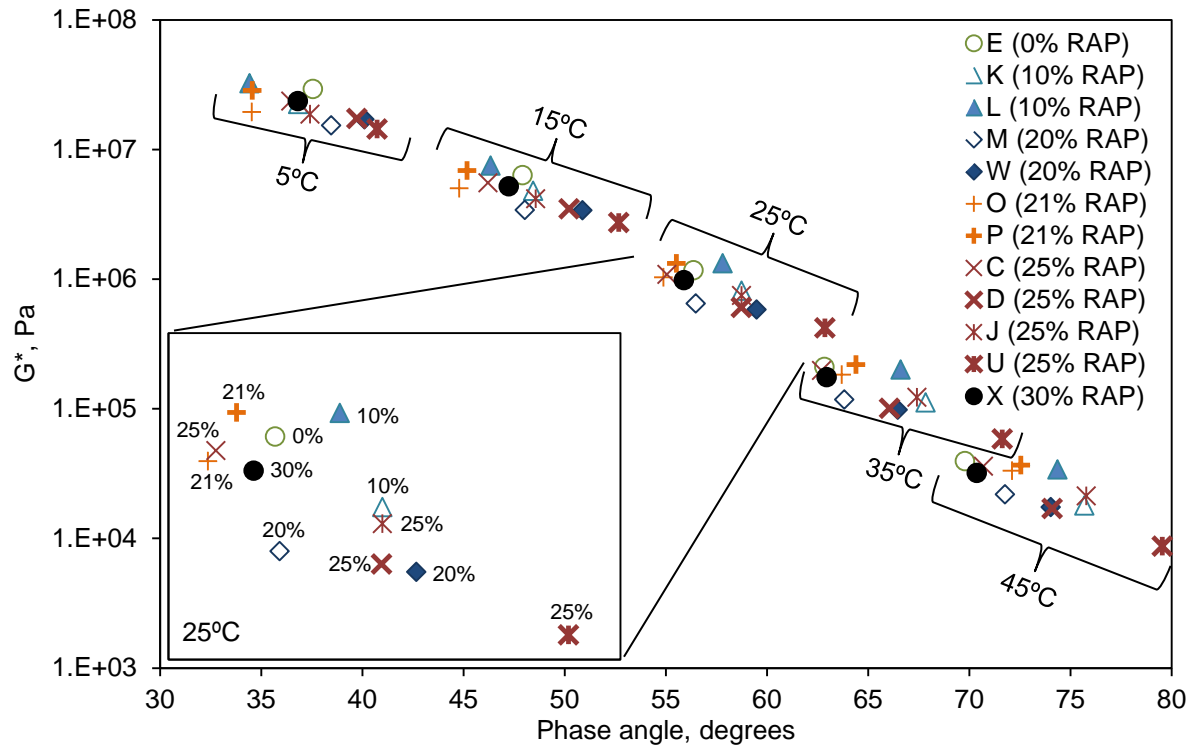


Figure 22. Black Space Plot. Plot is of extracted binders from sections with mixtures having various RAP contents at a frequency of 0.09959 rad/sec and temperatures of 5°C, 15°C, 25°C, 35°C, and 45°C. The callout shows enlarged distribution of response at 25°C for clarity.

Figure 23 shows the Black Space plots for extracted binder from mixtures with varying RAP contents at temperatures from 45 to 85°C at a test frequency of 0.09959 rad/sec (0.01585 Hz) using a 25 mm plate size. Clearly it can be seen that the responses overlap more at the higher temperatures, especially at 65°C and above. By investigation of the callout in Figure 21, which shows the details of the 65°C data, it is still evident that neither the binder stiffness nor phase angle responses follow any trend with RAP content.

GPC

In an effort to investigate further the trend shown in Table 13 as it related to the stiffness levels of the top and bottom of the cores, GPC was employed to investigate the percentage of LMS in the mixture. Small samples of the binder (25 mg) were collected after recovery and after aging in the pressure aging vessel (PAV) and dissolved in tetrahydrofuran, the elution solvent for the GPC. These samples were then injected into the GPC in triplicate, and the LMS was calculated from the resultant molecular weight distribution. The percentage of LMS and failure temperatures are shown in Figure 24 for the recovered samples and in Figure 25 for the PAV-aged samples.

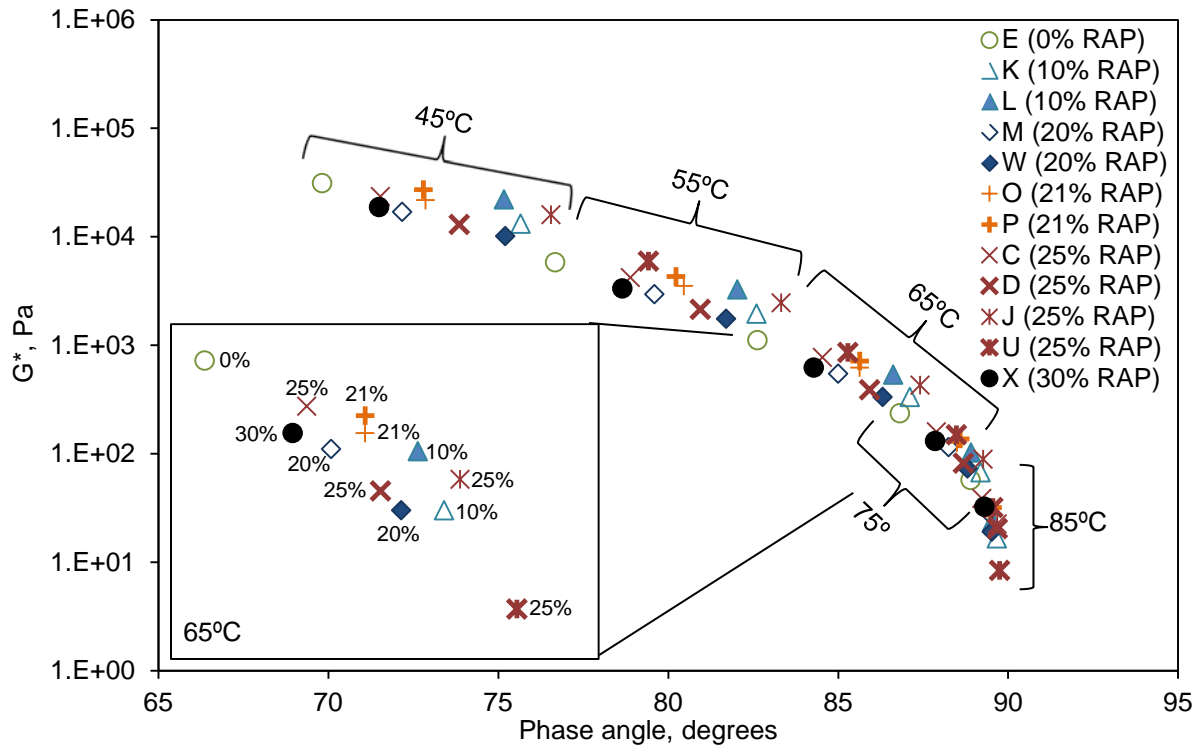


Figure 23. Black Space Plot. Plot is of extracted binders from sections with mixtures having various RAP contents at a frequency of 0.09959 rad/sec and temperatures of 45°C, 55°C, 65°C, 75°C, and 85°C. The callout shows enlarged distribution of response at 65°C.

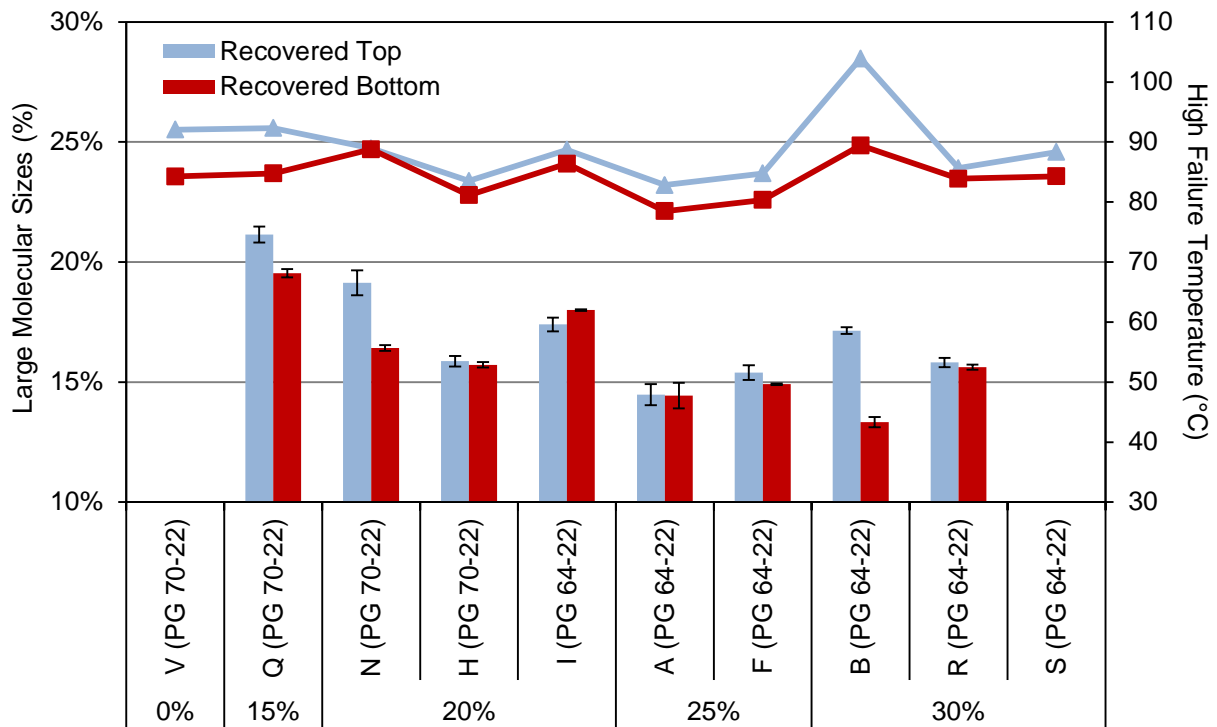


Figure 24. LMS and Failure Temperature for Recovered Binders. Bars indicate LMS values, and lines indicate failure temperature. Error bars indicate 1 standard deviation. Recovered LMS values were not available for Samples V and S. LMS = large molecular sizes.

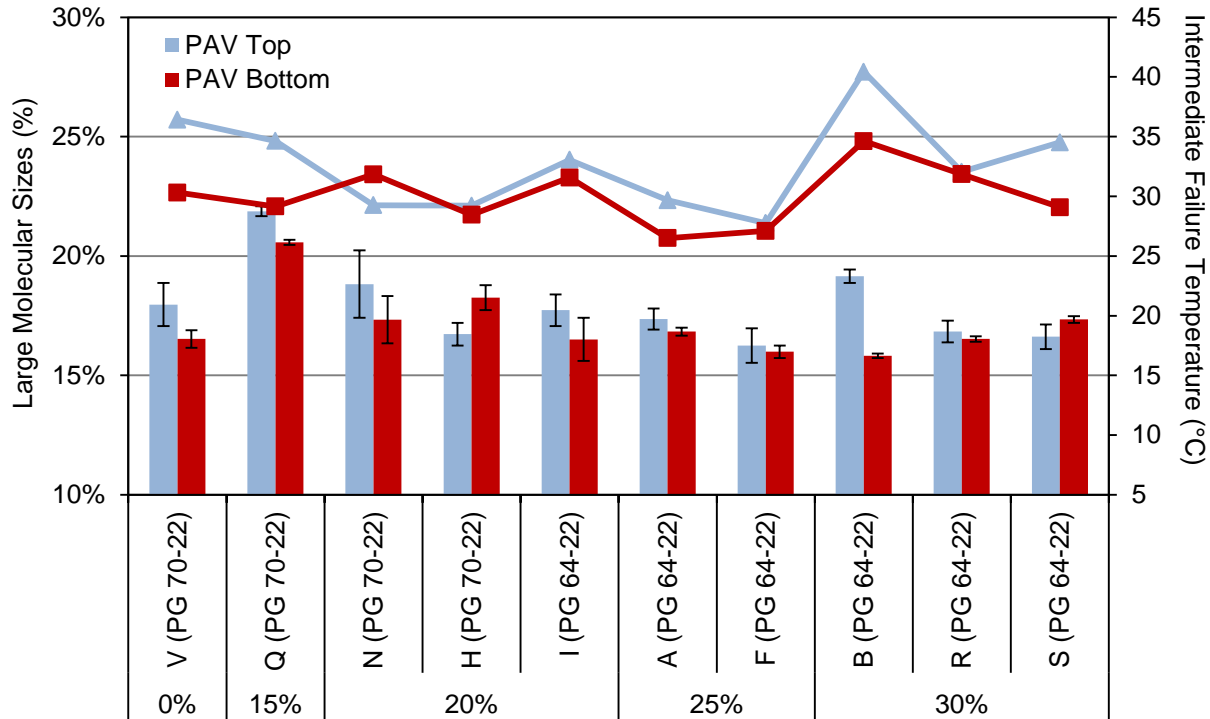


Figure 25. LMS and Failure Temperature for Recovered Binders After PAV Aging. Bars indicate LMS values, and lines indicate failure temperature. Error bars indicate 1 standard deviation. LMS = large molecular sizes.

The molecular weight distributions were generally in agreement with the trends found for failure temperatures of the binders. However, there are cases, such as that of rolling thin film oven (RTFO) Binder I and PAV Binders H and S, for which the molecular weight distributions actually show the bottom half of the core to be more highly oxidized. The failure temperature was not in agreement in these cases, showing that the top half was actually stiffer than the bottom half. However, in the case of PAV Binder N, the failure temperature grade showed that the bottom half of the core was stiffer than the top half. Overall, it was found that the top half of cores was stiffer and/or more highly oxidized than their respective bottom half.

Supplementary Analysis

Because of concerns expressed regarding the use of sites with WMA and the inclusion of RAP sites with 21% RAP, which would not be acceptable under specifications adopted since 2007, selected additional analyses were performed to assess if these sites were significantly affecting overall results. For this assessment, WMA Sites H, K, and M and RAP Sites O and P were eliminated from the dataset. The analyses included consideration of the visual survey results; dynamic modulus, RLPD, and Texas overlay test results; and binder grading information. All information and analyses are presented in Appendix G.

SUMMARY OF FINDINGS

Literature Review

- The survey of the literature indicated that few studies have been performed on long-term performance of RAP-containing mixtures.
- Case studies of pre-Superpave mixtures indicated that RAP mixtures generally performed as well as virgin mixtures.
- Test track studies of mixtures containing 45% RAP found that softer virgin binder grades may improve the performance of these mixtures.
- Test track studies of HMA and WMA mixtures containing 50% RAP found performance equivalent to that of a control virgin mixture.

Condition Data

- Visual survey data of the sites indicated that there were no significant differences ($\alpha = 0.05$) between the percentage of sites with mixtures having RAP contents $\leq 20\%$ and the percentage of sites with mixtures having RAP contents of 21% to 30% exhibiting each distress.
- Visual survey data and coring showed a number of distresses in both sets of sections: top-down and bottom-up fatigue cracking, longitudinal and transverse cracking, raveling, delamination of layers, and moisture damage in underlying layers. It should be noted that some of these distresses are not influenced by the surface mixture; rather, they are indicative of the structural condition of the underlying pavement.
- Distress data extracted from PMS indicated that most of the pavements were in acceptable ride condition and had low rut depths of less than 0.16 in. Only Sites A and B had a higher rut depth of 0.23 in.

Laboratory Analysis of Field Cores

- Air-void contents and permeability of cores were comparable between both sets of sections overall. Only one section (Section N, with a mixture having 20% RAP) did not meet design permeability requirements.
- Dynamic modulus test results indicated that neither RAP content nor virgin binder grade appeared to have discernable or trending influences on the measured modulus.
- RLPD test results on eight mixtures indicated that none of the mixtures reached tertiary flow in confined testing. Visual investigation of the slope and intercept of the secondary portion of the strain accumulation indicated a correlation between RAP content and increasing slope,

which may indicate some susceptibility to rutting related to virgin binder grade, blending and effective binder content, or test error.

- The results of the Texas overlay test showed no conclusive trends indicating that increased RAP contents positively or negatively affected mixtures.

Analysis of Extracted Binder

- Extracted binder from the top half and bottom half of cores indicated that in nearly every case, the binder extracted from the top half of the core was stiffer than that from the bottom half.
- The differences in failure temperature of binder extracted from the top half and bottom half of cores decreased with increasing RAP content.
- Comparison of binder grades determined from mixture collected during construction and from cores at 6 years of service indicated that all mixtures, regardless of RAP content, gained one to two high-temperature performance grades over the 6-year in-service period evaluated. Low-temperature grades were similarly affected, with only one section found to retain the as-constructed low-temperature grade in service.
- RAP content appeared to have an influence on the rate of aging of virgin binder–RAP blends. The difference in binder failure temperature before and after 6 to 7 years of service increased with decreasing RAP content.
- Data plots indicated that the mixtures containing less RAP aged over the 6-year period to a greater extent than those containing higher RAP contents; Sections V and Q (top half) containing 0% and 15% RAP, respectively, had the highest true grade results and the lowest RAP contents, whereas the sections with mixtures containing 25% to 30% RAP resulted in lower true grades. This may support the hypothesis that since RAP has already undergone significant aging (assuming the RAP source is from milled pavement and not from plant waste), it may not continue to stiffen and age further as extensively when reclaimed.
- Examination of the critical cracking temperatures suggested that although there are concerns about the cracking potential of the binders, these concerns are independent of the mixture RAP contents.
- Construction and comparison of binder shear modulus mastercurves indicated that the difference in the modulus between the top half and bottom half of cores was consistent irrespective of RAP content.
- Black Space analysis indicated that neither the phase angle nor the shear stiffness of the extracted binders followed any trend with respect to RAP content. This result was likely influenced by the various base binders used in the mixtures and the varying stiffness of each RAP source.

- Molecular weight distributions determined by GPC and binder failure temperatures were generally in agreement that the top half of cores was stiffer and more oxidized than the bottom half of cores.

CONCLUSIONS

- *Laboratory testing, including dynamic modulus determination, RLPD analysis, and extracted binder grading and analysis consistently showed no trends in results with RAP content. These results should not be extrapolated to RAP contents above the 30% maximum evaluated in this study.*
- *Overlay test results were influenced by more than just RAP (air-void content, etc.), and therefore no trend directly related to RAP content was shown.*
- *No trends in field performance could be determined because of the underlying structural conditions. Individual locations were found to show better or worse pavement performance, but this was attributed primarily to structural differences in the pavements and preexisting conditions. Surface deterioration observed in numerous test sections included fatigue cracking, longitudinal cracking, transverse cracking, raveling, and potholes.*
- *Binder analysis indicated that depth within a layer (in this case, top half versus bottom half) significantly affects binder properties, with stiffness decreasing with depth. However, increasing RAP contents appeared to mitigate the differences between the top half and bottom half of layers, possibly because of the preexisting aged composition of the RAP and its influence on the virgin binder properties.*

RECOMMENDATIONS

1. *VDOT's Material Division should not make any changes to the allowance of RAP contents of up to 30% as currently specified.*
2. *VDOT's Materials Division and the Virginia Transportation Research Council (VTRC) should continue to evaluate the use of RAP contents to assess the potential for performance and economic benefits. This effort should include evaluating potential ways to make these mixtures more durable and longer lasting; this may include investigating current and emerging technologies such as softer binder grades or rejuvenating agents. This work should be performed using plant-produced material placed to evaluate actual production, construction, and in-service performance. Accelerated performance testing of these mixtures would be appropriate.*
3. *VDOT's Materials Division and VTRC should further investigate the causes and solutions to the structural issues observed in this study such as layer debonding and moisture damage. Although this study did not target these deficiencies, they were widely observed and indicate a need for attention.*

BENEFITS AND IMPLEMENTATION

Benefits

The benefit of implementing Recommendation 1 is that the use of RAP will continue as currently permitted in the specifications. No changes to practice are necessary.

The benefit of implementing Recommendation 2 is that it will provide VDOT with the most current feasible options for improving mixture durability. Techniques and technologies are continually evolving to improve mixture durability while using RAP for economic and environmental benefits; without continued attention to this emerging area, VDOT may miss opportunities to improve mixture durability and realize cost savings.

The benefit of implementing Recommendation 3 is that if structural issues can be addressed or mitigated through optimized maintenance treatments and rehabilitation efforts, lifetime cost savings can be achieved.

Implementation

With regard to Recommendation 1, VDOT's Materials Division will make no changes to VDOT's specifications regarding the use of RAP contents up to 30% based on the outcomes of this study.

With regard to Recommendation 2, VTRC, with the assistance of the Materials Division, will continue to evaluate the use of RAP contents to assess the potential for performance and economic benefits. This will be accomplished through a combination of current work to evaluate the feasibility of RAP contents greater than 30% and a currently proposed project to assess the use of rejuvenators. As appropriate, when additional opportunities are identified to assess new advancements in the use of RAP, additional work will be proposed through VTRC's Asphalt Research Advisory Committee.

With regard to Recommendation 3, the Materials Division has been addressing tack issues that affect delamination with the support of VTRC.

ACKNOWLEDGMENTS

The authors thank Troy Deeds and Donnie Dodds, of VTRC, and Samuel Deloach, Ben Earl, Ken Elliton, Shane Moomaw, and Kim Snead, formerly of VTRC, for their outstanding efforts in sample collection and testing. In addition, the assistance of Andrew Wallis, formerly of the University of Virginia, in compiling visual survey data is acknowledged. Appreciation is also extended to Linda Evans of VTRC for her editorial assistance. The authors are also appreciative of the project's technical review panel for their expertise and guidance: Bill Bailey, Rob Crandol, Raja Shekharan, Bryan Smith, Alex Teklu, Chaz Weaver, and Mike Wells of VDOT; Brian Diefenderfer of VTRC; and Trenton Clark of the Virginia Asphalt Association.

REFERENCES

- Al-Azri, N.A., S.H. Jung, K.M. Lunsford, A. Ferry, J.A. Bullin, R.R. Davison, and C.J. Glover. Binder Oxidative Aging in Texas Pavements: Hardening Rates, Hardening Susceptibilities, and Impact of Pavement Depth. *Transportation Research Record: Journal of the Transportation Research Board*, No. 1962, 2006, pp. 12-20.
- Al-Khateeb, G., X. Qi, A. Shenoy, K. Stuart, and T. Mitchell. Assessment of Aging at FHWA's Pavement Testing Facility. *Transportation Research Record: Journal of the Transportation Research Board*, No. 1940, 2005, pp. 146-155.
- American Association of State Highway and Transportation Officials. *Standard Specifications for Transportation Materials and Methods of Sampling and Testing, 33rd Edition, and AASHTO Provisional Standards*. Washington, DC, 2014.
- Anderson, E.D., and J.S. Daniel. Long-Term Performance of Pavement With High Recycled Asphalt Content: Case Studies. *Transportation Research Record: Journal of the Transportation Research Board*, No. 2371, 2013, pp. 1-12.
- Anderson, R.M., G.N. King, D.I. Hanson, and P.B. Blankenship. Evaluation of the Relationship Between Asphalt Binder Properties and Non-Load Related Cracking. *Journal of the Association of Asphalt Paving Technologists*, Vol. 80, 2011, pp. 615-663.
- Apeageyi, A.K., B.K. Diefenderfer, and S.D. Diefenderfer. Rutting Resistance of Asphalt Concrete Mixtures That Contain Recycled Asphalt Pavement. *Transportation Research Record: Journal of the Transportation Research Board*, No. 2208, 2011, pp. 9-16.
- Bowers, B.F., Diefenderfer, B.K., and Diefenderfer, S.D. Evaluation of Dynamic Modulus in Asphalt Paving Mixtures Utilizing Small-Scale Specimen Geometries. *Journal of the Association of Asphalt Paving Technologists*, Vol. 84, 2015a, pp. 497-526.
- Bowers, B.F., B. Huang, X. Shu, and B.C. Miller. Investigation of Reclaimed Asphalt Pavement Blending Efficiency Through GPC and FTIR. *Construction and Building Material*, Vol. 50, No. 15, 2014, pp. 517-523.
- Bowers, B.F., J. Moore, B. Huang, and X. Shu. Blending Efficiency of Reclaimed Asphalt Pavement: An Approach Utilizing Rheological Properties and Molecular Weight Distributions. *FUEL*, Vol. 135, 2015b, pp. 63-68.
- Christensen, D.W., Jr., and Anderson, D.A. Interpretation of Dynamic Mechanical Test Data for Paving Grade Asphalt Cements. *Journal of the Association of Asphalt Paving Technologists*, Vol. 61, 1992, pp. 67-117.
- Copeland, A. *Reclaimed Asphalt Pavement in Asphalt Mixtures: State of the Practice*. FHWA-HRT-11-021. Federal Highway Administration, Washington, DC, 2011.

- Decker, D. Hot-Mix Recycling: State of the Practice. *Journal of the Association of Asphalt Paving Technologists*, Vol. 66, 1997, pp. 704-722.
- Doh, Y.S., S.N. Amirkhanian, and K.W. Kim. Analysis of Unbalanced Binder Oxidation Level in Recycled Asphalt Mixture Using GPC. *Construction and Building Materials*, Vol. 22, No.6, 2008, pp. 1253-1260.
- Glover C.J., A.E. Martin, A. Chowdhury, R. Han, N. Prapaitrakul, X. Jin, and J. Lawrence. *Evaluation of Binder Aging and Its Influence in Aging of Hot Mix Asphalt Concrete: Literature Review and Experimental Design*. FHWA/TX-08/0-6009-1. Texas Department of Transportation, Austin, 2008.
- Glover, C.J., R. Han, X. Jin, N. Prapaitrakul, Y. Cui, A. Rose, J.J. Lawrence, M. Padigala, E. Arambula, E.S. Park, and A. Epps Martin. *Evaluation of Binder Aging and Its Influence in Aging of Hot Mix Asphalt Concrete: Technical Report*. FHWA/TX-14/0-6009-2. Texas Department of Transportation, Austin, 2014.
- Hansen, K.E., and D.E. Newcomb. *Asphalt Pavement Mix Production Survey on Reclaimed Asphalt Pavement, Reclaimed Asphalt Shingles, and Warm-Mix Asphalt Usage: 2009-2010*. Information Series 138. National Asphalt Pavement Association, Lanham, MD, 2011.
- Kandhal, P. Recycling of Asphalt Pavements: An Overview. *Journal of the Association of Asphalt Paving Technologists*, Vol. 66, 1997, pp. 686-703.
- Khosravifar, S., I. Haider, Z. Afsharikia, and C.W. Schwartz. Application of Time-Temperature Superposition to Develop Master Curves of Cumulative Plastic Strain in Repeated Load Permanent Deformation Tests. *International Journal of Pavement Engineering*, Vol. 16, No. 3, 2015, pp. 214-223.
- Kim, K.W., K. Kim, Y.S. Dog, and S.N. Amirkhanian. Estimation of RAP's Binder Viscosity Using GPC Without Binder Recovery. *Journal of Materials in Civil Engineering*, Vol. 18, No. 4, 2006, pp. 1253-1260.
- Lee, S.J., S.N. Amirkhanian, and K. Shatanawi. Effects of Reaction Time on Physical and Chemical Properties of Rubber-modified Binders. *International Rubber Conference 2006, Compendium of Papers CD-ROM*, Lyon, France, May 16-18, 2006.
- Li, X., and N. Gibson. Using Small Scale Specimens for AMPT Dynamic Modulus and Fatigue Tests. *Journal of the Association of Asphalt Paving Technologists*, Vol. 82, 2013, pp. 579-615.
- Maupin, G.W., Jr., S.D. Diefenderfer, and J.S. Gillespie. *Evaluation of Using Higher Percentages of Recycled Asphalt Pavement in Asphalt Mixes in Virginia*. VTRC 08-R22. Virginia Transportation Research Council, Charlottesville, 2008.

- McDaniel, R., and R.M. Anderson. *NCHRP Report 452: Recommended Use of Reclaimed Asphalt Pavement in the Superpave Mix Design Method: Technician's Manual*. Transportation Research Board, Washington, DC, 2001.
- McDaniel, R.S., and A. Shah. Use of Reclaimed Asphalt Pavement Under Superpave Specifications. *Journal of the Association of Asphalt Paving Technologists*, Vol. 72, 2003, pp. 226-252.
- Miller, J.S., and W.Y. Bellinger. *Distress Identification Manual for the Long Term Pavement Performance Program (Fourth Revised Edition)*. FHWA-RD-03-031. Federal Highway Administration, Washington, DC, 2003.
- National Cooperative Highway Research Program. *Recommended Use of Reclaimed Asphalt Pavement in the Superpave Mix Design Method: Guidelines*. NCHRP Research Results Digest No. 253. Transportation Research Board, Washington, DC, 2001.
- Reinke, G., Hanz, A., Anderson, R.M., Ryan, M., Engber, S., and Herlitzka, D. *Impact of Re-refined Engine Oil Bottoms on Binder Properties and Mix Performance on Two Pavements in Minnesota*. 6th Eurasphalt & Eurobitume Congress, Prague, Czech Republic, 2016.
- Rowe, G.M. Prepared Discussion for Paper by Anderson et al.: Evaluation of the Relationship Between Asphalt Binder Properties and Non-Load Related Cracking. *Journal of the Association of Asphalt Paving Technologists*, Vol. 80, 2011, pp. 649-662.
- Texas Department of Transportation. *Test Procedure for Overlay Test Tex-248-F. Effective Dates: January 2009–October 2013*. 2009. http://ftp.dot.state.tx.us/pub/txdot-info/cst/TMS/200-F_series/archives/248-80109.pdf. Accessed August 2, 2015.
- Virginia Department of Transportation. *Road and Bridge Specifications*. Richmond, 2007.
- Virginia Department of Transportation. Separate-Cover Contract Documents: Special Provision Copied Notes, Special Provisions, and Supplemental Specifications for Plant Mix Schedules—Statewide. 2013 Paving Season. Volume 2 (F) 2013 PM-10-22-12 Rev. 09-07-12. Richmond, 2012.
- Virginia Department of Transportation. Mileage Tables—The State Highway Systems. 2013. http://www.virginiadot.org/VDOT/Projects/asset_upload_file789_5535.pdf. Accessed December 8, 2014.
- Virginia Department of Transportation. Virginia Test Methods. 2014. <http://www.virginiadot.org/business/resources/Materials/bu-mat-VTMs.pdf>. Accessed May 19, 2015.

- Von Quintus, H.L., J. Mallela, R. Bonaquist, C.W. Schwartz, and R.L. Carvalho. *NCHRP Report 719: Calibration of Rutting Models for Structural and Mix Design*. Transportation Research Board, Washington, DC, 2012.
- West, R., J. Michael, R. Turochy, and S. Maghsoodloo. Use of Data From Specific Pavement Studies Experiment 5 in the Long-Term Pavement Performance Program to Compare Virgin and Recycled Asphalt Pavements. *Transportation Research Record: Journal of the Transportation Research Board*, No. 2208, 2011, pp. 82-89.
- West, R., D. Timms, J.R. Willis, B. Powell, N. Tran, D. Watson, M. Sakhaeifar, R. Brown, M. Robbins, A. Vargas-Nordbeck, F. Villacorta, X. Guo, and J. Nelson. *Phase IV NCAT Pavement Test Track Findings*. NCAT Report 12-10. National Center for Asphalt Technology, Auburn, 2012.
- West, R.C., J.R. Willis, and M. Marasteanu. *NCHRP Report 752: Improved Mix Design, Evaluation, and Materials Management Practices for Hot-Mix Asphalt with High Reclaimed Asphalt Pavement Content*. Transportation Research Board, Washington, DC, 2013.
- Willis, J.R., P. Turner, G. Julian, A. Taylor, N. Tran, and F. Padula. *Effects of Changing Virgin Binder Grade and Content on RAP Mixture Properties*. NCAT Report 12-03. National Center for Asphalt Technology, Auburn, 2012.
- Woo, W.J., A. Chowdhury, and C.J. Glover. Field Aging of Unmodified Asphalt Binder in Three Texas Long-Term Performance Pavements. *Transportation Research Record: Journal of the Transportation Research Board*, No. 2051, 2008, pp. 15-22.
- Zhao, S., B.F. Bowers, B. Huang, and X. Shu. Characterizing Rheological Properties of Binder and Blending Efficiency of Asphalt Paving Mixtures Containing RAS Through GPC. *Journal of Materials in Civil Engineering*, Vol. 26, No. 5, 2014, pp. 941-946.

APPENDIX A
MIX DESIGNS

Table A1. Job Mix 4047-739 Used in Sections A and B

Mix Information		
Plant Type	Drum Mix Plant	
Job Mix ID	4047-739	
Mix Type	SM-12.5D	
Asphalt Content	5.60%	
Asphalt Type	PG 64-22	
Volumetric Data		
VTM	-	
VMA	-	
VFA	-	
FA Ratio	-	
P _{be}	-	
G _{mm}	-	
Sieve Data		
Sieve	Percent Passing	
19.0 mm (3/4 in)	100.0%	
12.5 mm (1/2 in)	96.0%	
9.5 mm (3/8 in)	89.0%	
2.36 mm (No. 8)	46.0%	
0.075 mm (No. 200)	6.5%	
Aggregate Information		
Size	Type	Percent
No. 29	Granite	60%
Recycled 1/2 in	Recycled	25%
Sand	Sand	15%

Table A2. Job Mix 4047-738 Used in Section B

Mix Information	
Plant Type	Drum Mix Plant
Job Mix ID	4047-739
Mix Type	IM-19.0D
Asphalt Content	5.00%
Asphalt Type	PG 64-22

Volumetric Data	
VTM	-
VMA	-
VFA	-
FA Ratio	-
P _{be}	-
G _{mm}	-

Sieve Data	
Sieve	Percent Passing
25.0 mm (1 in)	100.0%
19.0 mm (3/4 in)	96.0%
12.5 mm (1/2 in)	77.0%
2.36 mm (No. 8)	34.0%
0.075 mm (No. 200)	5.0%

Aggregate Information		
Size	Type	Percent
No. 68	Granite	50%
Recycled 1/2 in	Recycled	30%
Sand	Sand	20%

Table A3. Job Mix 4015-722 Used in Sections C and D

Mix Information		
Plant Type	Drum Mix Plant	
Job Mix ID	4015-722	
Mix Type	SM-12.5D	
Asphalt Content	5.50%	
Asphalt Type	PG 64-22	
Volumetric Data		
VTM	-	
VMA	-	
VFA	-	
FA Ratio	-	
P _{be}	-	
G _{mm}	-	
Sieve Data		
Sieve	Percent Passing	
19.0 mm (3/4 in)	100.0%	
12.5 mm (1/2 in)	96.0%	
9.5 mm (3/8 in)	89.0%	
2.36 mm (No. 8)	41.0%	
0.075 mm (No. 200)	5.0%	
Aggregate Information		
Size	Type	Percent
No. 8	Granite	42%
Recycled 1/2 in	Recycled	25%
No. 10 Screenings	Screenings	15%
Sand	Sand	10%
No. 10 Screenings	Screenings	8%

Table A4. Job Mix 4047-608 Used in Section E

Mix Information		
Plant Type	Drum Mix Plant	
Job Mix ID	4047-608	
Mix Type	SM-9.5D	
Asphalt Content	5.60%	
Asphalt Type	PG 70-22	
Volumetric Data		
VTM	-	
VMA	-	
VFA	-	
FA Ratio	-	
P _{be}	-	
G _{mm}	-	
Sieve Data		
Sieve	Percent Passing	
12.5 mm (1/2 in)	100.0%	
9.5 mm (3/8 in)	94.0%	
4.75 mm (No. 4)	69.0%	
2.36 mm (No. 8)	51.0%	
0.075 mm (No. 200)	5.5%	
Aggregate Information		
Size	Type	Percent
Top Size 1/2 in (No. 28)	Granite	70%
Sand	Sand	20%
Recycled 1/2 in	Recycled	10%

Table A5. Job Mix 3007-2007-15 Used in Section F

Mix Information	
Plant Type	Drum Mix Plant
Job Mix ID	3014-2007-15
Mix Type	SM-9.5D
Asphalt Content	5.50%
Asphalt Type	PG 64-22

Volumetric Data	
VTM	3.9%
VMA	15.7%
VFA	75.2%
FA Ratio	-
P _{be}	-
G _{mm}	2.598

Sieve Data	
Sieve	Percent Passing
12.5 mm (1/2 in)	100.0%
9.5 mm (3/8 in)	94.0%
4.75 mm (No. 4)	58.0%
2.36 mm (No. 8)	44.0%
0.075 mm (No. 200)	4.8%

Aggregate Information		
Size	Type	Percent
No. 8	Greenstone	43%
Recycled 1/2 in	Recycled	25%
Sand	Sand	22%
Sand	Greenstone	10%

Table A6. Job Mix 7008-200615 Used in Sections H and I

Mix Information		
Plant Type	Drum Mix Plant	
Job Mix ID	7008-200615	
Mix Type	SM-9.5A	
Asphalt Content	5.50%	
Asphalt Type	PG 64-22	
Volumetric Data		
VTM	-	
VMA	-	
VFA	-	
FA Ratio	-	
P _{bc}	-	
G _{mm}	-	
Sieve Data		
Sieve	Percent Passing	
12.5 mm (1/2 in)	100.0%	
9.5 mm (3/8 in)	92.0%	
4.75 mm (No. 4)	60.0%	
2.36 mm (No. 8)	43.0%	
0.075 mm (No. 200)	5.7%	
Aggregate Information		
Size	Type	Percent
No. 8	Silstone	43%
Sand	Sand	16%
No. 10 Screenings	Granite	15%
No. 10 Screenings	Silstone	14%
Recycled 1/2 in	Recycled	12%

Table A7. Job Mix 4015-719 Used in Section J

Mix Information	
Plant Type	Drum Mix Plant
Job Mix ID	4015-719
Mix Type	SM-9.5A
Asphalt Content	5.87%
Asphalt Type	PG 64-22

Volumetric Data	
VTM	-
VMA	-
VFA	-
FA Ratio	-
P _{be}	-
G _{mm}	-

Sieve Data	
Sieve	Percent Passing
12.5 mm (1/2 in)	100.0%
9.5 mm (3/8 in)	96.0%
4.75 mm (No. 4)	63.0%
2.36 mm (No. 8)	44.0%
0.075 mm (No. 200)	5.0%

Aggregate Information		
Size	Type	Percent
No. 8	Granite	35%
No. 10 Screenings	Screenings	25%
Recycled 1/2 in	Recycled	25%
Sand	Sand	10%

Table A8. Job Mix 48012-612 Used in Sections K and L

Mix Information		
Plant Type	Batch Plant	
Job Mix ID	4015-722	
Mix Type	SM-12.5A	
Asphalt Content	5.20%	
Asphalt Type	PG 64-22	
Volumetric Data		
VTM	3.3%	
VMA	-	
VFA	-	
FA Ratio	-	
P _{be}	-	
G _{mm}	-	
Sieve Data		
Sieve	Percent Passing	
19.0 mm (3/4 in)	100.0%	
12.5 mm (1/2 in)	96.0%	
9.5 mm (3/8 in)	86.0%	
2.36 mm (No. 8)	34.0%	
0.075 mm (No. 200)	6.0%	
Aggregate Information		
Size	Type	Percent
No. 78	Granite	35%
No. 8	Granite	23%
No. 10 Screenings	Limestone	17%
Sand	Sandstone	14%
Recycled 1/2 in	Recycled	10%
0	Hydrated Lime	1%

Table A9. Job Mix 5011-200610 Used in Sections M and N

Mix Information		
Plant Type	Drum Mix Plant	
Job Mix ID	4015-719	
Mix Type	SM-9.5A	
Asphalt Content	5.87%	
Asphalt Type	PG 64-22	
Volumetric Data		
VTM	3.6%	
VMA	16.2%	
VFA	77.8%	
FA Ratio	0.90	
P _{be}	5.5%	
G _{mm}	2.475	
Sieve Data		
Sieve	Percent Passing	
12.5 mm (1/2 in)	100.0%	
9.5 mm (3/8 in)	93.0%	
4.75 mm (No. 4)	61.0%	
2.36 mm (No. 8)	44.0%	
0.075 mm (No. 200)	5.0%	
Aggregate Information		
Size	Type	Percent
Top Size 1/2 in (No. 28)	Granite	29%
No. 8	Granite	26%
Sand	Sand	25%
Recycled 1/2 in	Recycled	20%

Table A10. Job Mix 3007-2007-18 Used in Sections O and P

Mix Information		
Plant Type	Drum Mix Plant	
Job Mix ID	3005-2007-06	
Mix Type	SM-9.5D	
Asphalt Content	5.90%	
Asphalt Type	PG 64-22	
Volumetric Data		
VTM	3.8%	
VMA	15.8%	
VFA	74.6%	
FA Ratio	1.10	
P _{bc}	5.3%	
G _{mm}	2.436	
Sieve Data		
Sieve	Percent Passing	
12.5 mm (1/2 in)	100.0%	
9.5 mm (3/8 in)	94.0%	
4.75 mm (No. 4)	63.0%	
2.36 mm (No. 8)	46.0%	
0.075 mm (No. 200)	5.8%	
Aggregate Information		
Size	Type	Percent
No. 8	Granite	40%
No. 10 Screenings	Granite	27%
Recycled 1/2 in	Recycled	21%
Sand	Sand	12%

Table A11. Job Mix 2025-200531 Used in Section Q

Mix Information	
Plant Type	Drum Mix Plant
Job Mix ID	2025-200531
Mix Type	SM-9.5D
Asphalt Content	5.87%
Asphalt Type	PG 70-22

Volumetric Data	
VTM	3.5%
VMA	15.3%
VFA	80.0%
FA Ratio	1.08
P _{be}	5.5%
G _{mm}	2.466

Sieve Data	
Sieve	Percent Passing
12.5 mm (1/2 in)	100.0%
9.5 mm (3/8 in)	90.0%
4.75 mm (No. 4)	57.0%
2.36 mm (No. 8)	38.0%
0.075 mm (No. 200)	6.0%

Aggregate Information		
Size	Type	Percent
No. 8	Quartzite	45%
No. 10 Screenings	Quartzite	25%
Recycled 1/2 in	Recycled	15%
Sand	Sand	15%

Table A12. Job Mix 2065-2007-04 Used in Sections R and S

Mix Information		
Plant Type	Drum Mix Plant	
Job Mix ID	2065-2007-04	
Mix Type	SM-9.5D	
Asphalt Content	5.50%	
Asphalt Type	PG 64-22	
Volumetric Data		
VTM	3.4%	
VMA	16.0%	
VFA	78.9%	
FA Ratio	1.12	
P _{be}	5.4%	
G _{mm}	2.488	
Sieve Data		
Sieve	Percent Passing	
12.5 mm (1/2 in)	100.0%	
9.5 mm (3/8 in)	94.0%	
4.75 mm (No. 4)	58.0%	
2.36 mm (No. 8)	42.0%	
0.075 mm (No. 200)	6.0%	
Aggregate Information		
Size	Type	Percent
No. 8	Quartzite	40%
Recycled 1/2 in	Recycled	30%
Sand	Sand	17%
No. 10 Screenings	Quartzite	13%

Table A13. Job Mix 5024-200605 Used in Section T

Mix Information		
Plant Type	Drum Mix Plant	
Job Mix ID	5024-200605	
Mix Type	SM-9.5A	
Asphalt Content	5.50%	
Asphalt Type	PG 64-22	
Volumetric Data		
VTM	3.9%	
VMA	16.0%	
VFA	75.4%	
FA Ratio	1.10	
P_{be}	5.3%	
G_{mm}	2.463	
Sieve Data		
Sieve	Percent Passing	
12.5 mm (1/2 in)	100.0%	
9.5 mm (3/8 in)	96.0%	
4.75 mm (No. 4)	67.0%	
2.36 mm (No. 8)	48.0%	
0.075 mm (No. 200)	6.0%	
Aggregate Information		
Size	Type	Percent
No. 78	Granite	42%
No. 10 Screenings	Granite	29%
Sand	Sand	19%
Recycled 1/2 in	Recycled	10%

Table A14. Job Mix 3005-2007-06 Used in Section U

Mix Information		
Plant Type	Drum Mix Plant	
Job Mix ID	3005-2007-06	
Mix Type	SM-12.5D	
Asphalt Content	5.70%	
Asphalt Type	PG 64-22	
Volumetric Data		
VTM	4.0%	
VMA	16.1%	
VFA	75.0%	
FA Ratio	1.00	
P _{bc}	5.1%	
G _{mm}	2.558	
Sieve Data		
Sieve	Percent Passing	
19.0 mm (3/4 in)	100.0%	
12.5 mm (1/2 in)	96.0%	
9.5 mm (3/8 in)	86.0%	
2.36 mm (No. 8)	44.0%	
0.075 mm (No. 200)	5.1%	
Aggregate Information		
Size	Type	Percent
Sand	Aplite	30%
No. 78	Aplite	30%
Recycled 1/2 in	Recycled	25%
No. 8	Aplite	15%

Table A15. Job Mix 7017-200710 Used in Section V

Mix Information		
Plant Type	Drum Mix Plant	
Job Mix ID	7017-200710	
Mix Type	SM-9.5D	
Asphalt Content	5.70%	
Asphalt Type	PG 64-22	
Volumetric Data		
VTM	-	
VMA	-	
VFA	-	
FA Ratio	-	
P _{be}	-	
G _{mm}	-	
Sieve Data		
Sieve	Percent Passing	
12.5 mm (1/2 in)	100.0%	
9.5 mm (3/8 in)	97.0%	
4.75 mm (No. 4)	62.0%	
2.36 mm (No. 8)	44.0%	
0.075 mm (No. 200)	5.0%	
Aggregate Information		
Size	Type	Percent
No. 8	Greenstone Manufactured	48%
Manufactured Sand	Sand	25%
Sand	Sand	15%
No. 10 Screenings	Greenstone	12%

Table A16. Job Mix 4051-720 Used in Section W

Mix Information		
Plant Type	Drum Mix Plant	
Job Mix ID	4051-720	
Mix Type	SM-12.5D	
Asphalt Content	5.70%	
Asphalt Type	PG 70-22	
Volumetric Data		
VTM	4.0%	
VMA	16.1%	
VFA	75.0%	
FA Ratio	1.00	
P _{be}	5.1%	
G _{mm}	2.558	
Sieve Data		
Sieve	Percent Passing	
19.0 mm (3/4 in)	100.0%	
12.5 mm (1/2 in)	96.0%	
9.5 mm (3/8 in)	83.0%	
2.36 mm (No. 8)	40.0%	
0.075 mm (No. 200)	5.5%	
Aggregate Information		
Size	Type	Percent
No. 78	Granite	41%
No. 10 Screenings	Screenings	24%
Recycled 1/2 in	Recycled	20%
Sand	Natural Sand	15%

Table A17. Job Mix 5029-2007-04 Used in Section X

Mix Information		
Plant Type	Drum Mix Plant	
Job Mix ID	5029-2007-04	
Mix Type	SM-12.5D	
Asphalt Content	5.40%	
Asphalt Type	PG 64-22	
Volumetric Data		
VTM	3.8%	
VMA	16.2%	
VFA	76.3%	
FA Ratio	1.00	
P _{be}	5.3%	
G _{mm}	2.460	
Sieve Data		
Sieve	Percent Passing	
19.0 mm (3/4 in)	100.0%	
12.5 mm (1/2 in)	97.0%	
9.5 mm (3/8 in)	86.0%	
2.36 mm (No. 8)	45.0%	
0.075 mm (No. 200)	5.4%	
Aggregate Information		
Size	Type	Percent
No. 78	Granite	36%
Recycled 1 in	Recycled	30%
Sand	Sand	22%
No. 10 Screenings	Granite	9%
No. 8	Granite	3%

APPENDIX B

PAVEMENT MANAGEMENT SYSTEM DISTRESS DATA

Table B1. PMS Distress Data for Sections A and B, SR 6, Goochland County

Parameter	Year						
	2008	2009	2010	2011	2012	2013	2014
CCI	97	95	87	82	82	72	75
LDR	100	96	89	82	82	72	75
NDR	97	97	94	90	97	80	91
IRI	92	93	95	96	102	108	109
Rut Depth	0.05	0.07	0.1	0.12	0.16	0.21	0.23
Number of Trucks	164	164	164	119	120	121	121

CCI = Critical Condition Index; LDR = load related distress rating; NDR = non-load related distress rating; IRI = International Roughness Index.

Table B2. PMS Distress Data for Section C, CR 703, Dinwiddie County

Parameter	Year						
	2008	2009	2010	2011	2012	2013	2014
CCI			95				
LDR			95				
NDR			100				
IRI			128				
Rut Depth			0.15				
Number of Trucks			48				

CCI = Critical Condition Index; LDR = load related distress rating; NDR = non-load related distress rating; IRI = International Roughness Index.

Table B3. PMS Distress Data for Section D, SR 40, Dinwiddie County

Parameter	Year						
	2008	2009	2010	2011	2012	2013	2014
CCI	-	99	96	99	98	95	82
LDR	-	99	97	99	98	95	83
NDR	-	100	99	100	100	98	87
IRI	-	86	89	89	89	91	90
Rut Depth	-	0.06	0.12	0.1	0.12	0.13	0.12
Number of Trucks	-	78	74	62	72	67	67

CCI = Critical Condition Index; LDR = load related distress rating; NDR = non-load related distress rating; IRI = International Roughness Index.

Table B4. PMS Distress Data for Section F, SR 24, Appomattox County

Parameter	Year						
	2008	2009	2010	2011	2012	2013	2014
CCI	99	96	90	98	95	97	94
LDR	100	97	92	99	96	98	95
NDR	99	99	96	99	97	98	97
IRI	70	72	74	75	75	96	84
Rut Depth	0.09	0.11	0.09	0.09	0.09	0.1	0.12
Number of Trucks	184	184	187	190	189	160	160

CCI = Critical Condition Index; LDR = load related distress rating; NDR = non-load related distress rating; IRI = International Roughness Index.

Table B5. PMS Distress Data for Section H, SR 211, Rappahannock County

Parameter	Year						
	2008	2009	2010	2011	2012	2013	2014
CCI	85	83	92	76	77	54	52
LDR	85	83	100	76	80	54	54
NDR	98	94	92	95	85	75	65
IRI	77	78	76	78	82	81	90
Rut Depth	0.08	0.06	0.08	0.07	0.09	0.07	0.09
Number of Trucks	79	79	81	58	54	-	-

CCI = Critical Condition Index; LDR = load related distress rating; NDR = non-load related distress rating; IRI = International Roughness Index.

Table B6. PMS Distress Data for Section I, SR 211, Rappahannock County

Parameter	Year						
	2008	2009	2010	2011	2012	2013	2014
CCI	95	71	84	71	56	51	27
LDR	95	71	92	71	56	51	27
NDR	100	94	84	94	80	71	68
IRI	56	60	58	57	59	60	60
Rut Depth	0.08	0.08	0.08	0.09	0.1	0.1	0.11
Number of Trucks	79	79	81	58	54	-	-

CCI = Critical Condition Index; LDR = load related distress rating; NDR = non-load related distress rating; IRI = International Roughness Index.

Table B7. PMS Distress Data for Sections K and L, US 220, Highland County

Parameter	Year						
	2008	2009	2010	2011	2012	2013	2014
CCI	99	100	87	75	43	50	40
LDR	100	100	89	75	43	50	40
NDR	99	100	87	84	62	69	62
IRI	70	77	68	76	79	79	78
Rut Depth	0.07	0.06	0.1	0.1	0.09	0.11	0.09
Number of Trucks	30	30	31	31	16	17	17

CCI = Critical Condition Index; LDR = load related distress rating; NDR = non-load related distress rating; IRI = International Roughness Index.

Table B8. PMS Distress Data for Section N, SR 143, York County

Parameter	Year						
	2008	2009	2010	2011	2012	2013	2014
CCI	90	96	84	80	77	40	46
LDR	99	99	97	96	95	95	96
NDR	90	96	84	80	77	40	46
IRI	94	89	89	97	97	101	106
Rut Depth	0.05	0.05	0.07	0.07	0.07	0.09	0.08
Number of Trucks	149	149	75	82	82	82	82

CCI = Critical Condition Index; LDR = load related distress rating; NDR = non-load related distress rating; IRI = International Roughness Index.

Table B9. PMS Distress Data for Section O, US 29, Pittsylvania County

Parameter	Year						
	2008	2009	2010	2011	2012	2013	2014
CCI	100	92	96	98	94	92	86
LDR	100	99	97	99	98	95	87
NDR	100	93	98	99	95	95	91
IRI	71	80	75	74	74	96	75
Rut Depth	0.04	0.09	0.11	0.11	0.11	0.14	0.15
Number of Trucks	962	966	922	859	869	889	889

CCI = Critical Condition Index; LDR = load related distress rating; NDR = non-load related distress rating; IRI = International Roughness Index.

Table B10. PMS Distress Data for Section Q, US 11, Montgomery County

Parameter	Year						
	2008	2009	2010	2011	2012	2013	2014
CCI	100	99	87	91	78	89	78
LDR	100	99	91	91	79	90	79
NDR	100	100	91	99	93	95	93
IRI	82	83	84	88	86	88	90
Rut Depth	0.07	0.09	0.14	0.12	0.11	0.12	0.13
Number of Trucks	89	89	89	85	82	81	81

CCI = Critical Condition Index; LDR = load related distress rating; NDR = non-load related distress rating; IRI = International Roughness Index.

Table B11. PMS Distress Data for Section R, US 221, Floyd County

Parameter	Year						
	2008	2009	2010	2011	2012	2013	2014
CCI	100	98	87	89	67	69	61
LDR	100	98	87	90	71	70	62
NDR	100	99	96	96	79	84	82
IRI	87	92	98	96	100	101	114
Rut Depth	0.07	0.07	0.11	0.09	0.13	0.11	0.11
Number of Trucks	107	105	114	114	112	100	60

CCI = Critical Condition Index; LDR = load related distress rating; NDR = non-load related distress rating; IRI = International Roughness Index.

Table B12. PMS Distress Data for Section S, US 58, Carroll County

Parameter	Year						
	2008	2009	2010	2011	2012	2013	2014
CCI	100	97	85	89	81	78	66
LDR	100	99	86	90	84	79	66
NDR	100	97	95	96	88	90	86
IRI	94	99	105	99	103	100	113
Rut Depth	0.06	0.09	0.14	0.11	0.1	0.12	0.14
Number of Trucks	108	108	125	119	96	95	57

CCI = Critical Condition Index; LDR = load related distress rating; NDR = non-load related distress rating; IRI = International Roughness Index.

Table B13. PMS Distress Data for Section U, US 29, Nelson County

Parameter	Year						
	2008	2009	2010	2011	2012	2013	2014
CCI	93	88	95	99	98	93	93
LDR	96	88	95	99	98	93	94
NDR	93	94	98	100	99	99	96
IRI	71	71	69	70	93	92	73
Rut Depth	0.1	0.17	0.14	0.1	0.11	0.14	0.16
Number of Trucks	826	826	351	914	831	806	806

CCI = Critical Condition Index; LDR = load related distress rating; NDR = non-load related distress rating; IRI = International Roughness Index.

Table B14. PMS Distress Data for Section X, I 664, Chesapeake County

Parameter	Year						
	2008	2009	2010	2011	2012	2013	2014
CCI	92	91	91	87	90	90	89
LDR	94	91	91	89	93	92	90
NDR	96	98	97	92	93	96	93
IRI	82	86	76	79	78	86	81
Rut Depth	0.16	0.18	0.15	0.15	0.17	0.17	0.16
Number of Trucks	2385	2461	2514	1909	2253	2197	2163

CCI = Critical Condition Index; LDR = load related distress rating; NDR = non-load related distress rating; IRI = International Roughness Index.

APPENDIX C
DYNAMIC MODULUS TEST RESULTS

Table C1. Section B Dynamic Modulus Data

Section	B	Mix Type SM-12.5D				RAP Content	25%
Specimen		B3		B4		B5	
Air Voids		6.6%		4.5%		8.2%	
Temperature	Frequency, Hz	Dynamic Modulus, MPa	Phase Angle, °	Dynamic Modulus, MPa	Phase Angle, °	Dynamic Modulus, MPa	Phase Angle, °
4.4°C	25	22028	12.84	29110	36.72	18717	3.97
	10	20595	6.49	22711	6.96	18158	4.33
	5	19561	6.89	21610	7.44	17642	4.60
	1	17093	8.17	18866	8.92	16317	5.47
	0.5	16026	8.82	17643	9.67	15726	5.89
	0.1	13591	10.59	14814	11.83	14273	7.11
21.1°C	25	12887	13.19	13862	14.37	13810	7.96
	10	11327	14.69	12105	16.06	12694	9.12
	5	10150	16.05	10762	17.53	11811	10.17
	1	7549	19.80	7825	21.48	9717	12.91
	0.5	6555	21.40	6723	23.03	8817	14.29
	0.1	4463	25.79	4441	27.19	6757	18.00
37.8°C	25	5591	24.82	5735	25.95	7132	18.58
	10	4416	26.81	4463	28.06	6016	20.76
	5	3618	28.40	3593	29.51	5177	22.63
	1	2116	31.69	2015	32.40	3421	27.24
	0.5	1645	32.32	1535	32.72	2803	28.77
	0.1	859.7	33.44	774.7	33.12	1615	32.36

Table C2. Section C Dynamic Modulus Data

Section	C	Mix Type SM-12.5D				RAP Content	25%
Specimen		C1		C9		C10	
Air Voids		6.7%		4.3%		5.3%	
Temperature	Frequency, Hz	Dynamic Modulus, MPa	Phase Angle, °	Dynamic Modulus, MPa	Phase Angle, °	Dynamic Modulus, MPa	Phase Angle, °
4.4°C	25	13222	8.86	18195	6.54	18882	6.17
	10	12014	9.62	16822	7.03	17801	6.64
	5	11083	10.26	15958	7.56	16933	7.09
	1	8968	11.83	13916	9.02	14858	8.37
	0.5	8097	12.52	13039	9.73	13949	9.03
	0.1	6220	14.08	10969	11.80	11844	10.91
21.1°C	25	5969	15.21	10374	13.72	11105	12.99
	10	4953	15.29	9075	15.22	9791	14.3
	5	4241	15.71	8127	16.52	8809	15.57
	1	2832	15.75	5990	20.01	6619	18.92
	0.5	2383	16.18	5185	21.52	5790	20.30
	0.1	1522	17.81	3522	25.38	4038	24.18
37.8°C	25	2147	20.30	4376	25.69	4843	24.23
	10	1741	22.09	3479	27.31	3900	25.96
	5	1415	23.54	2846	28.67	3229	27.31
	1	841.2	26.77	1681	31.41	1956	30.41
	0.5	675.3	28.53	1320	31.91	1549	31.06
	0.1	388.4	32.32	714.9	32.87	834.3	32.38

Table C3. Section D Dynamic Modulus Data

Section	D	Mix Type SM-12.5D				RAP Content	25%
Specimen		D4		D6		D9	
Air Voids		6.2%		7.2%		7.2%	
Temperature	Frequency, Hz	Dynamic Modulus, MPa	Phase Angle, °	Dynamic Modulus, MPa	Phase Angle, °	Dynamic Modulus, MPa	Phase Angle, °
4.4°C	25	20084	6.72	17614	7.62	17999	6.43
	10	18812	7.27	16366	8.51	16889	7.15
	5	17792	7.82	15353	9.30	15943	7.77
	1	15346	9.41	12929	11.55	13644	9.50
	0.5	14279	10.20	11863	12.68	12644	10.41
	0.1	11805	12.53	9380	15.83	10291	12.96
21.1°C	25	11294	14.75	9234	17.51	9899	14.10
	10	9771	16.52	7782	19.52	8557	16.58
	5	8633	18.05	6756	21.19	7526	18.33
	1	6183	22.25	4581	25.49	5308	22.86
	0.5	5291	23.96	3826	26.94	4510	24.62
	0.1	3426	28.65	2339	30.58	2872	29.47
37.8°C	25	4417	28.05	3273	30.52	3984	28.82
	10	3412	29.84	2472	31.52	3089	30.74
	5	2724	31.16	1923	32.38	2449	32.15
	1	1492	33.65	1028	33.09	1352	34.05
	0.5	1123	33.87	773.3	32.85	1029	33.96
	0.1	552.6	34.02	396.9	31.75	538.2	33.06

Table C4. Section E Dynamic Modulus Data

Section	E	Mix Type SM-9.5D				RAP Content	0%
Specimen		E5		E7		E9	
Air Voids		5.9%		5.9%		6.0%	
Temperature	Frequency, Hz	Dynamic Modulus, MPa	Phase Angle, °	Dynamic Modulus, MPa	Phase Angle, °	Dynamic Modulus, MPa	Phase Angle, °
4.4°C	25	22985	5.43	23230	5.02	21632	5.79
	10	21907	5.93	22172	5.46	20464	6.27
	5	20980	6.36	21303	5.87	19523	6.79
	1	18669	7.62	19105	7.04	17196	8.23
	0.5	17630	8.26	18113	7.63	16171	8.92
	0.1	15166	10.03	15771	9.25	13819	10.93
21.1°C	25	14216	11.57	14867	11.02	13140	12.47
	10	12689	13.48	13337	12.29	11571	14.04
	5	11496	14.81	12141	13.39	10380	15.40
	1	8800	18.39	9444	16.45	7719	19.27
	0.5	7715	19.99	8360	17.87	6697	20.98
	0.1	5436	24.17	6011	21.74	4549	25.44
37.8°C	25	6776	22.37	7229	21.36	6021	24.56
	10	5460	24.93	5871	23.52	4759	26.92
	5	4534	26.76	4927	25.19	3893	28.65
	1	2764	30.68	3079	29.16	2253	32.37
	0.5	2188	31.40	2466	30.29	1738	33.21
	0.1	1183	33.11	1362	32.90	896.6	34.31

Table C5. Section J Dynamic Modulus Data

Section	J	Mix Type SM-9.5D				RAP Content	25%
Specimen		J1 6.3%		J2 7.2%		J4 7.3%	
Air Voids		Dynamic	Phase	Dynamic	Phase	Dynamic	Phase
Temperature	Frequency, Hz	Modulus, MPa	Angle, °	Modulus, MPa	Angle, °	Modulus, MPa	Angle, °
4.4°C	25	15991	7.81	17252	7.13	18075	6.90
	10	14960	8.56	16126	7.67	16912	7.32
	5	14103	9.09	15199	8.17	16009	7.82
	1	12035	10.59	13010	9.56	13847	9.32
	0.5	11154	11.33	12089	10.28	12908	10.08
	0.1	9157	13.43	9937	12.31	10823	12.21
21.1°C	25	8796	15.54	9548	14.23	10191	14.66
	10	7657	17.04	8215	15.71	8838	16.35
	5	6787	18.31	7231	17.11	7837	17.74
	1	4875	21.84	5168	20.77	5695	21.61
	0.5	4176	23.24	4419	22.39	4907	23.11
	0.1	2743	26.99	2885	26.69	3293	27.25
37.8°C	25	3618	27.47	3812	27.42	4129	26.89
	10	2835	29.11	2956	29.18	3234	28.63
	5	2286	30.36	2374	30.60	2621	30.00
	1	1288	32.94	1309	33.29	1495	32.91
	0.5	984.7	33.24	982.5	33.70	1145	33.47
	0.1	511.7	33.61	475.3	34.26	575.8	34.43

Table C6. Section L Dynamic Modulus Data

Section	L	Mix Type SM-9.5A				RAP Content	10%
Specimen		L1		L4		L7	
Air Voids		6.9%		7.2%		7.4%	
Temperature	Frequency, Hz	Dynamic Modulus, MPa	Phase Angle, °	Dynamic Modulus, MPa	Phase Angle, °	Dynamic Modulus, MPa	Phase Angle, °
4.4°C	25	19651	5.51	15184	5.36	13085	6.77
	10	18628	5.91	14533	6.45	12641	7.85
	5	17799	6.35	13958	6.95	12212	8.67
	1	15755	7.53	12393	8.47	11030	11.89
	0.5	14830	8.18	11737	9.26	10525	13.38
	0.1	12639	10.00	10050	11.47	9205	16.24
21.1°C	25	11899	11.86	9546	13.57	9405	10.22
	10	10519	13.20	8533	14.84	8512	11.53
	5	9480	14.42	7712	16.14	7810	12.67
	1	7152	17.76	5763	19.68	6165	15.67
	0.5	6262	19.27	5039	21.18	5531	17.17
	0.1	4358	23.39	3428	25.14	4077	21.17
37.8°C	25	5198	23.76	4195	25.89	4293	27.41
	10	4168	25.87	3356	27.57	3733	26.80
	5	3437	27.38	2746	28.89	3164	27.29
	1	2046	30.13	1610	31.25	2041	30.73
	0.5	1610	30.65	1265	31.71	1676	31.48
	0.1	870.1	31.27	693.2	31.59	993	33.65

Table C7. Section M Dynamic Modulus Data

Section	M	Mix Type SM-9.5A (WMA)				RAP Content	20%
Specimen		M3		M7		M9	
Air Voids		7.7%		6.6%		7.5%	
Temperature	Frequency, Hz	Dynamic Modulus, MPa	Phase Angle, °	Dynamic Modulus, MPa	Phase Angle, °	Dynamic Modulus, MPa	Phase Angle, °
4.4°C	25	16134	7.13	18189	7.14	18789	6.81
	10	15152	7.61	17039	7.91	17595	7.3
	5	14356	8.13	16074	8.46	16666	7.77
	1	12362	9.52	13774	10.06	14426	9.07
	0.5	11519	10.23	12750	10.9	13433	9.71
	0.1	9571	12.37	10444	13.38	11198	11.74
	21.1°C	25	9231	14.26	10206	14.84	11212
10		8068	15.66	8818	16.53	9775	15.3
5		7189	16.95	7803	17.99	8684	16.74
1		5301	20.38	5598	21.9	6350	20.63
0.5		4577	21.86	4778	23.57	5461	22.26
0.1		3098	25.84	3113	27.9	3637	26.79
37.8°C		25	3840	26.06	4045	28.11	4595
	10	3043	27.67	3150	29.85	3582	28.77
	5	2489	29.01	2535	31.17	2897	30.25
	1	1473	31.63	1435	33.73	1660	33.46
	0.5	1162	32.25	1109	34.12	1291	34.11
	0.1	632.8	33.31	581.9	34.45	685.1	35.15

Table C8. Section N Dynamic Modulus Data

Section	N	Mix Type SM-9.5A				RAP Content	20%
Specimen		N6 10.1%		N7 8.7%		N10 8.4%	
Air Voids		Dynamic	Phase	Dynamic	Phase	Dynamic	Phase
Temperature	Frequency, Hz	Modulus, MPa	Angle, °	Modulus, MPa	Angle, °	Modulus, MPa	Angle, °
4.4°C	25	16699	6.27	16060	7.37	16060	7.37
	10	15702	6.90	15012	8.03	15012	8.03
	5	14882	7.52	14160	8.57	14160	8.57
	1	12901	9.14	12165	10.14	12165	10.14
	0.5	12058	9.96	11335	10.89	11335	10.89
	0.1	10072	12.26	9434	13.03	9434	13.03
21.1°C	25	9695	14.44	8849	15.02	8849	28.24
	10	8427	16.15	7669	16.72	7669	30.04
	5	7480	17.67	6785	18.23	6785	31.49
	1	5398	21.84	4888	22.26	4888	34.01
	0.5	4621	23.54	4189	23.90	4189	34.31
	0.1	3023	27.96	2771	28.09	2771	34.21
37.8°C	25	3922	28.07	3518	28.24	3518	28.24
	10	3028	30.08	2725	30.04	2725	30.04
	5	2422	31.64	2179	31.49	2179	31.49
	1	1346	34.41	1224	34.01	1224	34.01
	0.5	1028	34.77	939	34.31	939	34.31
	0.1	521.7	35.00	483.2	34.21	483.2	34.21

Table C9. Section O Dynamic Modulus Data

Section	O	Mix Type SM-9.5D				RAP Content	21%
Specimen		2		0		0	
Air Voids		5.8%		5.6%		6.3%	
Temperature	Frequency, Hz	Dynamic Modulus, MPa	Phase Angle, °	Dynamic Modulus, MPa	Phase Angle, °	Dynamic Modulus, MPa	Phase Angle, °
4.4°C	25	19782	5.64	20082	6.19	18805	5.99
	10	18703	6.16	18944	6.74	17589	7.28
	5	17807	6.63	18033	7.27	16574	7.84
	1	15606	7.95	15826	8.79	14135	9.36
	0.5	14609	8.63	14844	9.56	13089	10.09
	0.1	12287	10.52	12582	11.7	10718	12.05
21.1°C	25	11706	13.10	11975	13.54	10326	15.09
	10	10236	14.58	10554	15.15	8852	16.66
	5	9147	15.96	9457	16.53	7771	18.07
	1	6731	19.61	7020	20.12	5489	21.68
	0.5	5822	21.16	6099	21.51	4671	23.12
	0.1	3920	25.22	4150	25.20	3023	26.94
37.8°C	25	4874	25.22	5290	25.77	3927	27.48
	10	3836	27.23	4199	27.38	3030	29.44
	5	3116	28.78	3426	28.68	2410	30.79
	1	1804	31.83	2017	31.35	1335	33.56
	0.5	1408	32.39	1580	31.78	1020	34.03
	0.1	757.5	33.32	850.9	32.68	527.1	35.18

Table C10. Section P Dynamic Modulus Data

Section	P	Mix Type SM-9.5D				RAP Content	21%
Specimen		P1 7.3%		P6 7.2%		P8 7.6%	
Air Voids		Dynamic	Phase	Dynamic	Phase	Dynamic	Phase
Temperature	Frequency, Hz	Modulus, MPa	Angle, °	Modulus, MPa	Angle, °	Modulus, MPa	Angle, °
4.4°C	25	17325	6.65	19703	6.44	19760	5.98
	10	16256	7.52	18574	6.92	18668	6.40
	5	15358	8.13	17683	7.31	17788	6.76
	1	13179	9.78	15553	8.40	15725	7.80
	0.5	12210	10.66	14620	8.97	14806	8.38
	0.1	9984	13.10	12439	10.72	12693	9.94
21.1°C	25	9451	15.40	11384	13.18	11577	12.73
	10	8110	17.14	9992	14.63	10216	14.03
	5	7124	18.56	8949	15.92	9203	15.17
	1	5029	22.23	6680	19.52	6961	18.53
	0.5	4273	23.58	5816	21.09	6089	19.91
	0.1	2753	26.99	3995	25.27	4284	23.90
37.8°C	25	3619	28.46	4806	25.45	4898	24.63
	10	2793	29.79	3812	27.33	3895	26.51
	5	2222	30.88	3134	28.75	3211	27.95
	1	1237	32.65	1852	32.00	1917	31.15
	0.5	945.6	32.80	1445	32.70	1508	31.84
	0.1	491.5	32.44	747.4	34.19	795	33.26

Table C11. Section R Dynamic Modulus Data

Section	R	Mix Type SM-9.5D				RAP Content	30%
Specimen		R4 7.0%		R6 9.3%		R9 8.3%	
Air Voids		Dynamic	Phase	Dynamic	Phase	Dynamic	Phase
Temperature	Frequency, Hz	Modulus, MPa	Angle, °	Modulus, MPa	Angle, °	Modulus, MPa	Angle, °
4.4°C	25	19388	5.81	18250	5.50	17595	5.68
	10	18319	6.22	17380	5.74	16692	5.96
	5	17493	6.60	16685	6.02	15971	6.31
	1	15511	7.70	15024	6.78	14227	7.36
	0.5	14650	8.28	14292	7.22	13458	7.93
	0.1	12575	10.13	12557	8.56	11673	9.54
21.1°C	25	11509	12.67	10899	6.93	10031	10.06
	10	10154	14.03	10494	11.67	9874	13.04
	5	9139	15.34	9595	12.68	8950	14.27
	1	6873	19.10	7579	15.60	6873	17.59
	0.5	5987	20.78	6756	17.03	6068	19.09
	0.1	4114	25.38	4945	21.05	4326	23.15
37.8°C	25	4931	25.47	5544	21.46	4978	23.12
	10	3893	27.58	4545	23.66	4033	25.10
	5	3186	29.21	3831	25.38	3344	26.78
	1	1859	32.80	2428	29.50	2020	30.64
	0.5	1440	33.59	1962	30.69	1590	31.63
	0.1	732.9	35.01	1098	33.42	831.3	33.77

Table C12. Section S Dynamic Modulus Data

Section	S	Mix Type SM-9.5D				RAP Content	30%
Specimen		S4 5.9%		S6 8.2%		S9 7.7%	
Air Voids		Dynamic	Phase	Dynamic	Phase	Dynamic	Phase
Temperature	Frequency, Hz	Modulus, MPa	Angle, °	Modulus, MPa	Angle, °	Modulus, MPa	Angle, °
4.4°C	25	20122	6.04	17598	5.81	-	-
	10	19023	6.52	16677	6.24	-	-
	5	18144	6.91	15907	6.67	-	-
	1	16013	8.10	14044	7.91	-	-
	0.5	15071	8.75	13223	8.57	-	-
	0.1	12789	10.69	11258	10.45	-	-
21.1°C	25	11938	13.17	10574	12.73	11383	12.56
	10	10448	14.71	9337	14.20	10023	14.02
	5	9336	16.12	8395	15.57	8989	15.42
	1	6889	20.18	6260	19.26	6674	19.23
	0.5	5955	21.95	5429	20.90	5770	20.89
	0.1	3965	26.87	3669	25.22	3874	25.22
37.8°C	25	4916	26.79	4583	25.58	4893	25.47
	10	3820	29.02	3615	27.52	3836	27.58
	5	3071	30.70	2946	29.08	3103	29.14
	1	1710	33.98	1711	32.25	1778	32.01
	0.5	1295	34.55	1330	32.84	1375	32.55
	0.1	635.3	34.92	692.8	33.74	722.4	33.07

Table C13. Section T Dynamic Modulus Data

Section	T	Mix Type SM-9.5A				RAP Content	10%
Specimen		T3		T4		-	-
Air Voids		6.9%		5.8%		-	-
Temperature	Frequency, Hz	Dynamic Modulus, MPa	Phase Angle, °	Dynamic Modulus, MPa	Phase Angle, °	Dynamic Modulus, MPa	Phase Angle, °
4.4°C	25	17498	8.14	19881	7.51	-	-
	10	16124	8.86	18467	8.18	-	-
	5	15038	9.54	17341	8.83	-	-
	1	12512	11.35	14701	10.59	-	-
	0.5	11441	12.27	13566	11.51	-	-
	0.1	9023	14.94	11079	14.00	-	-
21.1°C	25	8618	17.95	10375	16.45	-	-
	10	7227	19.83	8826	18.35	-	-
	5	6234	21.36	7695	19.94	-	-
	1	4212	25.43	5354	24.20	-	-
	0.5	3517	26.91	4542	25.77	-	-
	0.1	2172	30.66	2905	29.96	-	-
37.8°C	25	2922	32.41	3864	30.18	-	-
	10	2218	33.26	2953	31.67	-	-
	5	1738	34.08	2350	32.76	-	-
	1	932	35.37	1287	34.87	-	-
	0.5	703.3	35.23	980.5	34.89	-	-
	0.1	349.1	35.25	489.8	34.64	-	-

Table C14. Section U Dynamic Modulus Data

Section U		Mix Type SM-9.5D				RAP Content 25%	
Specimen		U1 6.1%		U3 6.0%		U7 7.2%	
Air Voids							
Temperature	Frequency, Hz	Dynamic Modulus, MPa	Phase Angle, °	Dynamic Modulus, MPa	Phase Angle, °	Dynamic Modulus, MPa	Phase Angle, °
4.4°C	25	15667	7.24	15276	8.44	13401	8.43
	10	14399	8.86	14074	9.27	12307	9.02
	5	13387	9.85	13118	9.99	11426	9.58
	1	10975	12.30	10863	12.09	9379	10.97
	0.5	9953	13.61	9895	13.10	8551	11.60
	0.1	7658	16.93	7738	16.04	6699	13.03
21.1°C	25	7647	19.82	7660	18.58	6820	15.82
	10	6357	22.05	6372	20.62	5758	17.18
	5	5422	23.83	5450	22.4	4983	18.36
	1	3504	28.47	3553	26.79	3382	20.86
	0.5	2862	29.89	2899	28.38	2837	22.04
	0.1	1640	33.37	1680	32.03	1778	24.46
37.8°C	25	2449	34.93	2267	33.12	2495	27.64
	10	1809	35.29	1667	34.46	1919	28.92
	5	1358	35.68	1270	35.47	1513	29.84
	1	672.8	35.08	637.9	35.59	835.4	31.56
	0.5	492.8	34.04	464.3	34.79	641.8	31.87
	0.1	250.7	31.46	231	32.33	343.0	32.70

Table C15. Section V Dynamic Modulus Data

Section	V	Mix Type SM-9.5D				RAP Content	0%
Specimen		V1		V8		V9	
Air Voids		7.9%		7.3%		6.7%	
Temperature	Frequency, Hz	Dynamic Modulus, MPa	Phase Angle, °	Dynamic Modulus, MPa	Phase Angle, °	Dynamic Modulus, MPa	Phase Angle, °
4.4°C	25	21056	5.92	20836	5.70	20889	7.20
	10	19794	6.42	19641	6.21	19523	7.96
	5	18808	6.89	18669	6.73	18425	8.62
	1	16350	8.24	16262	8.15	15738	10.46
	0.5	15237	8.94	15170	8.87	14542	11.36
	0.1	12583	10.92	12585	10.80	11795	13.87
21.1°C	25	12143	12.94	11992	13.59	11518	15.29
	10	10568	14.41	10415	15.24	9869	17.21
	5	9376	15.64	9251	16.62	8632	18.68
	1	6756	18.83	6680	20.22	6018	22.53
	0.5	5793	20.18	5728	21.86	5087	24.08
	0.1	3811	23.62	3762	25.96	3223	27.93
37.8°C	25	4761	24.20	4702	26.34	4327	28.82
	10	3705	26.09	3641	28.40	3306	30.46
	5	2994	27.53	2924	30.00	2630	31.64
	1	1712	30.37	1646	33.10	1454	33.84
	0.5	1332	31.02	1266	33.78	1114	33.95
	0.1	706.5	32.45	659.2	34.87	585.4	33.84

Table C16. Section W Dynamic Modulus Data

Section	W	Mix Type SM-12.5D				RAP Content	25%
Specimen		W5		W6		W7	
Air Voids		5.4%		3.8%		3.8%	
Temperature	Frequency, Hz	Dynamic Modulus, MPa	Phase Angle, °	Dynamic Modulus, MPa	Phase Angle, °	Dynamic Modulus, MPa	Phase Angle, °
4.4°C	25	19768	7.11	20842	8.84	22558	7.46
	10	18407	7.69	19079	9.92	20994	8.32
	5	17298	8.26	17659	10.85	19716	9.06
	1	14597	9.82	14334	13.50	16582	11.34
	0.5	13406	10.57	12922	14.80	15230	12.47
	0.1	10646	12.62	9737	18.39	12062	15.62
21.1°C	25	10384	12.39	10210	19.9	12296	16.93
	10	8800	13.83	8377	22.25	10427	19.16
	5	7649	14.96	7090	24.12	9051	21.00
	1	5180	17.58	4474	28.94	6121	25.8
	0.5	4339	18.87	3615	30.44	5089	27.54
	0.1	2682	22.46	2025	33.77	3056	31.8
37.8°C	25	3864	24.15	3166	35.12	4355	32.32
	10	2964	26.28	2294	35.83	3267	33.90
	5	2349	28.02	1738	36.17	2538	34.83
	1	1324	31.26	870.8	35.77	1312	36.06
	0.5	1027	32.13	639.4	34.81	964.4	35.64
	0.1	554.4	34.15	315.5	32.67	464.1	34.11

Table C17. Section X Dynamic Modulus Data

Section	X	Mix Type SM-12.5D				RAP Content	25%
Specimen		X2		X5		X7	
Air Voids		5.2%		5.4%		5.1%	
Temperature	Frequency, Hz	Dynamic Modulus, MPa	Phase Angle, °	Dynamic Modulus, MPa	Phase Angle, °	Dynamic Modulus, MPa	Phase Angle, °
4.4°C	25	21052	6.26	22666	4.78	19919	3.15
	10	19815	6.79	21727	5.08	18302	7.33
	5	18821	7.31	20943	5.46	17363	7.93
	1	16419	8.84	18938	6.53	15045	9.67
	0.5	15363	9.56	18014	7.05	14029	10.55
	0.1	12867	11.62	15788	8.51	11677	12.95
21.1°C	25	12181	13.63	14945	10.41	11519	15.03
	10	10683	15.22	13477	11.53	10035	16.75
	5	9551	16.49	12330	12.55	8913	18.17
	1	7063	19.92	9687	15.30	6453	21.97
	0.5	6129	21.26	8606	16.56	5568	23.38
	0.1	4182	24.94	6291	19.85	3693	27.12
37.8°C	25	5497	26.05	7209	20.42	4868	27.37
	10	4418	27.61	5898	22.2	3816	28.97
	5	3623	29.00	4963	23.65	3085	30.19
	1	2157	32.09	3154	27.01	1748	32.56
	0.5	1702	32.56	2541	28.10	1349	32.79
	0.1	936.6	33.39	1465	30.63	704.6	32.95

APPENDIX D

DYNAMIC MODULUS STATISTICAL ANALYSIS

Table D1. *t*-test Comparisons of Mixtures at 4.4°C (40°F) and 0.1 Hz (lower left half of table) and 0.5 Hz (upper right half of table)

Section (% RAP)	E (0%)	V (0%)	K (10%)	L (10%)	T (10%)	M (20%)	N (20%)	W (20%)	O (21%)	P (21%)	B (25%)	C (25%)	D (25%)	J (25%)	U (25%)	B-IM (30%)	R (30%)	S (30%)	X (30%)
E (0%)		0.0440	0.4320	0.0438	0.0811	0.0090	0.0040	0.0207	0.0177	0.0336	0.3709	0.0793	0.0098	0.0026	0.0006	0.0058	0.0153	0.1139	0.3357
V (0%)	0.0300		0.8388	0.1744	0.2463	0.0500	0.0228	0.2445	0.2805	0.3163	0.1175	0.2108	0.0910	0.0165	0.0020	0.0003	0.1243	0.5279	0.5588
K (10%)	0.3898	0.8012		0.2630	0.2768	0.3455	0.1864	0.5049	0.5867	0.5162	0.6472	0.2300	0.3214	0.2138	0.0817	0.1740	0.5701	0.5926	0.8761
L (10%)	0.0336	0.2397	0.3719		0.9386	0.6325	0.6601	0.3812	0.2923	0.3867	0.0671	0.7802	0.7248	0.8366	0.1409	0.5661	0.2997	0.3412	0.1193
T (10%)	0.0742	0.2546	0.2843	0.7201		0.6788	0.5840	0.4062	0.3277	0.4077	0.1067	0.7273	0.7725	0.7486	0.1724	0.5118	0.3498	0.3654	0.1340
M (20%)	0.0097	0.0838	0.3910	0.8761	0.5887		0.1074	0.4077	0.1923	0.4569	0.0174	0.5246	0.8510	0.1871	0.0080	0.0771	0.1332	0.4465	0.1386
N (20%)	0.0050	0.0177	0.2374	0.4905	0.8222	0.1665		0.0776	0.0328	0.1082	0.0068	0.9994	0.2270	0.6095	0.0322	0.6718	0.0230	0.1961	0.0626
W (20%)	0.0105	0.1438	0.3934	0.8900	0.6016	0.9943	0.2595		0.7328	0.9822	0.0485	0.3606	0.4079	0.1129	0.0096	0.0696	0.7452	0.8222	0.2415
O (21%)	0.0201	0.5261	0.6541	0.3718	0.2890	0.2291	0.0527	0.3060		0.7801	0.0483	0.3034	0.2406	0.0468	0.0031	0.0291	0.9463	0.9783	0.3034
P (21%)	0.0438	0.5560	0.6171	0.4711	0.3277	0.4257	0.1425	0.4650	0.8883		0.0720	0.3598	0.4369	0.1499	0.0177	0.0972	0.7992	0.8460	0.2592
B (25%)	0.3748	0.0148	0.5451	0.0610	0.1233	0.0116	0.0032	0.0206	0.0341	0.0843		0.1083	0.0200	0.0052	0.0010	0.0090	0.0385	0.1802	0.6489
C (25%)	0.0834	0.2681	0.2825	0.6682	0.8659	0.5831	0.9698	0.5929	0.3381	0.3765	0.1160		0.5786	0.8659	0.3447	0.9200	0.3108	0.3212	0.1424
D (25%)	0.0092	0.1092	0.3356	0.9174	0.7583	0.7104	0.4187	0.7580	0.2108	0.3404	0.0188	0.6986		0.3773	0.0206	0.1738	0.2289	0.3989	0.1187
J (25%)	0.0031	0.0219	0.2604	0.6059	0.9531	0.2600	0.7294	0.3732	0.0680	0.1741	0.0028	0.8840	0.5805		0.0197	0.3867	0.0333	0.2140	0.0682
U (25%)	0.0011	0.0004	0.0952	0.0754	0.2065	0.0120	0.0174	0.0208	0.0054	0.0254	0.0001	0.3156	0.0308	0.0146		0.0335	0.0017	0.0746	0.0211
B-IM (30%)	0.0028	0.0008	0.1624	0.2191	0.4379	0.0475	0.1409	0.0835	0.0196	0.0680	0.0004	0.6789	0.1307	0.1277	0.0294		0.0068	0.2014	0.0631
R (30%)	0.0266	0.9010	0.7830	0.2499	0.2566	0.0840	0.0162	0.1524	0.5770	0.5898	0.0142	0.2748	0.1137	0.0220	0.0004	0.0011		0.9908	0.2880
S (30%)	0.0880	0.7660	0.7110	0.3583	0.2734	0.3345	0.1693	0.3396	0.8813	0.8015	0.1669	0.3168	0.2544	0.1649	0.0644	0.1162	0.8060		0.3490
X (30%)	0.3585	0.4566	0.8099	0.1555	0.1262	0.1570	0.0863	0.1526	0.3302	0.3163	0.5932	0.1604	0.1217	0.0897	0.0308	0.0570	0.4393	0.3978	

Shaded bold cells indicate significant differences at a level of significance of $\alpha = 0.05$.

Table D2. *t*-test Comparisons of Mixtures at 4.4°C (40°F) and 1.0 Hz (lower left half of table) and 5.0 Hz (upper right half of table)

Section (% RAP)	E (0%)	V (0%)	K (10%)	L (10%)	T (10%)	M (20%)	N (20%)	W (20%)	O (21%)	P (21%)	B (25%)	C (25%)	D (25%)	J (25%)	U (25%)	B-IM (30%)	R (30%)	S (30%)	X (30%)
E (0%)		0.0641	0.4878	0.0572	0.1133	0.0076	0.0027	0.0689	0.0126	0.0238	0.4918	0.0709	0.0118	0.0021	0.0007	0.0094	0.0060	0.1422	0.2754
V (0%)	0.0506		0.8384	0.1369	0.2777	0.0537	0.0384	0.6424	0.1170	0.1643	0.4866	0.1586	0.0874	0.0202	0.0086	0.0000	0.0416	0.3849	0.7330
K (10%)	0.4490	0.8463		0.1478	0.2752	0.2754	0.1246	0.7041	0.4774	0.3708	0.8123	0.1612	0.2738	0.1522	0.0591	0.1848	0.3252	0.4120	0.9959
L (10%)	0.0487	0.1591	0.2205		0.5015	0.4087	0.9429	0.1504	0.2253	0.3037	0.0772	0.9995	0.4199	0.8172	0.3491	0.6776	0.3378	0.3203	0.1002
T (10%)	0.0898	0.2536	0.2759	0.7788		0.9018	0.3701	0.2855	0.4534	0.6450	0.1379	0.5272	0.9117	0.5109	0.1440	0.6370	0.7291	0.6545	0.1825
M (20%)	0.0088	0.0465	0.3271	0.5391	0.7315		0.0619	0.1215	0.1353	0.5558	0.0982	0.4448	0.9933	0.1415	0.0151	0.1704	0.5602	0.6622	0.1153
N (20%)	0.0036	0.0267	0.1652	0.7480	0.4992	0.0876		0.0258	0.0151	0.0783	0.0380	0.9471	0.1176	0.4425	0.0800	0.2165	0.0319	0.2442	0.0384
W (20%)	0.0279	0.3129	0.5564	0.2732	0.3613	0.2733	0.0502		0.4497	0.3065	0.3793	0.1775	0.1516	0.0328	0.0051	0.0642	0.1759	0.4713	0.5617
O (21%)	0.0164	0.2160	0.5563	0.2655	0.3591	0.1802	0.0261	0.9848		0.6014	0.1953	0.2571	0.2811	0.0312	0.0042	0.0416	0.2980	0.7618	0.2681
P (21%)	0.0299	0.2519	0.4727	0.3535	0.4649	0.4848	0.0951	0.7623	0.7275		0.1375	0.3382	0.6200	0.1383	0.0146	0.1992	0.8182	0.9575	0.1885
B (25%)	0.4015	0.2204	0.6959	0.0697	0.1055	0.0346	0.0127	0.0953	0.0797	0.0801		0.0942	0.0871	0.0409	0.0121	0.0674	0.1143	0.2152	0.7349
C (25%)	0.0767	0.1913	0.2076	0.8462	0.6636	0.4945	0.9818	0.2908	0.2872	0.3510	0.1024		0.4548	0.8326	0.3844	0.7040	0.3737	0.3480	0.1210
D (25%)	0.0102	0.0873	0.3091	0.6032	0.8073	0.8832	0.1783	0.3007	0.2501	0.4819	0.0296	0.5362		0.2477	0.0188	0.3404	0.7052	0.6723	0.1107
J (25%)	0.0024	0.0172	0.1941	0.9539	0.6652	0.1639	0.5489	0.0720	0.0406	0.1422	0.0110	0.8564	0.3246		0.0413	0.5949	0.0877	0.3011	0.0432
U (25%)	0.0005	0.0038	0.0749	0.1909	0.1625	0.0092	0.0436	0.0072	0.0029	0.0155	0.0025	0.3563	0.0189	0.0252		0.0416	0.0075	0.1005	0.0107
B-IM (30%)	0.0080	0.0003	0.1784	0.8118	0.5512	0.1076	0.7630	0.0682	0.0360	0.1179	0.0219	0.9624	0.2098	0.6435	0.0410		0.0962	0.3919	0.0733
R (30%)	0.0115	0.0659	0.4859	0.3149	0.4295	0.2007	0.0250	0.7752	0.7029	0.9179	0.0607	0.3278	0.3255	0.0437	0.0029	0.0184		0.8313	0.1417
S (30%)	0.1221	0.4638	0.5346	0.3341	0.4370	0.5126	0.2084	0.9171	0.9019	0.8834	0.1841	0.3272	0.4754	0.2375	0.0798	0.2480	0.9320		0.2933
X (30%)	0.3201	0.6112	0.9113	0.1103	0.1452	0.1333	0.0541	0.3035	0.2949	0.2380	0.6748	0.1352	0.1166	0.0600	0.0174	0.0670	0.2358	0.3272	

Shaded bold cells indicate significant differences at a level of significance of $\alpha = 0.05$.

Table D3. *t*-Test Comparisons of Mixtures at 4.4°C (40°F) and 10.0 Hz (lower left half of table) and 25.0 Hz (upper right half of table)

Section (% RAP)	E (0%)	V (0%)	K (10%)	L (10%)	T (10%)	M (20%)	N (20%)	W (20%)	O (21%)	P (21%)	B (25%)	C (25%)	D (25%)	J (25%)	U (25%)	B-IM (30%)	R (30%)	S (30%)	X (30%)
E (0%)		0.0743	0.5462	0.0674	0.1467	0.0061	0.0019	0.1914	0.0096	0.0245	0.8484	0.0724	0.0161	0.0025	0.0013	0.0791	0.0044	0.1694	0.2227
V (0%)	0.0696		0.8171	0.1246	0.3107	0.0664	0.0370	0.8886	0.0669	0.1295	0.5222	0.1446	0.0903	0.0231	0.0121	0.1373	0.0388	0.3483	0.7550
K (10%)	0.5085	0.8284		0.1052	0.2864	0.2292	0.0942	0.8771	0.3974	0.2884	0.6221	0.1349	0.2358	0.1161	0.0450	0.1124	0.2174	0.3205	0.9371
L (10%)	0.0612	0.1309	0.1257		0.3192	0.3228	0.8543	0.1042	0.2018	0.2638	0.1268	0.7783	0.3132	0.6246	0.6103	0.9294	0.3346	0.3007	0.0983
T (10%)	0.1262	0.2925	0.2791	0.4095		0.8947	0.2876	0.2465	0.5972	0.8834	0.2721	0.4361	0.9389	0.3879	0.1258	0.3170	0.8575	0.9307	0.2267
M (20%)	0.0073	0.0580	0.2552	0.3657	0.9884		0.0409	0.0748	0.1176	0.6491	0.2575	0.4367	0.9327	0.1410	0.0224	0.3266	0.9056	0.8189	0.0633
N (20%)	0.0024	0.0412	0.1105	0.9645	0.3305	0.0514		0.0191	0.0085	0.0730	0.1517	0.8497	0.0910	0.3710	0.1397	0.7845	0.0465	0.2853	0.0167
W (20%)	0.1068	0.8565	0.7797	0.1246	0.2654	0.0951	0.0216		0.1985	0.1360	0.5470	0.1229	0.0900	0.0204	0.0046	0.1191	0.0620	0.2909	0.8974
O (21%)	0.0114	0.0922	0.4442	0.2127	0.5078	0.1172	0.0117	0.3051		0.5339	0.3476	0.2554	0.3335	0.0349	0.0084	0.2145	0.1593	0.6791	0.1618
P (21%)	0.0230	0.1461	0.3337	0.2837	0.7417	0.5900	0.0741	0.2076	0.5620		0.2891	0.3552	0.7597	0.1493	0.0182	0.2720	0.6216	0.9676	0.1137
B (25%)	0.5282	0.5906	0.8650	0.0822	0.1725	0.1322	0.0523	0.5580	0.2511	0.1741		0.1572	0.2605	0.1773	0.1025	0.1212	0.2508	0.2872	0.5730
C (25%)	0.0690	0.1482	0.1448	0.9172	0.4733	0.4269	0.9264	0.1451	0.2469	0.3333	0.0960		0.4288	0.8707	0.3867	0.7238	0.4575	0.4086	0.1147
D (25%)	0.0131	0.0892	0.2586	0.3639	0.9697	0.9648	0.1020	0.1175	0.2998	0.6827	0.1253	0.4266		0.2135	0.0222	0.3170	0.8769	0.8627	0.0751
J (25%)	0.0021	0.0216	0.1361	0.7255	0.4539	0.1361	0.4057	0.0256	0.0304	0.1394	0.0593	0.8281	0.2253		0.0672	0.5882	0.1801	0.3730	0.0171
U (25%)	0.0008	0.0105	0.0527	0.4502	0.1364	0.0185	0.1012	0.0047	0.0056	0.0154	0.0193	0.3931	0.0196	0.0504		0.7201	0.0166	0.1322	0.0039
B-IM (30%)	0.0076	0.0004	0.1857	0.5300	0.6582	0.1817	0.1287	0.0600	0.0369	0.2560	0.0960	0.6159	0.4168	0.4027	0.0379		0.3370	0.2991	0.1131
R (30%)	0.0049	0.0402	0.2723	0.3395	0.9113	0.8065	0.0367	0.1031	0.2076	0.7129	0.1367	0.3971	0.9093	0.1204	0.0107	0.2012		0.7860	0.0509
S (30%)	0.1517	0.3663	0.3685	0.3106	0.7698	0.7290	0.2606	0.3692	0.7171	0.9914	0.2361	0.3605	0.7589	0.3297	0.1118	0.4776	0.8008		0.2681
X (30%)	0.2561	0.7941	0.9492	0.0999	0.2073	0.1089	0.0333	0.7371	0.2584	0.1738	0.7606	0.1168	0.1100	0.0371	0.0088	0.0744	0.1128	0.2883	

Shaded bold cells indicate significant differences at a level of significance of $\alpha = 0.05$.

Table D4. *t*-test Comparisons of Mixtures at 21.1°C (70°F) and 0.1 Hz (lower left half of table) and 0.5 Hz (upper right half of table)

Section (% RAP)	E (0%)	V (0%)	K (10%)	L (10%)	T (10%)	M (20%)	N (20%)	W (20%)	O (21%)	P (21%)	B (25%)	C (25%)	D (25%)	J (25%)	U (25%)	B-IM (30%)	R (30%)	S (30%)	X (30%)
E (0%)		0.0344	0.2887	0.0341	0.0217	0.0251	0.0128	0.0076	0.0347	0.0431	0.8108	0.0781	0.0094	0.0126	0.0103	0.0039	0.0942	0.0499	0.4908
V (0%)	0.0388		0.7508	0.8692	0.1655	0.4215	0.0419	0.0891	0.9920	0.8310	0.1181	0.4113	0.1285	0.0293	0.0068	0.0033	0.0919	0.5458	0.3166
K (10%)	0.2637	0.7256		0.7962	0.2326	0.5466	0.3067	0.2935	0.7547	0.6893	0.3668	0.3879	0.3436	0.3303	0.1139	0.1381	0.8113	0.8550	0.6127
L (10%)	0.0627	0.3537	0.9938		0.1288	0.3988	0.0639	0.0871	0.8942	0.7633	0.1219	0.3879	0.1275	0.0684	0.0162	0.0078	0.2096	0.8013	0.3430
T (10%)	0.0171	0.1592	0.2500	0.0848		0.2370	0.5968	0.6744	0.1360	0.1777	0.0332	0.7431	0.5119	0.5195	0.2638	0.3555	0.0945	0.1634	0.0862
M (20%)	0.0304	0.5590	0.5840	0.2328	0.2175		0.2415	0.2534	0.5128	0.7075	0.0765	0.5981	0.3676	0.2774	0.0950	0.0439	0.1102	0.2981	0.2144
N (20%)	0.0223	0.0536	0.3544	0.0471	0.5000	0.2871		0.9125	0.1116	0.2182	0.0465	0.9683	0.7926	0.7766	0.0869	0.0481	0.0121	0.0379	0.1208
W (20%)	0.0083	0.0573	0.2593	0.0290	0.9259	0.1471	0.4230		0.1246	0.2190	0.0332	0.9327	0.7619	0.7696	0.0732	0.1146	0.0264	0.0706	0.1058
O (21%)	0.0427	0.8164	0.8025	0.5928	0.1199	0.5098	0.1351	0.0732		0.8569	0.1118	0.4206	0.1797	0.1276	0.0257	0.0179	0.2323	0.7183	0.3206
P (21%)	0.0599	0.8876	0.7956	0.6436	0.1527	0.6148	0.2347	0.1348	0.9739		0.1032	0.4867	0.2998	0.2512	0.0465	0.0468	0.2581	0.6281	0.2895
B (25%)	0.9066	0.1631	0.3466	0.2359	0.0582	0.1283	0.0906	0.0605	0.1758	0.1765		0.0929	0.0397	0.0492	0.0251	0.0202	0.2681	0.1467	0.6418
C (25%)	0.0753	0.5376	0.4721	0.3524	0.6093	0.7032	0.8816	0.6359	0.4879	0.5176	0.1135		0.9425	0.9681	0.2697	0.3821	0.2214	0.3509	0.1756
D (25%)	0.0118	0.1362	0.3500	0.0626	0.5434	0.3139	0.9614	0.5398	0.1540	0.2402	0.0770	0.8708		0.9356	0.0580	0.0772	0.0347	0.0953	0.1251
J (25%)	0.0200	0.0681	0.3832	0.0493	0.4292	0.3358	0.7364	0.3406	0.1578	0.2697	0.0938	0.9512	0.8066		0.0163	0.0256	0.0058	0.0126	0.1295
U (25%)	0.0128	0.0075	0.1262	0.0131	0.2587	0.0921	0.0460	0.0958	0.0269	0.0510	0.0441	0.2254	0.0617	0.0124		0.2577	0.0049	0.0026	0.0527
B-IM (30%)	0.0059	0.0033	0.1342	0.0046	0.2646	0.0370	0.0225	0.1192	0.0157	0.0432	0.0404	0.2588	0.0596	0.0138	0.5625		0.0012	0.0033	0.0555
R (30%)	0.1691	0.0550	0.6372	0.2444	0.0523	0.0697	0.0136	0.0095	0.1533	0.2354	0.4317	0.1951	0.0185	0.0109	0.0068	0.0015		0.1412	0.6520
S (30%)	0.0667	0.3407	0.9006	0.7159	0.1591	0.3078	0.0267	0.0445	0.7303	0.7695	0.2121	0.4025	0.0834	0.0185	0.0003	0.0043	0.1166		0.3776
X (30%)	0.5472	0.2922	0.5603	0.4426	0.0982	0.2288	0.1462	0.1018	0.3309	0.3355	0.6760	0.2005	0.1341	0.1547	0.0627	0.0608	0.7804	0.3820	

Shaded bold cells indicate significant differences at a level of significance of $\alpha = 0.05$.

Table D5. *t*-test Comparisons of Mixtures at 21.1°C (70°F) and 1.0 Hz (lower left half of table) and 5.0 Hz (upper right half of table).

Section (% RAP)	E (0%)	V (0%)	K (10%)	L (10%)	T (10%)	M (20%)	N (20%)	W (20%)	O (21%)	P (21%)	B (25%)	C (25%)	D (25%)	J (25%)	U (25%)	B-IM (30%)	R (30%)	S (30%)	X (30%)
E (0%)		0.0325	0.3315	0.0179	0.0396	0.0212	0.0066	0.0123	0.0251	0.0272	0.5749	0.0813	0.0079	0.0051	0.0043	0.0027	0.0413	0.0242	0.4275
V (0%)	0.0331		0.7800	0.3215	0.1854	0.2654	0.0476	0.1760	0.6420	0.4240	0.0459	0.2890	0.1016	0.0109	0.0004	0.0024	0.6614	0.6432	0.3783
K (10%)	0.3005	0.7562		0.4937	0.2097	0.4607	0.2265	0.3781	0.6589	0.5286	0.4400	0.2835	0.3106	0.2485	0.0931	0.1472	0.8465	0.7002	0.7030
L (10%)	0.0259	0.8089	0.6989		0.2676	0.9084	0.1729	0.6473	0.5860	0.9216	0.0278	0.4745	0.4290	0.2034	0.0272	0.0545	0.2555	0.4370	0.2019
T (10%)	0.0241	0.1668	0.2249	0.1521		0.2976	0.8611	0.4006	0.1778	0.2521	0.0510	0.9568	0.5335	0.7401	0.2500	0.5503	0.1798	0.1956	0.0817
M (20%)	0.0238	0.3797	0.5284	0.5420	0.2427		0.1931	0.6970	0.4810	0.8326	0.0301	0.4986	0.4522	0.2179	0.0676	0.0747	0.2300	0.3420	0.1874
N (20%)	0.0103	0.0417	0.2858	0.0883	0.6443	0.2258		0.3266	0.0766	0.1848	0.0080	0.9641	0.4913	0.7678	0.0773	0.2101	0.0519	0.0483	0.0853
W (20%)	0.0081	0.1069	0.3114	0.1571	0.5803	0.3245	0.8455		0.3322	0.6027	0.0183	0.6154	0.7334	0.3989	0.0382	0.0956	0.1460	0.2318	0.1432
O (21%)	0.0314	0.9007	0.7273	0.9362	0.1421	0.5188	0.1022	0.1596		0.6846	0.0409	0.3494	0.2000	0.0811	0.0152	0.0235	0.4967	0.8569	0.2992
P (21%)	0.0379	0.7171	0.6454	0.8618	0.1891	0.7491	0.2106	0.2810	0.8165		0.0425	0.4511	0.4094	0.2179	0.0352	0.0689	0.3451	0.5517	0.2243
B (25%)	0.7502	0.0976	0.3849	0.0791	0.0290	0.0578	0.0310	0.0246	0.0862	0.0792		0.1015	0.0113	0.0056	0.0042	0.0028	0.0590	0.0339	0.6191
C (25%)	0.0791	0.3719	0.3558	0.4140	0.7997	0.5608	0.9976	0.9361	0.3990	0.4740	0.0924		0.7329	0.8897	0.3384	0.6709	0.2657	0.3227	0.1502
D (25%)	0.0087	0.1194	0.3349	0.1822	0.5082	0.3785	0.7135	0.8888	0.1846	0.3220	0.0271	0.8795		0.6092	0.0413	0.1270	0.0870	0.1305	0.1127
J (25%)	0.0100	0.0210	0.3073	0.0960	0.5622	0.2556	0.7909	0.9830	0.1144	0.2416	0.0332	0.9410	0.8446		0.0104	0.0936	0.0091	0.0171	0.0949
U (25%)	0.0088	0.0045	0.1089	0.0187	0.2607	0.0903	0.0864	0.0634	0.0236	0.0441	0.0185	0.2906	0.0542	0.0148		0.0508	0.0001	0.0012	0.0392
B-IM (30%)	0.0035	0.0030	0.1417	0.0134	0.4061	0.0508	0.0700	0.1127	0.0194	0.0515	0.0138	0.4541	0.0888	0.0340	0.1712		0.0024	0.0033	0.0556
R (30%)	0.0734	0.1336	0.9007	0.2083	0.1132	0.1386	0.0172	0.0419	0.2792	0.2777	0.1992	0.2332	0.0441	0.0052	0.0030	0.0013		0.3976	0.4280
S (30%)	0.0424	0.7024	0.8203	0.6248	0.1658	0.3076	0.0415	0.0909	0.7294	0.5954	0.1147	0.3382	0.0993	0.0125	0.0020	0.0029	0.1735		0.3239
X (30%)	0.4695	0.3342	0.6416	0.3007	0.0846	0.2130	0.1132	0.1138	0.3191	0.2765	0.6320	0.1692	0.1237	0.1219	0.0500	0.0565	0.5962	0.3739	

Shaded bold cells indicate significant differences at a level of significance of $\alpha = 0.05$.

Table D6. *t*-test Comparisons of Mixtures at 21.1°C (70°F) and 10.0 Hz (lower left half of table) and 25.0 Hz (upper right half of table)

Section (% RAP)	E (0%)	V (0%)	K (10%)	L (10%)	T (10%)	M (20%)	N (20%)	W (20%)	O (21%)	P (21%)	B (25%)	C (25%)	D (25%)	J (25%)	U (25%)	B-IM (30%)	R (30%)	S (30%)	X (30%)
E (0%)		0.0362	0.3457	0.0231	0.0627	0.0232	0.0058	0.0233	0.0188	0.0209	0.4130	0.0805	0.0083	0.0025	0.0011	0.0028	0.0084	0.0139	0.3838
V (0%)	0.0343		0.8126	0.1811	0.2117	0.2261	0.0620	0.3003	0.3999	0.2486	0.0179	0.2291	0.0920	0.0149	0.0004	0.0016	0.1144	0.2778	0.4431
K (10%)	0.3495	0.7818		0.3148	0.2030	0.3996	0.1689	0.4764	0.5930	0.4310	0.4879	0.2231	0.2798	0.1925	0.0737	0.1503	0.4240	0.5756	0.7566
L (10%)	0.0186	0.2364	0.4083		0.5653	0.6856	0.3533	0.5534	0.3435	0.6485	0.0428	0.5733	0.8963	0.4572	0.0569	0.2506	0.6029	0.3441	0.1260
T (10%)	0.0487	0.1977	0.2057	0.3667		0.3793	0.8463	0.3081	0.2343	0.3521	0.1047	0.8621	0.6079	0.9894	0.2257	0.6755	0.3467	0.2515	0.0921
M (20%)	0.0226	0.2506	0.4309	0.9031	0.3304		0.1641	0.7810	0.4529	0.9176	0.0508	0.4381	0.5253	0.1908	0.0447	0.1256	0.8874	0.4467	0.1675
N (20%)	0.0060	0.0528	0.2017	0.2364	0.9836	0.1841		0.1229	0.0545	0.1525	0.0130	0.9471	0.3243	0.7133	0.0711	0.6526	0.0929	0.0511	0.0615
W (20%)	0.0158	0.2191	0.4098	0.9890	0.3577	0.9114	0.2143		0.6824	0.8753	0.0440	0.3816	0.4150	0.1518	0.0206	0.0838	0.8606	0.6933	0.2103
O (21%)	0.0225	0.5324	0.6225	0.4614	0.2007	0.4738	0.0657	0.4525		0.5678	0.0300	0.3047	0.2090	0.0517	0.0059	0.0268	0.4782	0.9569	0.2800
P (21%)	0.0239	0.3334	0.4793	0.8030	0.2920	0.8730	0.1710	0.8076	0.6317		0.0397	0.4193	0.5082	0.1930	0.0242	0.1031	0.9917	0.5711	0.1836
B (25%)	0.4954	0.0286	0.4742	0.0301	0.0756	0.0366	0.0072	0.0251	0.0333	0.0390		0.1073	0.0158	0.0018	0.0001	0.0005	0.0088	0.0132	0.6113
C (25%)	0.0802	0.2589	0.2524	0.5083	0.9628	0.4688	0.9502	0.5021	0.3271	0.4355	0.1043		0.6095	0.8449	0.3842	0.9371	0.4104	0.3109	0.1347
D (25%)	0.0081	0.0985	0.2969	0.6124	0.5624	0.4885	0.4137	0.5903	0.2063	0.4527	0.0120	0.6734		0.4424	0.0291	0.1933	0.4231	0.1973	0.1033
J (25%)	0.0038	0.0111	0.2246	0.2935	0.8400	0.2122	0.7408	0.2658	0.0676	0.2078	0.0021	0.8639	0.5339		0.0156	0.3635	0.0918	0.0341	0.0699
U (25%)	0.0027	0.0002	0.0860	0.0359	0.2417	0.0599	0.0719	0.0301	0.0109	0.0305	0.0010	0.3595	0.0365	0.0111		0.0137	0.0043	0.0020	0.0278
B-IM (30%)	0.0027	0.0021	0.1494	0.1063	0.6073	0.0968	0.3383	0.0910	0.0250	0.0807	0.0011	0.7838	0.1530	0.1621	0.0266		0.0311	0.0119	0.0581
R (30%)	0.0334	0.7128	0.7332	0.2739	0.2131	0.2916	0.0672	0.2562	0.6394	0.3872	0.0268	0.2757	0.1158	0.0148	0.0001	0.0029		0.4527	0.1775
S (30%)	0.0187	0.4268	0.6377	0.3890	0.2168	0.3875	0.0484	0.3732	0.9334	0.5529	0.0158	0.3154	0.1559	0.0226	0.0014	0.0049	0.5642		0.2674
X (30%)	0.4079	0.4026	0.7394	0.1645	0.0846	0.1784	0.0745	0.1643	0.2902	0.2048	0.6145	0.1417	0.1082	0.0841	0.0344	0.0561	0.3659	0.2986	

Shaded bold cells indicate significant differences at a level of significance of $\alpha = 0.05$.

Table D7. *t*-test Comparisons of Mixtures at 37.8°C (100°F) and 0.1 Hz (lower left half of table) and 0.5 Hz (upper right half of table)

Section (% RAP)	E (0%)	V (0%)	K (10%)	L (10%)	T (10%)	M (20%)	N (20%)	W (20%)	O (21%)	P (21%)	B (25%)	C (25%)	D (25%)	J (25%)	U (25%)	B-IM (30%)	R (30%)	S (30%)	X (30%)
E (0%)		0.0423	0.1329	0.0821	0.0149	0.0351	0.0283	0.0125	0.0449	0.0414	0.7851	0.0502	0.0175	0.0294	0.0128	0.0088	0.1570	0.0624	0.5602
V (0%)	0.0589		0.7854	0.1463	0.1682	0.7697	0.0480	0.0757	0.6231	0.7678	0.2005	0.8530	0.1134	0.0781	0.0013	0.0069	0.0950	0.2725	0.2154
K (10%)	0.1276	0.8222		0.6685	0.2767	0.7175	0.3986	0.3004	0.9858	0.9159	0.2870	0.7252	0.3918	0.4616	0.1352	0.1453	0.4557	0.9792	0.3470
L (10%)	0.1532	0.1331	0.5075		0.0494	0.1361	0.0417	0.0218	0.4383	0.3820	0.3615	0.3349	0.0320	0.0478	0.0079	0.0054	0.5061	0.2847	0.4357
T (10%)	0.0203	0.1358	0.2693	0.0315		0.1831	0.4857	0.8635	0.1086	0.1362	0.0935	0.3389	0.5192	0.3728	0.2352	0.2677	0.0319	0.1667	0.0888
M (20%)	0.0505	0.8132	0.7648	0.1216	0.1448		0.2119	0.1218	0.5259	0.6549	0.1847	0.9516	0.2069	0.2832	0.0336	0.0224	0.0840	0.3703	0.1961
N (20%)	0.0391	0.0375	0.4004	0.0510	0.4392	0.2080		0.4776	0.1605	0.2133	0.1286	0.5298	0.9463	0.4976	0.0083	0.0381	0.0401	0.0370	0.1283
W (20%)	0.0194	0.0790	0.3030	0.0235	0.8174	0.1177	0.4984		0.0947	0.1302	0.1002	0.3725	0.5715	0.3163	0.0859	0.1321	0.0180	0.0581	0.0955
O (21%)	0.0654	0.5981	0.9510	0.3410	0.0915	0.5275	0.1571	0.0943		0.8880	0.2414	0.6483	0.1523	0.2064	0.0299	0.0260	0.2222	0.9887	0.2739
P (21%)	0.0535	0.8045	0.9292	0.2466	0.1156	0.7080	0.2000	0.1234	0.8139		0.2230	0.7302	0.2074	0.2757	0.0400	0.0370	0.1988	0.8674	0.2504
B (25%)	0.8445	0.2453	0.3086	0.4839	0.1234	0.2316	0.1611	0.1316	0.2978	0.2652		0.1794	0.1207	0.1400	0.0666	0.0667	0.5104	0.2444	0.8207
C (25%)	0.0577	0.9766	0.8312	0.2751	0.2352	0.9374	0.3946	0.2728	0.7106	0.8547	0.2410		0.5238	0.6399	0.1259	0.1380	0.2037	0.6206	0.2015
D (25%)	0.0291	0.0710	0.3890	0.0346	0.4685	0.1646	0.9112	0.5847	0.1403	0.1850	0.1549	0.3814		0.6329	0.0327	0.0509	0.0266	0.0693	0.1187
J (25%)	0.0386	0.0495	0.4392	0.0506	0.3635	0.2232	0.6353	0.3950	0.1780	0.2325	0.1685	0.4491	0.6917		0.0028	0.0230	0.0441	0.0189	0.1414
U (25%)	0.0182	0.0016	0.1446	0.0127	0.2470	0.0320	0.0116	0.1191	0.0334	0.0379	0.0917	0.1002	0.0264	0.0060		0.6733	0.0111	0.0015	0.0607
B-IM (30%)	0.0138	0.0088	0.1481	0.0086	0.2724	0.0234	0.0513	0.1601	0.0284	0.0335	0.0912	0.1002	0.0515	0.0346	0.8409		0.0072	0.0121	0.0599
R (30%)	0.2128	0.1523	0.4374	0.8133	0.0370	0.1352	0.0677	0.0345	0.2948	0.2213	0.5519	0.2360	0.0519	0.0695	0.0221	0.0166		0.1641	0.6433
S (30%)	0.0711	0.4928	0.9449	0.1852	0.1325	0.5014	0.0110	0.0616	0.7998	0.9594	0.2726	0.8060	0.0440	0.0145	0.0010	0.0095	0.1977		0.2719
X (30%)	0.6968	0.2271	0.3130	0.5106	0.1016	0.2121	0.1404	0.1090	0.2867	0.2493	0.8981	0.2263	0.1328	0.1473	0.0743	0.0724	0.5970	0.2574	

Shaded bold cells indicate significant differences at a level of significance of $\alpha = 0.05$.

Table D8. *t*-test Comparisons of Mixtures at 37.8°C (100°F) and 1.0 Hz (lower left half of table) and 5.0 Hz (upper right half of table)

Section (% RAP)	E (0%)	V (0%)	K (10%)	L (10%)	T (10%)	M (20%)	N (20%)	W (20%)	O (21%)	P (21%)	B (25%)	C (25%)	D (25%)	J (25%)	U (25%)	B-IM (30%)	R (30%)	S (30%)	X (30%)
E (0%)		0.0228	0.1471	0.0268	0.0157	0.0167	0.0112	0.0050	0.0261	0.0220	0.6290	0.0508	0.0065	0.0142	0.0070	0.0028	0.0594	0.0398	0.4403
V (0%)	0.0350		0.7724	0.3273	0.1995	0.6016	0.0582	0.1006	0.7074	0.9864	0.1289	0.5909	0.1643	0.0486	0.0009	0.0091	0.0690	0.2236	0.1996
K (10%)	0.1342	0.7744		0.9410	0.2532	0.6475	0.3539	0.3119	0.9200	0.7918	0.2667	0.5400	0.3924	0.4241	0.1164	0.1447	0.6061	0.9767	0.3833
L (10%)	0.0588	0.1679	0.7482		0.1074	0.2411	0.0415	0.0464	0.7367	0.5336	0.1835	0.3824	0.0738	0.0562	0.0074	0.0058	0.2930	0.7461	0.2985
T (10%)	0.0131	0.1772	0.2686	0.0624		0.2278	0.5521	0.7109	0.1285	0.1720	0.0431	0.5271	0.4871	0.4163	0.2616	0.3828	0.0699	0.1825	0.0661
M (20%)	0.0278	0.7201	0.6919	0.1515	0.1952		0.2148	0.1913	0.5016	0.7287	0.1032	0.7366	0.3228	0.3223	0.0545	0.0304	0.0752	0.3097	0.1622
N (20%)	0.0225	0.0487	0.3868	0.0380	0.4964	0.2133		0.7572	0.1407	0.2180	0.0667	0.7591	0.8232	0.4967	0.0334	0.0586	0.0155	0.0696	0.0985
W (20%)	0.0094	0.0810	0.3013	0.0246	0.8186	0.1361	0.5309		0.1178	0.1851	0.0491	0.6678	0.6655	0.4711	0.0654	0.1369	0.0173	0.0698	0.0779
O (21%)	0.0369	0.6375	0.9642	0.5111	0.1123	0.5140	0.1565	0.0991		0.7838	0.1488	0.4931	0.1844	0.1977	0.0280	0.0260	0.2705	0.8703	0.2463
P (21%)	0.0340	0.8002	0.8867	0.4332	0.1417	0.6558	0.2138	0.1393	0.8740		0.1209	0.6101	0.2877	0.3084	0.0379	0.0402	0.1980	0.6218	0.2007
B (25%)	0.7467	0.1780	0.2757	0.3040	0.0766	0.1595	0.1101	0.0846	0.2131	0.1936		0.0987	0.0604	0.0782	0.0325	0.0300	0.3270	0.1721	0.7706
C (25%)	0.0486	0.7745	0.6669	0.3545	0.3908	0.8889	0.6008	0.4476	0.6008	0.6858	0.1492		0.8422	0.9119	0.1786	0.2537	0.2188	0.4289	0.1506
D (25%)	0.0128	0.1367	0.3946	0.0381	0.4986	0.2457	0.9726	0.5808	0.1636	0.2270	0.1031	0.6206		0.8264	0.0428	0.0744	0.0248	0.0974	0.0962
J (25%)	0.0244	0.0791	0.4606	0.0483	0.3686	0.3141	0.4478	0.3243	0.2140	0.2929	0.1229	0.7403	0.6646		0.0016	0.0324	0.0183	0.0132	0.1157
U (25%)	0.0107	0.0011	0.1294	0.0070	0.2428	0.0386	0.0101	0.0773	0.0295	0.0396	0.0554	0.1422	0.0364	0.0020		0.3120	0.0042	0.0001	0.0441
B-IM (30%)	0.0064	0.0074	0.1436	0.0047	0.2915	0.0236	0.0401	0.1293	0.0256	0.0372	0.0550	0.1655	0.0555	0.0234	0.5652		0.0025	0.0131	0.0445
R (30%)	0.1207	0.0810	0.4869	0.4139	0.0359	0.0723	0.0300	0.0149	0.2206	0.1940	0.4637	0.2044	0.0220	0.0353	0.0083	0.0047		0.1604	0.5238
S (30%)	0.0557	0.2326	0.9860	0.3694	0.1717	0.3389	0.0576	0.0603	0.9499	0.7950	0.2251	0.5482	0.0808	0.0212	0.0014	0.0134	0.1588		0.2667
X (30%)	0.5221	0.2117	0.3577	0.3940	0.0829	0.1879	0.1220	0.0918	0.2681	0.2416	0.8029	0.1867	0.1146	0.1382	0.0565	0.0561	0.6216	0.2757	

Shaded bold cells indicate significant differences at a level of significance of $\alpha = 0.05$.

Table D9. T-test Comparisons of Mixtures at 37.8°C (100°F) and 10.0 Hz (lower left half of table) and 25.0 Hz (upper right half of table)

Section (% RAP)	E (0%)	V (0%)	K (10%)	L (10%)	T (10%)	M (20%)	N (20%)	W (20%)	O (21%)	P (21%)	B (25%)	C (25%)	D (25%)	J (25%)	U (25%)	B-IM (30%)	R (30%)	S (30%)	X (30%)
E (0%)		0.0173	0.1591	0.0115	0.0274	0.0136	0.0060	0.0043	0.0216	0.0153	0.4408	0.0574	0.0046	0.0074	0.0053	0.0016	0.0301	0.0253	0.3745
V (0%)	0.0199		0.7845	0.9274	0.2161	0.4880	0.0738	0.1328	0.8319	0.7485	0.0777	0.4345	0.1572	0.0214	0.0008	0.0103	0.0898	0.3143	0.2098
K (10%)	0.1515	0.7706		0.7652	0.2343	0.5978	0.3133	0.3420	0.8701	0.6868	0.2808	0.4187	0.3792	0.3598	0.1026	0.1499	0.7757	0.9431	0.4241
L (10%)	0.0191	0.5018	0.9598		0.1811	0.6074	0.1130	0.1785	0.8066	0.8285	0.0629	0.4587	0.2201	0.1431	0.0175	0.0192	0.2055	0.5453	0.1970
T (10%)	0.0188	0.2037	0.2413	0.1271		0.2603	0.6141	0.5603	0.1501	0.2143	0.0320	0.7077	0.4788	0.5005	0.2772	0.5297	0.1254	0.1914	0.0615
M (20%)	0.0145	0.5482	0.6218	0.3179	0.2375		0.2318	0.3207	0.4962	0.8228	0.0501	0.5966	0.3960	0.3021	0.0751	0.0486	0.1319	0.3064	0.1494
N (20%)	0.0085	0.0623	0.3337	0.0523	0.5713	0.2191		0.8635	0.1260	0.2218	0.0268	0.9427	0.6906	0.6474	0.0700	0.1048	0.0204	0.0650	0.0832
W (20%)	0.0046	0.1176	0.3218	0.0727	0.6339	0.2412	0.9218		0.1661	0.2974	0.0211	0.9949	0.8507	0.8881	0.0513	0.1326	0.0385	0.0898	0.0796
O (21%)	0.0243	0.7370	0.9034	0.8866	0.1323	0.4873	0.1324	0.1350		0.6799	0.0864	0.4007	0.2010	0.1610	0.0267	0.0298	0.3885	0.8299	0.2407
P (21%)	0.0181	0.9028	0.7405	0.5891	0.1851	0.7683	0.2169	0.2254	0.7229		0.0576	0.5340	0.3606	0.2877	0.0354	0.0488	0.2218	0.4814	0.1724
B (25%)	0.5608	0.1079	0.2689	0.1334	0.0341	0.0797	0.0492	0.0363	0.1233	0.0912		0.0855	0.0240	0.0338	0.0153	0.0105	0.1678	0.1040	0.7496
C (25%)	0.0531	0.5223	0.4857	0.3978	0.5918	0.6784	0.8300	0.8026	0.4482	0.5821	0.0882		0.9170	0.9459	0.2372	0.4324	0.2396	0.3488	0.1317
D (25%)	0.0055	0.1686	0.3891	0.1051	0.4664	0.3635	0.7411	0.7268	0.1932	0.3238	0.0444	0.9502		0.9235	0.0418	0.0976	0.0424	0.1016	0.0888
J (25%)	0.0110	0.0339	0.3930	0.0673	0.4449	0.3103	0.5582	0.6334	0.1792	0.2981	0.0589	0.9664	0.9579		0.0038	0.0522	0.0076	0.0087	0.0973
U (25%)	0.0061	0.0008	0.1097	0.0091	0.2681	0.0622	0.0470	0.0604	0.0275	0.0361	0.0246	0.1997	0.0419	0.0021		0.1468	0.0023	0.0001	0.0375
B-IM (30%)	0.0022	0.0100	0.1477	0.0080	0.4540	0.0371	0.0770	0.1440	0.0281	0.0435	0.0214	0.3214	0.0847	0.0411	0.2144		0.0030	0.0096	0.0413
R (30%)	0.0440	0.0720	0.6732	0.2598	0.0894	0.0898	0.0145	0.0243	0.3196	0.2000	0.2606	0.2278	0.0308	0.0127	0.0032	0.0026		0.2103	0.4210
S (30%)	0.0335	0.2388	0.9632	0.9863	0.1826	0.3000	0.0643	0.0784	0.8624	0.5459	0.1460	0.3913	0.1007	0.0097	0.0000	0.0117	0.1715		0.2673
X (30%)	0.4186	0.1979	0.3934	0.2578	0.0616	0.1529	0.0902	0.0762	0.2409	0.1827	0.7701	0.1390	0.0919	0.1057	0.0406	0.0427	0.4704	0.2622	

Shaded bold cells indicate significant differences at a level of significance of $\alpha=0.05$.

APPENDIX E
BINDER GRADING RESULTS

Table E1. Binder Test Results for Binder Extracted From Entire Core for Control Mixtures Containing 0%-20% RAP

Section	E	K	L	M	W
Portion of Core	Entire	Entire	Entire	Entire	Entire
RAP Content	0%	10%	10%	20%	20%
Dynamic Shear, 10 rad/sec, specification: $G^*/\sin \delta > 2.20$ kPa					
RTFO $G^*/\sin \delta$, 76°C	10.28	4.603	6.735	4.973	4.795
RTFO $G^*/\sin \delta$, 82°C	5.014	2.169	3.113	2.462	2.367
RTFO $G^*/\sin \delta$, 88°C	2.529		1.485	1.242	1.203
RTFO $G^*/\sin \delta$, 94°C	1.294				
RTFO $G^*/\sin \delta$, 100°C					
RTFO $G^*/\sin \delta$, 106°C					
RTFO G^* , 76°C	9.992	4.557	6.651	4.888	4.729
RTFO G^* , 82°C	4.923	2.158	3.091	2.437	2.348
RTFO G^* , 88°C	2.501		1.479	1.235	1.197
RTFO G^* , 94°C	1.286				
RTFO G^* , 100°C					
RTFO G^* , 106°C					
RTFO δ , 76°C	76.38	81.93	80.93	79.36	80.5
RTFO δ , 82°C	79.10	84.14	83.20	81.85	82.77
RTFO δ , 88°C	81.51		85.07	83.98	84.74
RTFO δ , 94°C	83.63				
RTFO δ , 100°C					
RTFO δ , 106°C					
<i>RTFO failure temp.</i>	89.29	82.89	84.84	83.03	82.72
Dynamic Shear, 10 rad/sec, specification: $G^* \sin \delta < 5000$ kPa					
PAV $G^* \sin \delta$, 25.0°C					
PAV $G^* \sin \delta$, 28.0°C				5195	6817
PAV $G^* \sin \delta$, 31.0°C		5362	6453	3782	4851
PAV $G^* \sin \delta$, 34.0°C	5681	3783	4598	2735	
PAV $G^* \sin \delta$, 37.0°C	4128				
PAV $G^* \sin \delta$, 40.0°C					
PAV G^* , 25.0°C					
PAV G^* , 28.0°C				3.84E+6	1.00E+7
PAV G^* , 31.0°C		7.70E+6	9.56E+6	5.54E+6	6.79E+6
PAV G^* , 34.0°C	8.04E+6	5.16E+6	6.44E+6	7.96E+6	
PAV G^* , 37.0°C	5.64E+6				
PAV G^* , 40.0°C					
PAV δ , 25.0°C					
PAV δ , 28.0°C				45.41	42.91
PAV δ , 31.0°C		47.10	42.48	43.10	45.61
PAV δ , 34.0°C	44.99	44.12	45.57	40.74	
PAV δ , 37.0°C	47.04				
PAV δ , 40.0°C					
<i>PAV failure temp.</i>	35.2	31.6	33.26	28.37	30.73
Creep Stiffness, 60 sec, specification: Stiffness < 300 MPa and m-value > 0.300					
Stiffness, 0°C	133		122		
M-value, 0°C	0.330		0.312		
Stiffness, -6°C	300	189	227	124	166
M-value, -6°C	0.291	0.305	0.276	0.320	0.310

Stiffness, -12°C		343		241	343
M-value, -12°C		0.253		0.276	0.272
<i>Stiffness failure temp.</i>	<i>-16.0</i>	<i>-20.7</i>	<i>-18.7</i>	<i>-24.0</i>	<i>-20.9</i>
<i>M-value failure temp.</i>	<i>-14.6</i>	<i>-16.6</i>	<i>-12.0</i>	<i>-18.7</i>	<i>-17.6</i>
Performance Grade	82-10	76-16	82-10	82-16	82-16

Shaded cells indicate the failure temperature.

Table E2. Binder Test Results for Binder Extracted From Entire Core for Mixtures Containing 21%-30% RAP

Section	O	P	C	D	J	U	B-IM	X
Portion of Core	Entire	Entire	Entire	Entire	Entire	Entire	Entire	Entire
RAP Content	21%	21%	25%	25%	25%	25%	30%	30%
Dynamic Shear, 10 rad/sec, specification: G*/sin delta >2.20 kPa								
RTFO G*/sin δ, 76°C	10.51		8.309	6.210	6.052	2.751	3.433	7.321
RTFO G*/sin δ, 82°C	5.000	2.891	4.032	2.959	2.859	1.298	1.662	3.582
RTFO G*/sin δ, 88°C	2.454	1.412	2.015	1.459	1.407			1.803
RTFO G*/sin δ, 94°C	1.226							
RTFO G*/sin δ, 100°C								
RTFO G*/sin δ, 106°C								
RTFO G*, 76°C	10.30		8.112	6.106	5.986	2.736	3.397	7.164
RTFO G*, 82°C	4.944	2.870	3.974	2.930	2.843	1.295	1.652	3.534
RTFO G*, 88°C	2.439	1.407	1.998	1.452	1.403			1.785
RTFO G*, 94°C	1.222							
RTFO G*, 100°C								
RTFO G*, 106°C								
RTFO δ, 76°C	78.64		77.52	79.50	81.53	83.95	81.74	78.11
RTFO δ, 82°C	81.35	83.06	80.27	82.00	83.84	85.79	83.87	80.69
RTFO δ, 88°C	83.61	85.04	82.60	84.10	85.70			82.95
RTFO δ, 94°C	85.37							
RTFO δ, 100°C								
RTFO δ, 106°C								
<i>RTFO failure temp.</i>	<i>89.00</i>	<i>84.29</i>	<i>87.21</i>	<i>84.55</i>	<i>84.27</i>	<i>77.79</i>	<i>79.68</i>	<i>86.25</i>
Dynamic Shear, 10 rad/sec, specification: G* sin delta <5000kPa								
PAV G* sin δ, 25.0°C						6490	6399	
PAV G* sin δ, 28.0°C				6117		4663	4538	6804
PAV G* sin δ, 31.0°C		5895	5525	4334	5361	3288	3163	4895
PAV G* sin δ, 34.0°C	6369	4309	3964	3014	3976		2167	
PAV G* sin δ, 37.0°C	4819							
PAV G* sin δ, 40.0°C								
PAV G*, 25.0°C						9.95E+6	9.30E+6	
PAV G*, 28.0°C				8.90E+6		6.75E+6	6.29E+6	1.03E+7
PAV G*, 31.0°C		9.21E+6	8.26E+6	6.02E+6	7.91E+6	4.52E+6	4.21E+6	7.05E+6
PAV G*, 34.0°C	9.79E+6	6.36E+6	5.64E+6	4.01E+6	5.63E+6		2.78E+6	
PAV G*, 37.0°C	7.09E+6							
PAV G*, 40.0°C								
PAV δ, 25.0°C						40.71	43.46	
PAV δ, 28.0°C				43.41		43.67	46.14	41.38
PAV δ, 31.0°C		39.80	41.96	46.10	42.65	46.65	48.76	44.02
PAV δ, 34.0°C	40.60	42.63	44.64	48.78	44.92		51.35	
PAV δ, 37.0°C	42.80							
PAV δ, 40.0°C								
<i>PAV failure temp.</i>	<i>36.6</i>	<i>32.58</i>	<i>30.9</i>	<i>29.74</i>	<i>31.7</i>	<i>27.33</i>	<i>27.12</i>	<i>30.81</i>
Creep Stiffness, 60 sec, specification: Stiffness < 300 MPa and m-value > 0.300								
Stiffness, 0°C	132	99	86		87			
M-value, 0°C	0.305	0.337	0.342		0.346			
Stiffness, -6°C	248	189	185	162	173	130	132	187
M-value, -6°C	0.260	0.264	0.297	0.328	0.297	0.319	0.346	0.308
Stiffness, -12°C				339		261	298	392

M-value, -12°C				0.277		0.273	0.297	0.263
<i>Stiffness failure temp.</i>	-17.8	-20.3	-19.8	-21.0	-20.8	-23.2	-22.0	-19.8
<i>M-value failure temp.</i>	-10.7	-13.0	-15.6	-19.3	-15.6	-18.5	-21.6	-17.1
Performance Grade	82-10	82-10	82-10	82-16	82-10	76-16	76-16	82-16

Shaded cells indicate the failure temperature.

Table E3. Binder Test Results for Binder Extracted From Top Half and Bottom Half of Cores for Mixtures Containing 21%-30% RAP

Section	V	V	Q	Q	H	H	I	I	N	N
Portion of Core	Bottom	Top	Bottom	Top	Bottom	Top	Bottom	Top	Bottom	Top
RAP Content	0%	0%	15%	15%	20%	20%	20%	20%	20%	20%
Dynamic Shear, 10 rad/sec, specification: G*/sin delta >2.20 kPa										
RTFO G*/sin δ, 76°C	5.796	14.16	6.378	15.93	4.200	5.460	7.737	10.22	7.832	9.409
RTFO G*/sin δ, 82°C	2.831	6.942	3.023	7.599	1.977	2.611	3.690	4.808	3.821	4.706
RTFO G*/sin δ, 88°C	1.429	3.477	1.498	3.667		1.292	1.820	2.348	1.917	2.413
RTFO G*/sin δ, 94°C		1.778		1.817				1.192		1.269
RTFO G*/sin δ, 100°C										
RTFO G*/sin δ, 106°C										
RTFO G*, 76°C	5.705	13.69	6.288	15.4	4.156	5.382	7.596	9.975	7.681	9.079
RTFO G*, 82°C	2.805	6.789	3.000	7.447	1.966	2.590	3.650	4.740	2.776	4.596
RTFO G*, 88°C	1.422	3.429	1.492	3.626		1.286	1.809	2.330	1.904	2.378
RTFO G*, 94°C		1.764		1.806				1.187		1.258
RTFO G*, 100°C										
RTFO G*, 106°C										
RTFO δ, 76°C	79.84	75.20	80.37	75.23	81.64	80.31	79.03	77.55	78.73	74.77
RTFO δ, 82°C	82.15	77.95	82.89	78.52	83.83	82.70	80.57	80.38	81.21	77.6
RTFO δ, 88°C	84.18	80.47	84.90	81.37		84.68	83.72	82.76	83.37	80.18
RTFO δ, 94°C		82.73		83.62				84.73		82.47
RTFO δ, 100°C										
RTFO δ, 106°C										
<i>RTFO failure temp.</i>	<i>84.26</i>	<i>92.06</i>	<i>84.76</i>	<i>92.33</i>	<i>81.15</i>	<i>83.52</i>	<i>86.38</i>	<i>88.71</i>	<i>88.79</i>	<i>88.94</i>
Dynamic Shear, 10 rad/sec, specification: G* sin delta <5000 kPa										
PAV G* sin δ, 25.0°C										
PAV G* sin δ, 28.0°C	6558		5596		5267	5699				5697
PAV G* sin δ, 31.0°C	4607		4175		3754	4133	5337	6236	5470	4187
PAV G* sin δ, 34.0°C		6561	3069	5259			3781	4522	3969	3023
PAV G* sin δ, 37.0°C		4685		4147						
PAV G* sin δ, 40.0°C										
PAV G*, 25.0°C										
PAV G*, 28.0°C	9.41E+6		9.16E+6		7.69E+6	8.67E+6				8.89E+6
PAV G*, 31.0°C	6.30E+6		6.46E+6		5.21E+6	5.96E+6	7.65E+0	9.41E+6	7.90E+6	6.23E+6
PAV G*, 34.0°C		9.56E+6	4.51E+6	8.63E+6			5.17E+0	6.48E+6	5.50E+6	4.30E+6
PAV G*, 37.0°C		6.52E+6		6.65E+6						
PAV G*, 40.0°C										
PAV δ, 25.0°C										
PAV δ, 28.0°C	44.21		37.65		43.25	41.12				39.85
PAV δ, 31.0°C	46.96		40.26		46.09	43.9	44.27	41.5	43.85	42.26
PAV δ, 34.0°C		43.32	42.92	37.54			47.01	44.25	46.17	44.66
PAV δ, 37.0°C		45.96		39.21						
PAV δ, 40.0°C										
<i>PAV failure temp.</i>	<i>30.31</i>	<i>36.42</i>	<i>29.15</i>	<i>34.64</i>	<i>28.46</i>	<i>29.22</i>	<i>31.57</i>	<i>33.06</i>	<i>31.84</i>	<i>29.26</i>
Creep Stiffness, 60 sec, specification: Stiffness < 300 MPa and m-value > 0.300										
Stiffness, 0°C		156	81	99				102		
M-value, 0°C		0.326	0.339	0.308				0.342		
Stiffness, -6°C	193	305	137	165	158	178	220	218	215	158
M-value, -6°C	0.322	0.277	0.297	0.281	0.319	0.308	0.305	0.283	0.3	0.313

Stiffness, -12°C	427				297	322	371		423	287
M-value, -12°C	0.274				0.274	0.268	0.247		0.256	0.268
<i>Stiffness failure temp.</i>	-19.3	-15.9	-24.9	-23.0	-22.1	-21.3	-19.6	-18.5	-19.0	-22.4
<i>M-value failure temp.</i>	-18.8	-13.2	-15.6	-11.8	-18.5	-17.2	-16.5	-14.3	-16.0	-17.7
Performance Grade	82-16	82-10	76-10	82-10	76-16	82-16	82-16	88-10	82-16	82-16

Shaded cells indicate the failure temperature.

Table E4. Binder Test Results for Binder Extracted From Top Half and Bottom Half of Cores for Mixtures Containing 21% to 30% RAP

Section	A	A	B	B	F	F	R	R	S	S
Portion of Core	Bottom	Top	Bottom	Top	Bottom	Top	Bottom	Top	Bottom	Top
RAP Content	25%	25%	25%	25%	25%	25%	30%	30%	30%	30%
Dynamic Shear, 10 rad/sec, specification: G*/sin delta >2.20 kPa										
RTFO G*/sin δ, 76°C	2.966	5.480	10.45	43.34	3.819	6.786	5.815	7.343	6.071	10.22
RTFO G*/sin δ, 82°C	1.436	2.648	50.62	22.49	1.784	3.088	2.730	2.414	2.842	4.706
RTFO G*/sin δ, 88°C		1.322	2.548	11.72		1.469	1.339	1.655	1.411	2.256
RTFO G*/sin δ, 94°C			1.324	6.198						1.113
RTFO G*/sin δ, 100°C				3.322						
RTFO G*/sin δ, 106°C				1.803						
RTFO G*, 76°C	2.945	5.407	101.7	39.26	3.787	6.687	5.748	7.234	5.991	10.03
RTFO G*, 82°C	1.431	2.628	4.978	20.82	1.777	3.064	2.714	3.386	2.821	4.657
RTFO G*, 88°C		1.317	2.522	10.60		1.463	1.335	1.648	1.406	2.244
RTFO G*, 94°C			1.317	5.946						1.110
RTFO G*, 100°C				3.229						
RTFO G*, 106°C				1.769						
RTFO δ, 76°C		80.66	76.80	64.96	82.57	80.24	81.27	80.10	80.66	79.08
RTFO δ, 82°C	83.16	82.96	79.49	67.76	84.75	82.89	83.65	82.68	83.05	81.72
RTFO δ, 88°C	85.08	84.89	81.86	70.72		85.01	85.56	84.77	85.01	83.96
RTFO δ, 94°C			83.92	73.59						85.86
RTFO δ, 100°C				76.35						
RTFO δ, 106°C				78.93						
<i>RTFO failure temp.</i>	<i>78.47</i>	<i>82.81</i>	<i>89.42</i>	<i>103.9</i>	<i>80.35</i>	<i>84.77</i>	<i>83.88</i>	<i>85.65</i>	<i>84.27</i>	<i>88.33</i>
Dynamic Shear, 10 rad/sec, specification: G* sin delta <5000 kPa										
PAV G* sin δ, 25.0°C	5999				6227					
PAV G* sin δ, 28.0°C	4181	5950			4559	6017			5581	
PAV G* sin δ, 31.0°C	2861	4355			3246	4385	5452	5558	4072	
PAV G* sin δ, 34.0°C			5339	8786			4018	4120	2920	5267
PAV G* sin δ, 37.0°C			3886	6901					2031	3903
PAV G* sin δ, 40.0°C				4721						
PAV G*, 25.0°C	8.55E+6									
PAV G*, 28.0°C	5.68E+6	8.77E+6			9.83E+6	9.46E+6			8.60E+6	
PAV G*, 31.0°C	3.72E+6	6.16E+6			6.73E+6	6.50E+6	8.35E+6	8.78E+6	5.95E+6	
PAV G*, 34.0°C			7.59E+6	1.48E+7	4.55E+6		5.83E+6	6.16E+6	4.06E+6	7.65E+6
PAV G*, 37.0°C			5.33E+6	1.12E+7					2.70E+6	5.42E+6
PAV G*, 40.0°C				7.19E+6						
PAV δ, 25.0°C	44.56				39.69					
PAV δ, 28.0°C	47.41	42.73			42.60	39.50			40.45	
PAV δ, 31.0°C	50.20	45.01			45.57	42.43	40.75	39.27	43.23	
PAV δ, 34.0°C			44.74	36.51			43.75	41.98	45.97	43.49
PAV δ, 37.0°C			46.85	38.19					48.82	45.82
PAV δ, 40.0°C				41.08						
<i>PAV failure temp.</i>	<i>26.50</i>	<i>29.67</i>	<i>34.62</i>	<i>40.43</i>	<i>27.10</i>	<i>27.76</i>	<i>31.85</i>	<i>32.06</i>	<i>29.08</i>	<i>34.52</i>
Creep Stiffness, 60 sec, specification: Stiffness < 300 MPa and m-value > 0.300										
Stiffness, 0°C			142	193		87	100	101		135
M-value, 0°C			0.338	0.276		0.341	0.333	0.32		0.314
Stiffness, -6°C	142	174	293	352	140	160	178	181	179	225
M-value, -6°C	0.350	0.317	0.289	0.248	0.319	0.294	0.284	0.282	0.304	0.272

Stiffness, -12°C	279	360			271				355	
M-value, -12°C	0.297	0.276			0.275				0.253	
Stiffness failure temp.	-22.6	-20.5	-16.2	-14.4	-22.9	-22.2	-21.4	-21.2	-20.5	-19.4
M-value failure temp.	-21.7	-18.5	-14.7	-4.9	-18.6	-15.2	-14.0	-13.2	-16.5	-12.0
Performance Grade	82-16	82-16	82-10	NA	82-16	82-10	82-10	82-10	82-16	82-10

Shaded cells indicate the failure temperature.

APPENDIX F
BINDER MASTERCURVE RESULTS

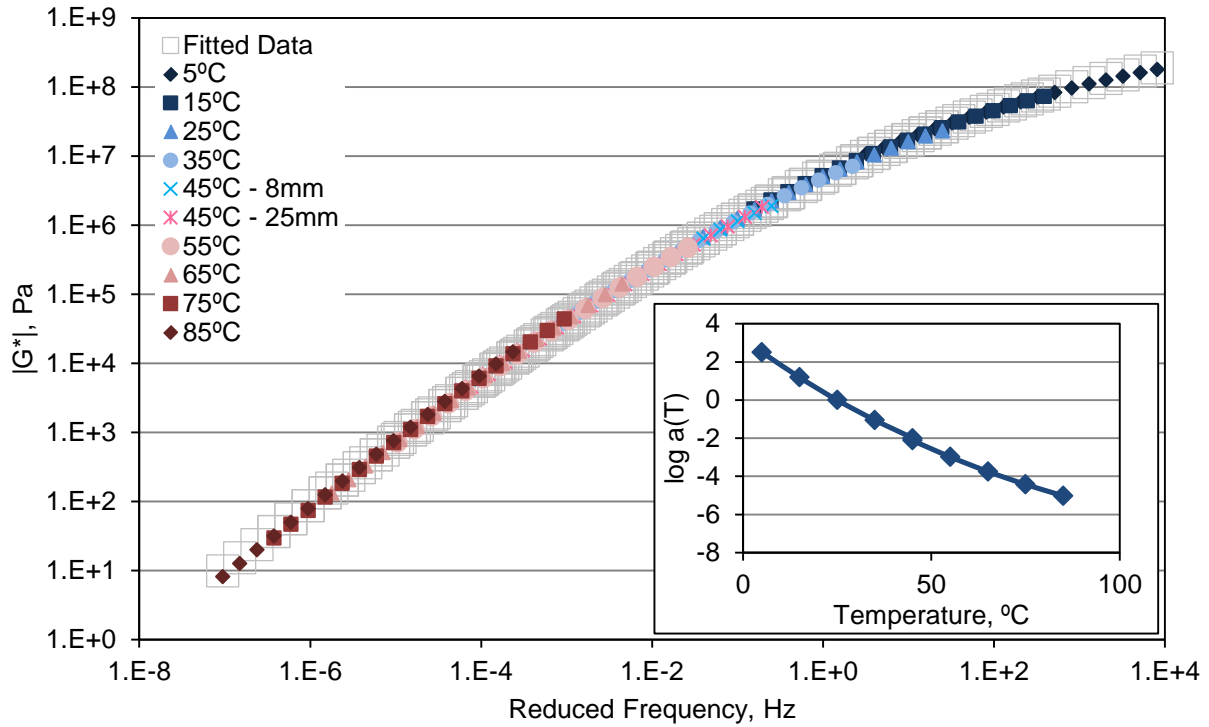


Figure F1. Extracted Binder Mastercurve for Section A, Bottom Half of Cores

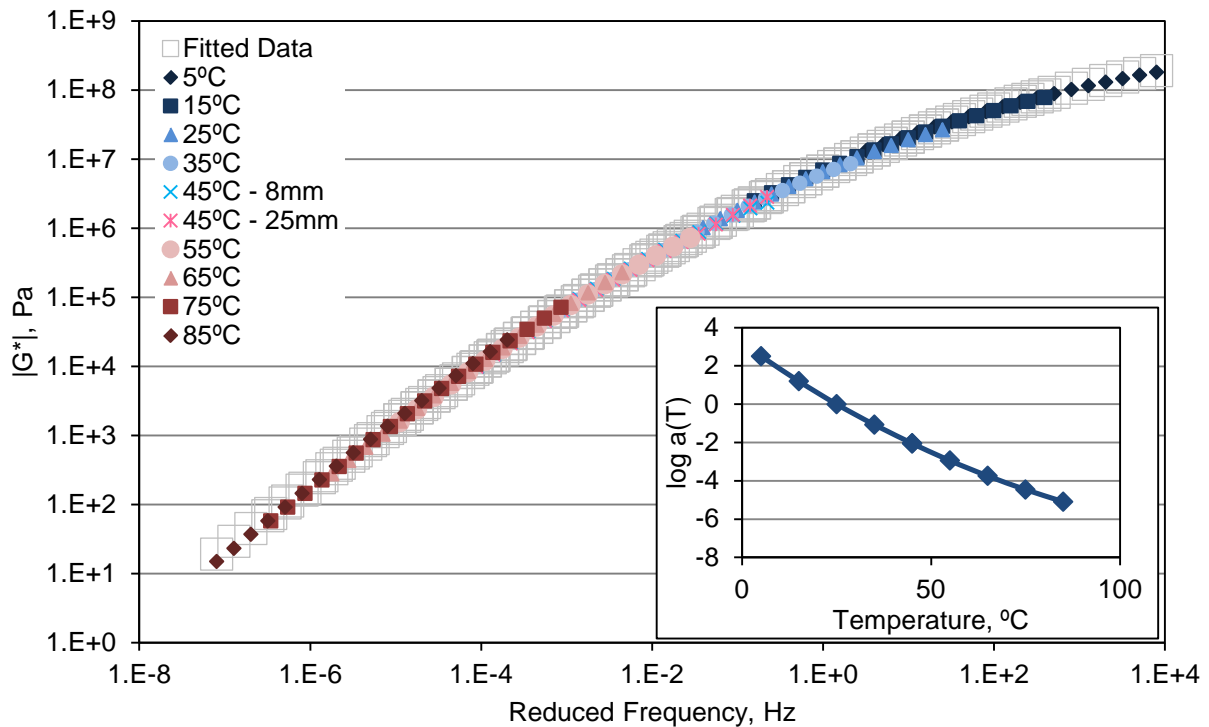


Figure F2. Extracted Binder Mastercurve for Section A, Top Half of Cores

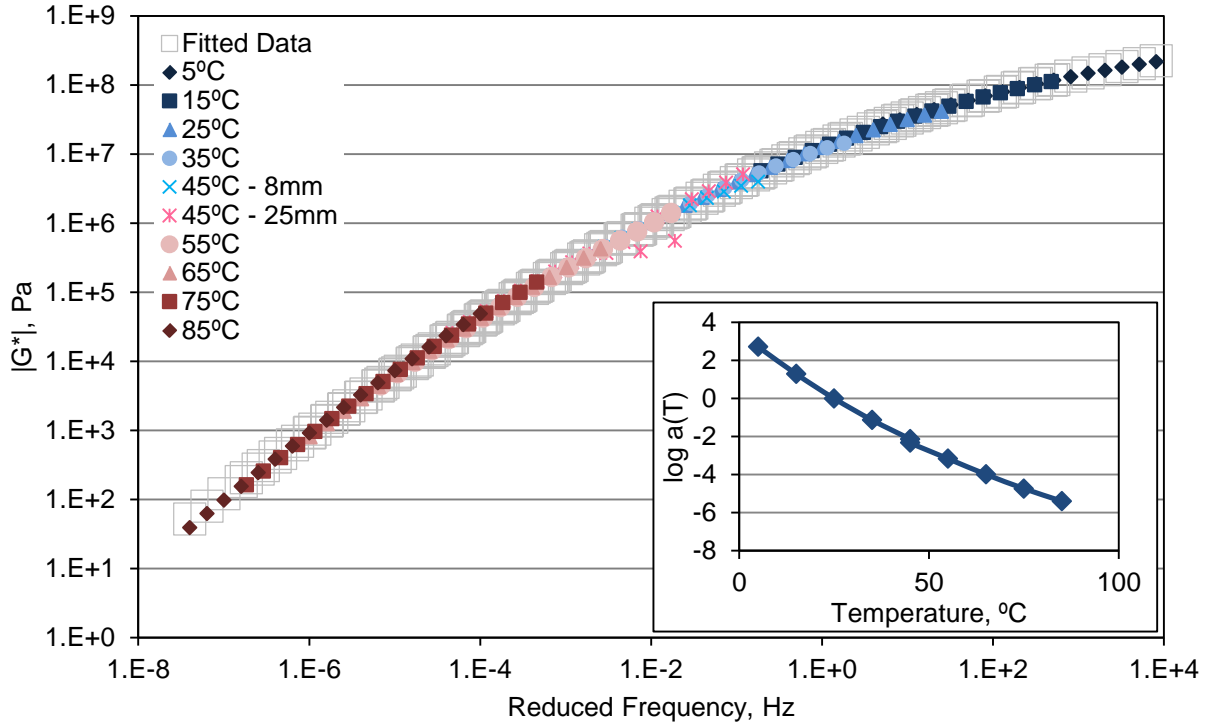


Figure F3. Extracted Binder Mastercurve for Section B, Bottom Half of Cores

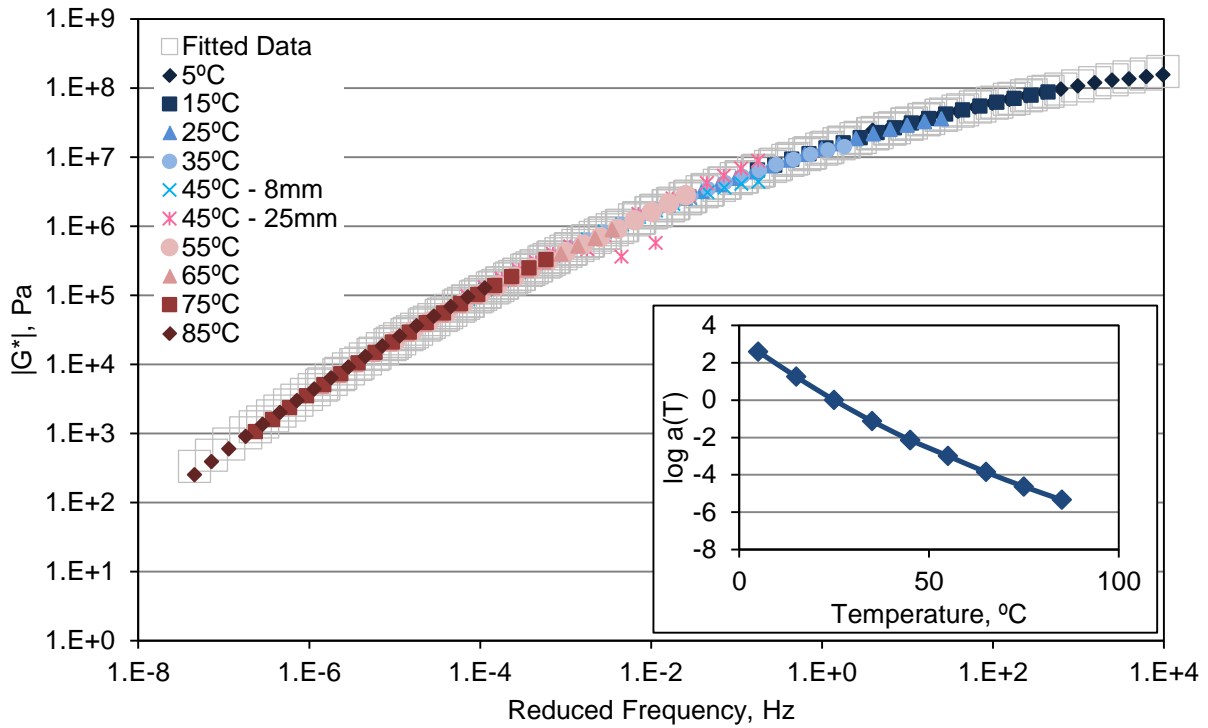


Figure F4. Extracted Binder Mastercurve for Section B, Top Half of Cores

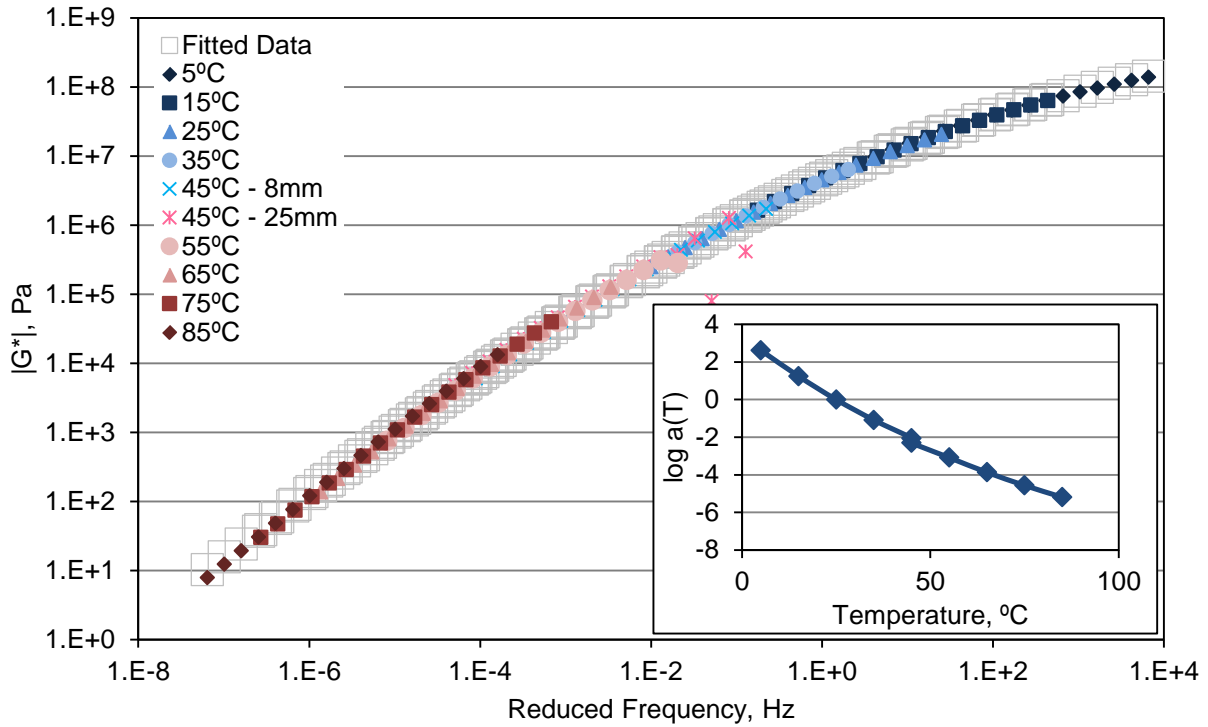


Figure F5. Extracted Binder Mastercurve for Section B, Intermediate Layer, Entire Core

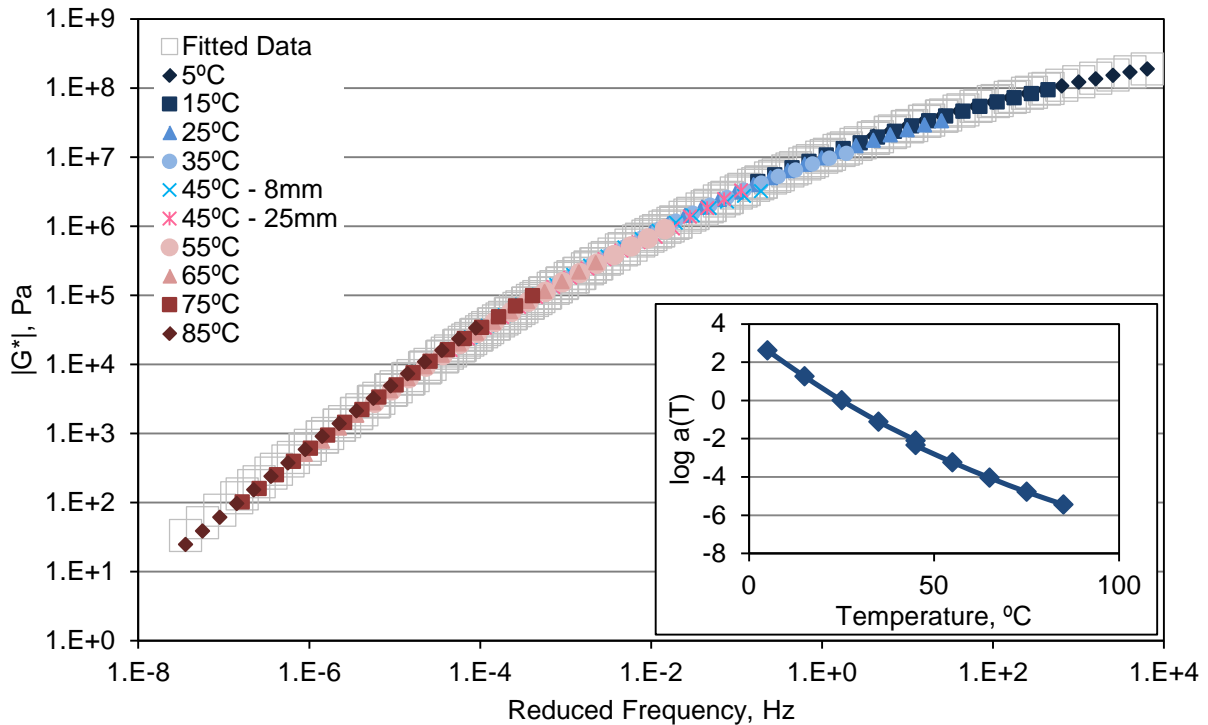


Figure F6. Extracted Binder Mastercurve for Section C, Entire Core

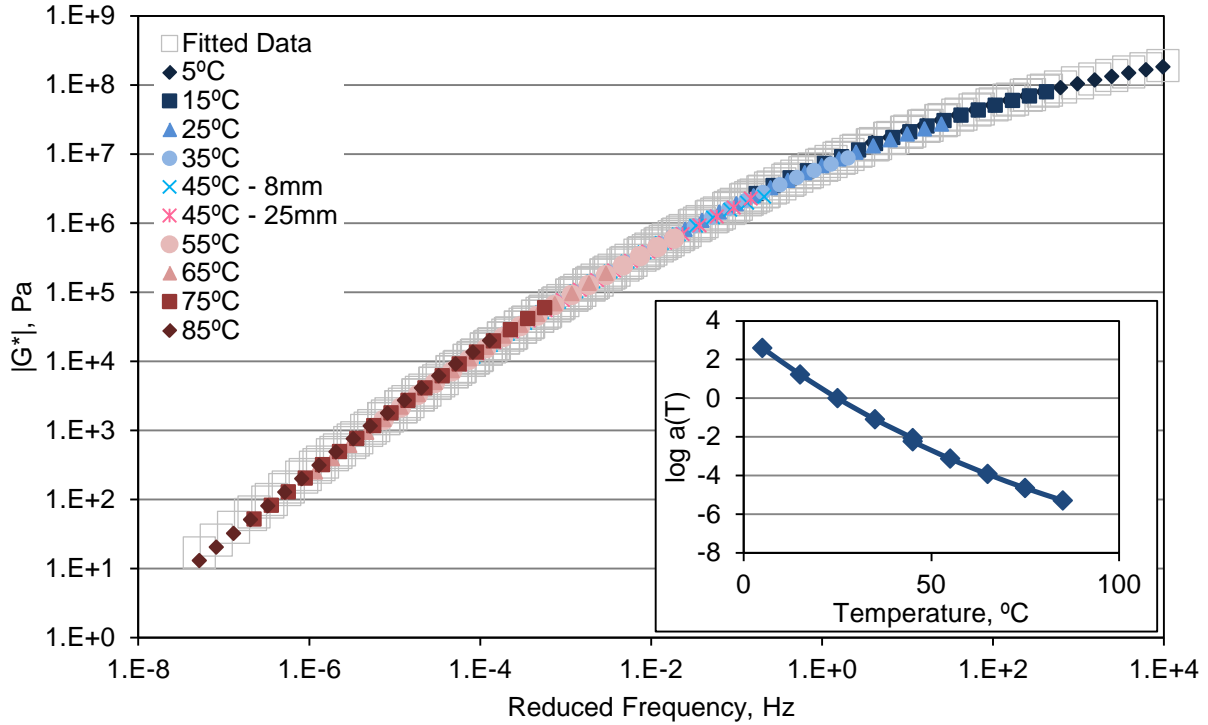


Figure F7. Extracted Binder Mastercurve for Section D, Entire Core

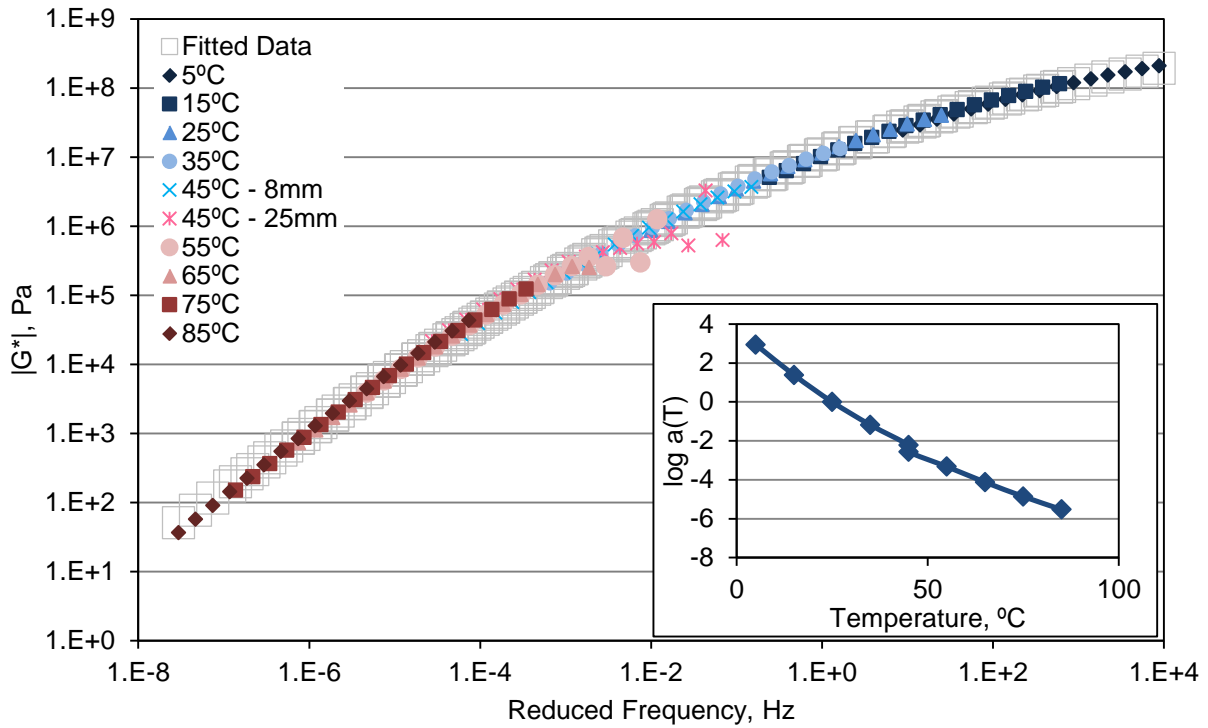


Figure F8. Extracted binder Mastercurve for Section E, Entire Core

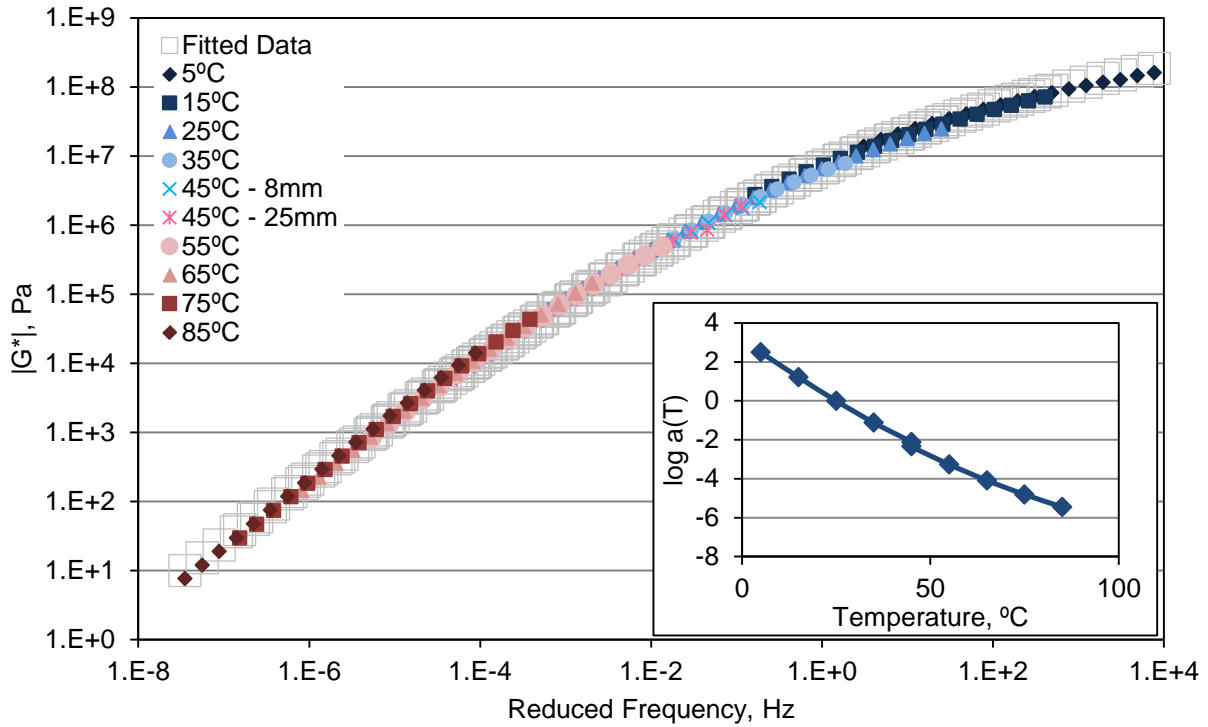


Figure F9. Extracted Binder Mastercurve for Section F, Bottom Half of Cores

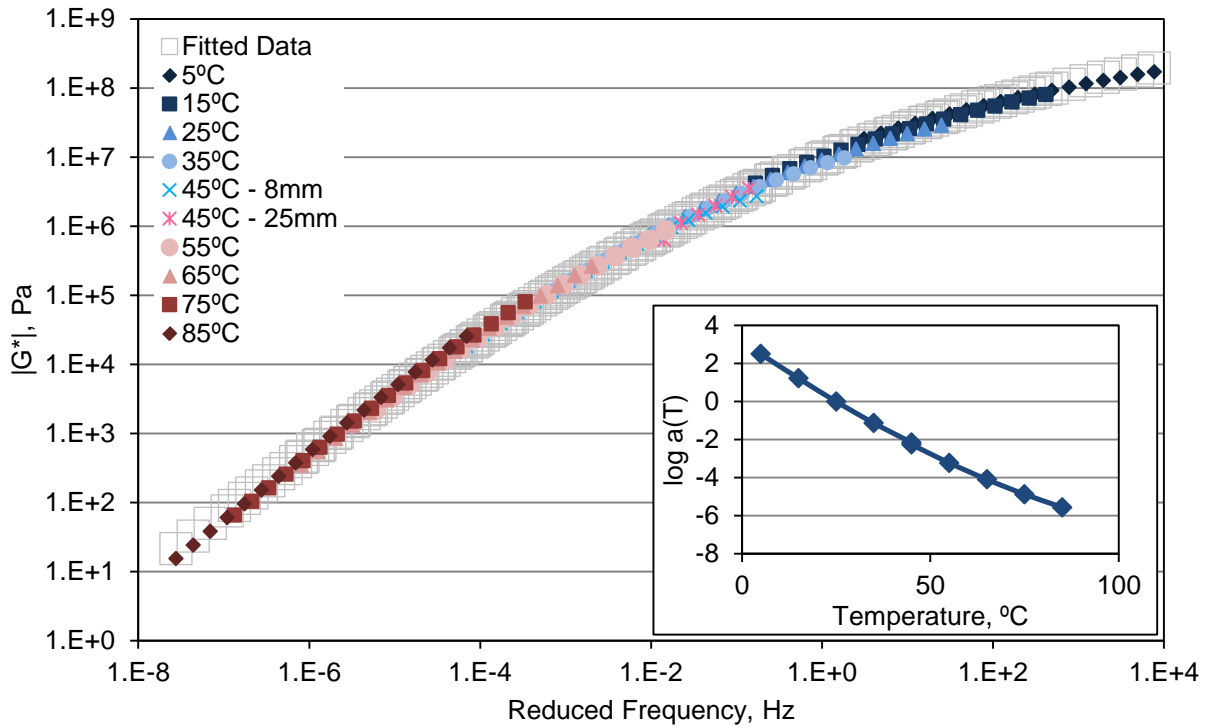


Figure F10. Extracted Binder Mastercurve for Section F, Top Half of Cores

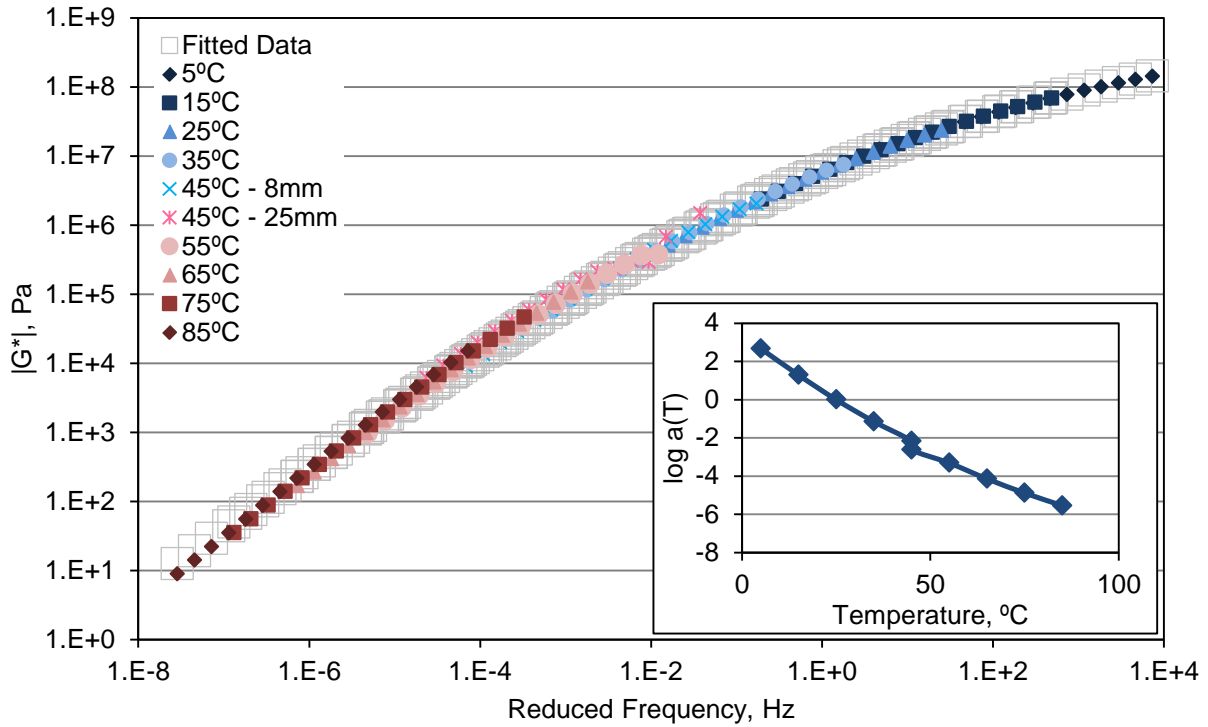


Figure F11. Extracted Binder Mastercurve for Section H, Bottom Half of Cores

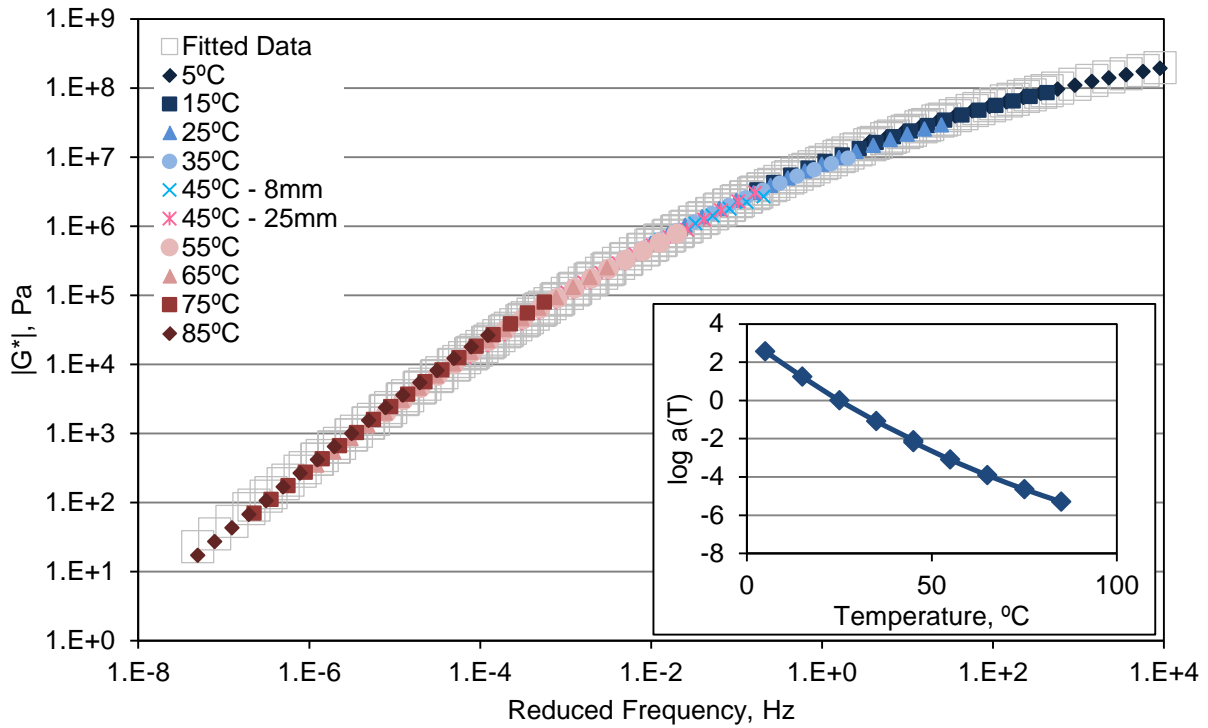


Figure F12. Extracted Binder Mastercurve for Section H, Top Half of Cores

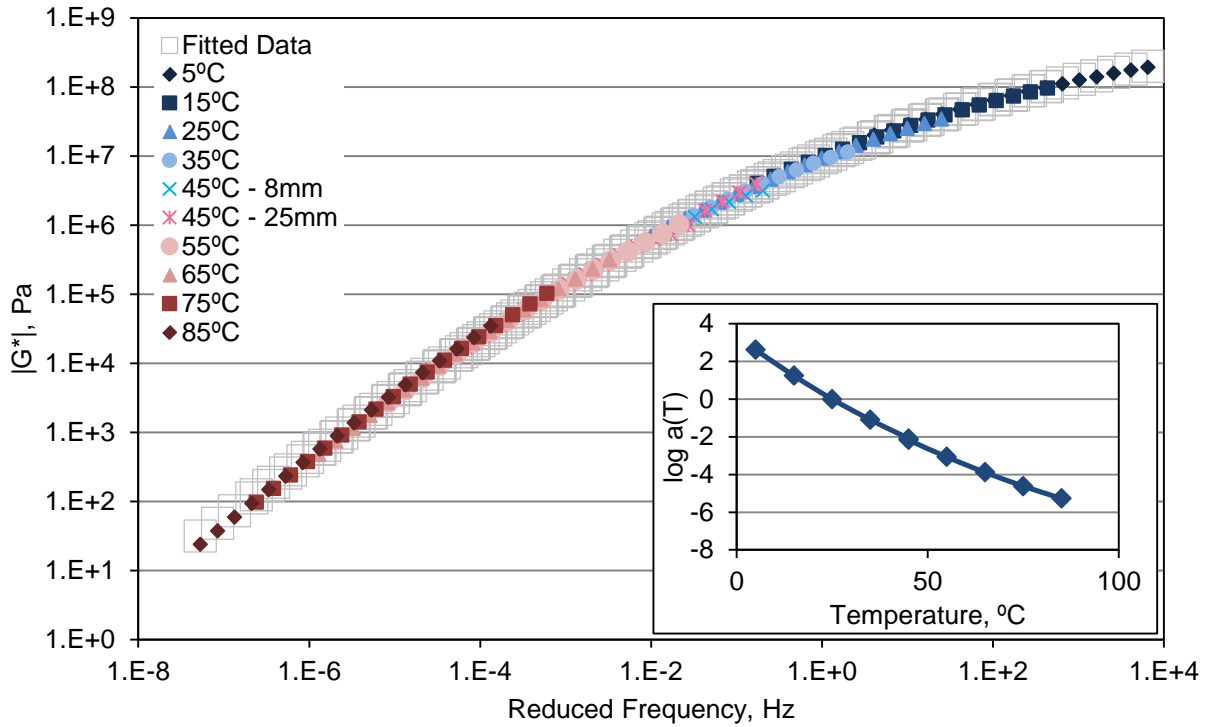


Figure F13. Extracted Binder Mastercurve for Section I, Bottom Half of Cores

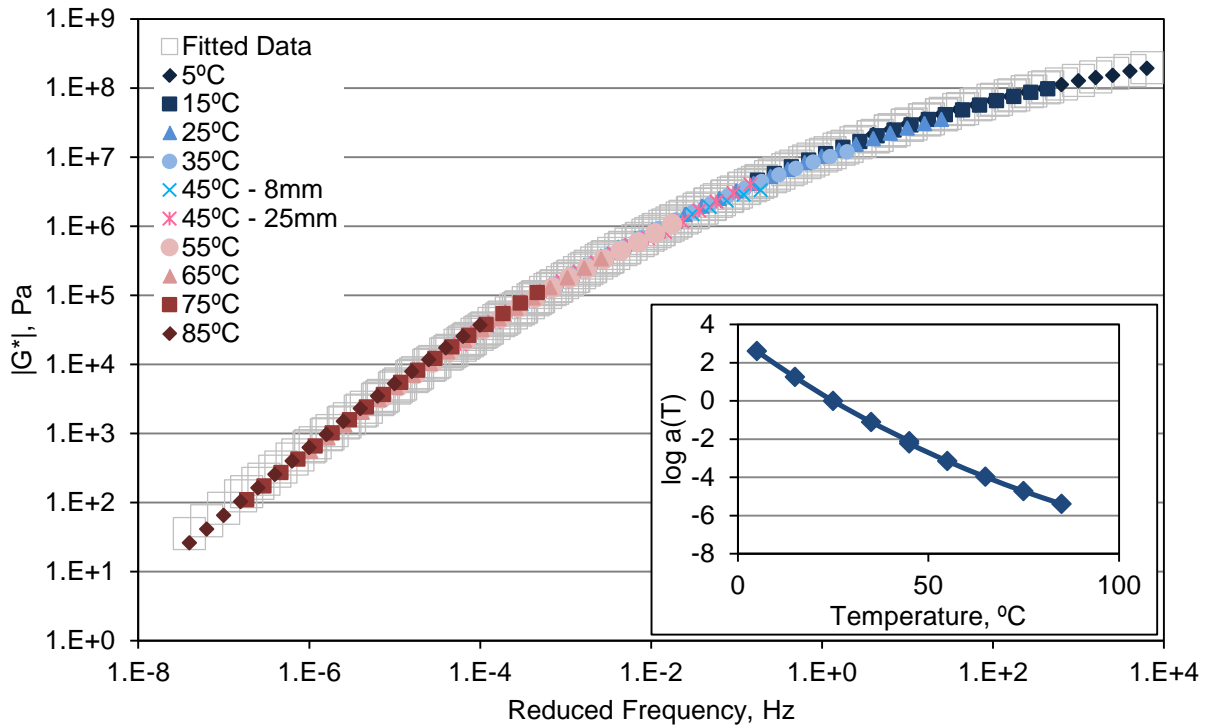


Figure F14. Extracted Binder Mastercurve for Section I, Top Half of Cores

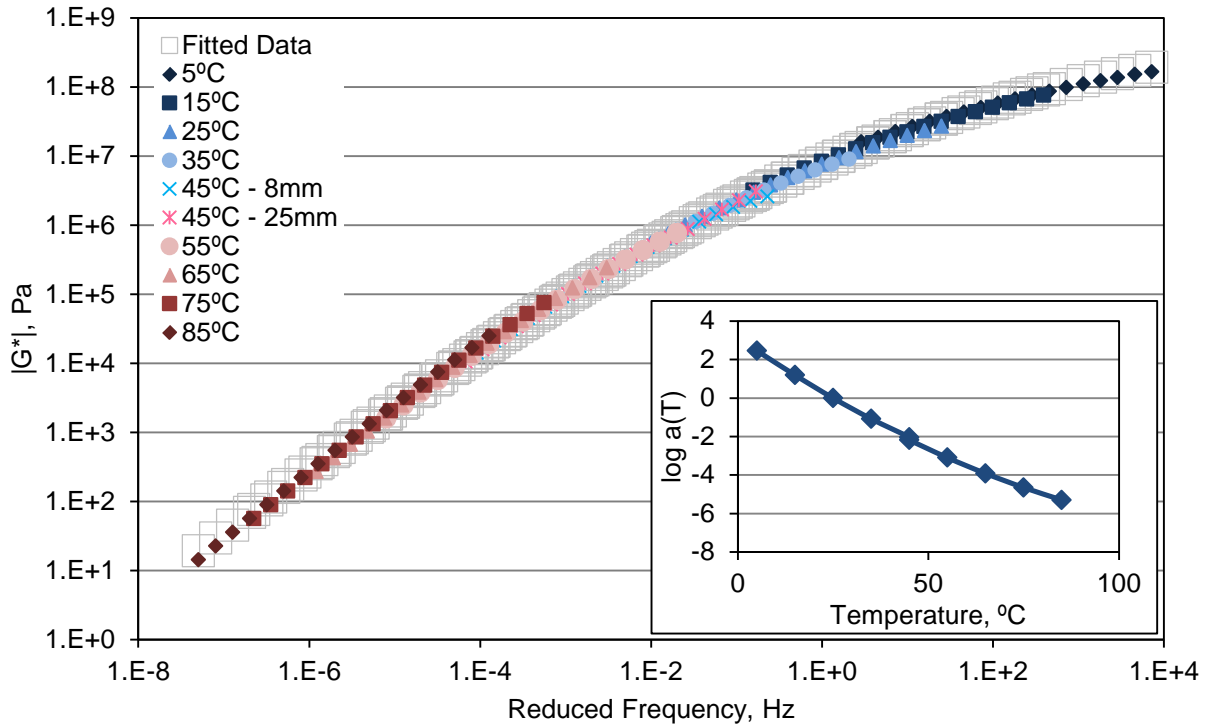


Figure F15. Extracted Binder Mastercurve for Section J, Entire Core

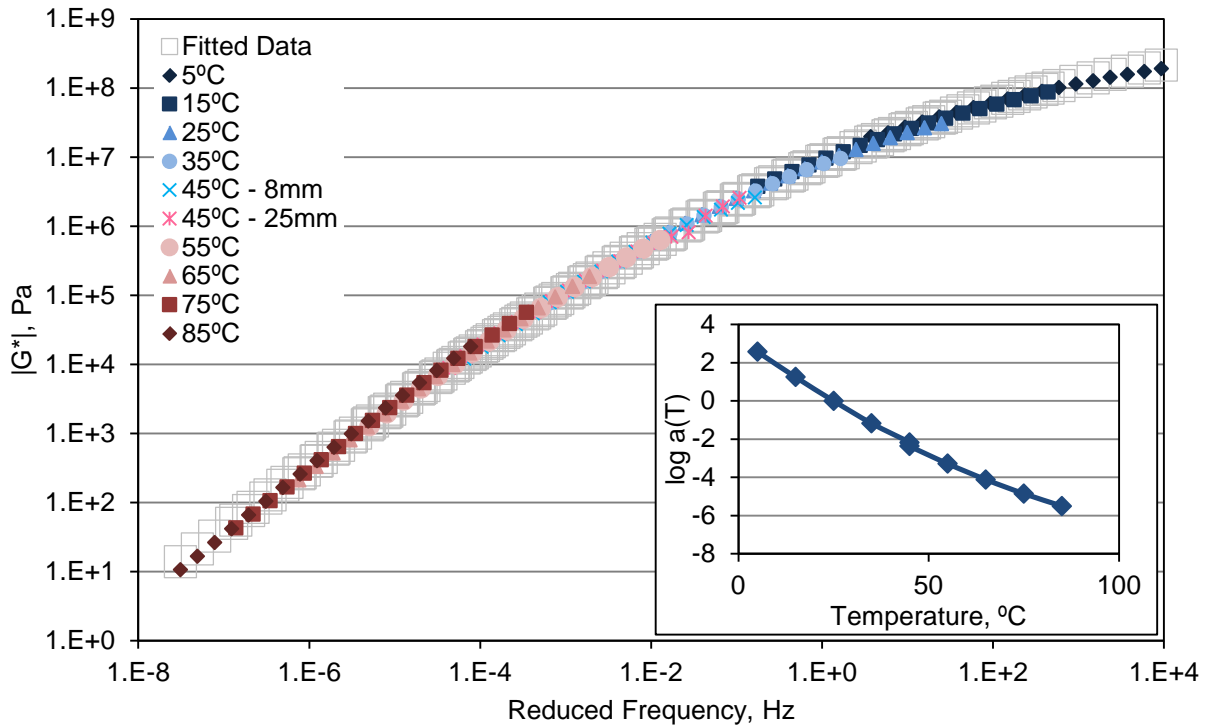


Figure F16. Extracted Binder Mastercurve for Section K, Entire Core

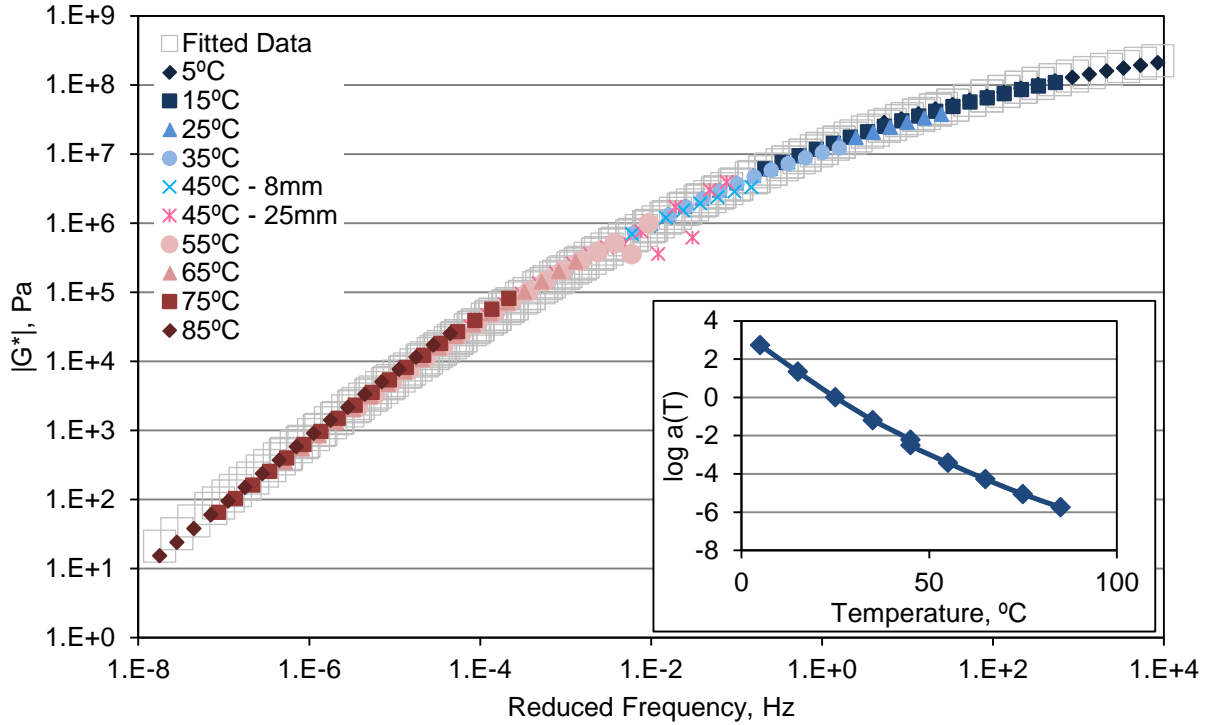


Figure F17. Extracted Binder Mastercurve for Section L, Entire Core

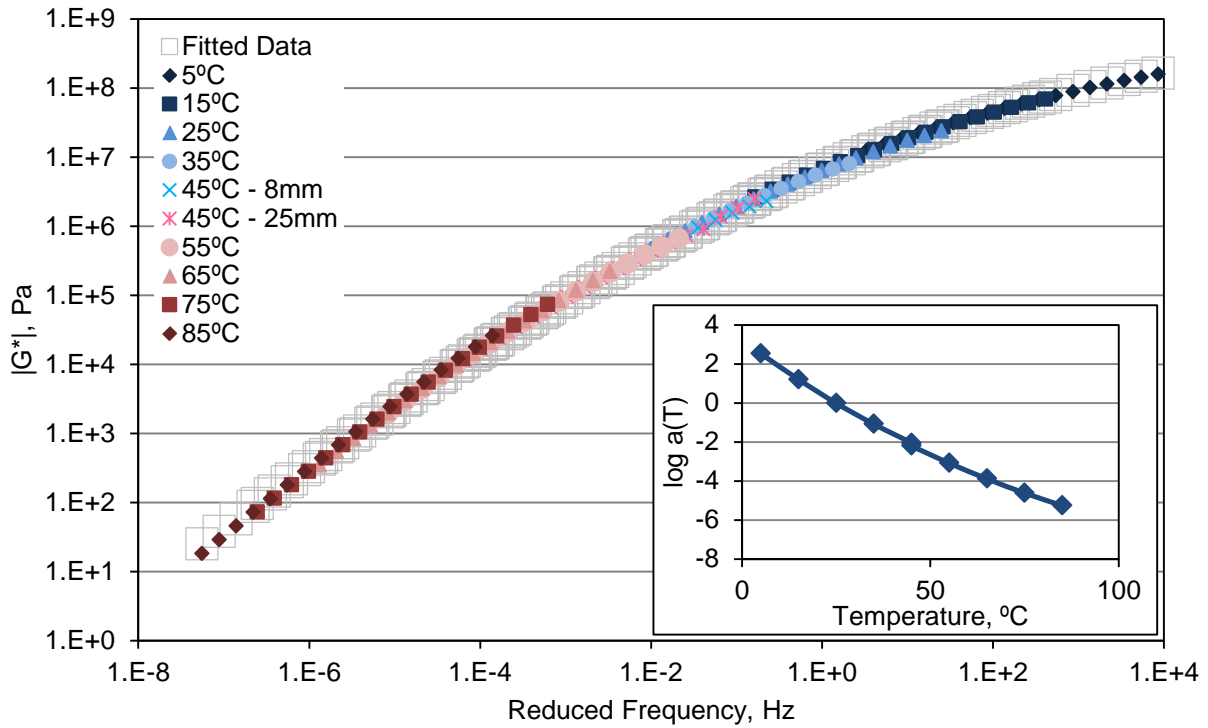


Figure F18. Extracted Binder Mastercurve for Section M, Entire Core

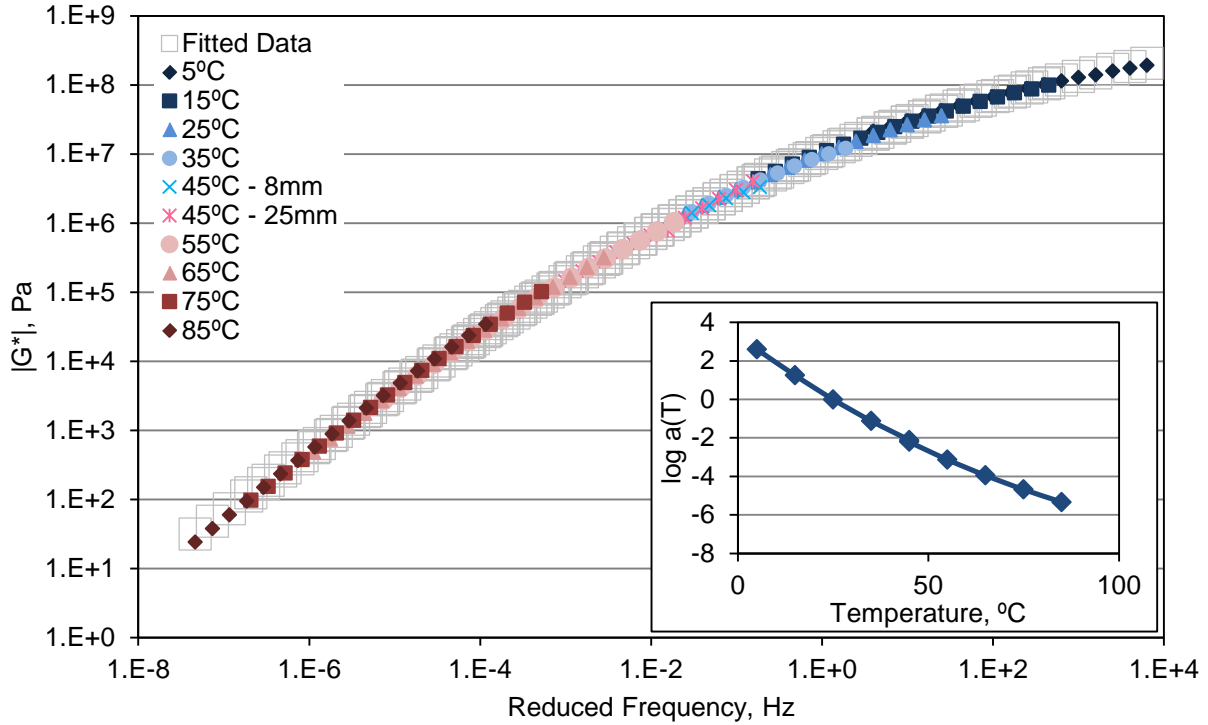


Figure F19. Extracted Binder Mastercurve for Section N, Bottom Half of Cores

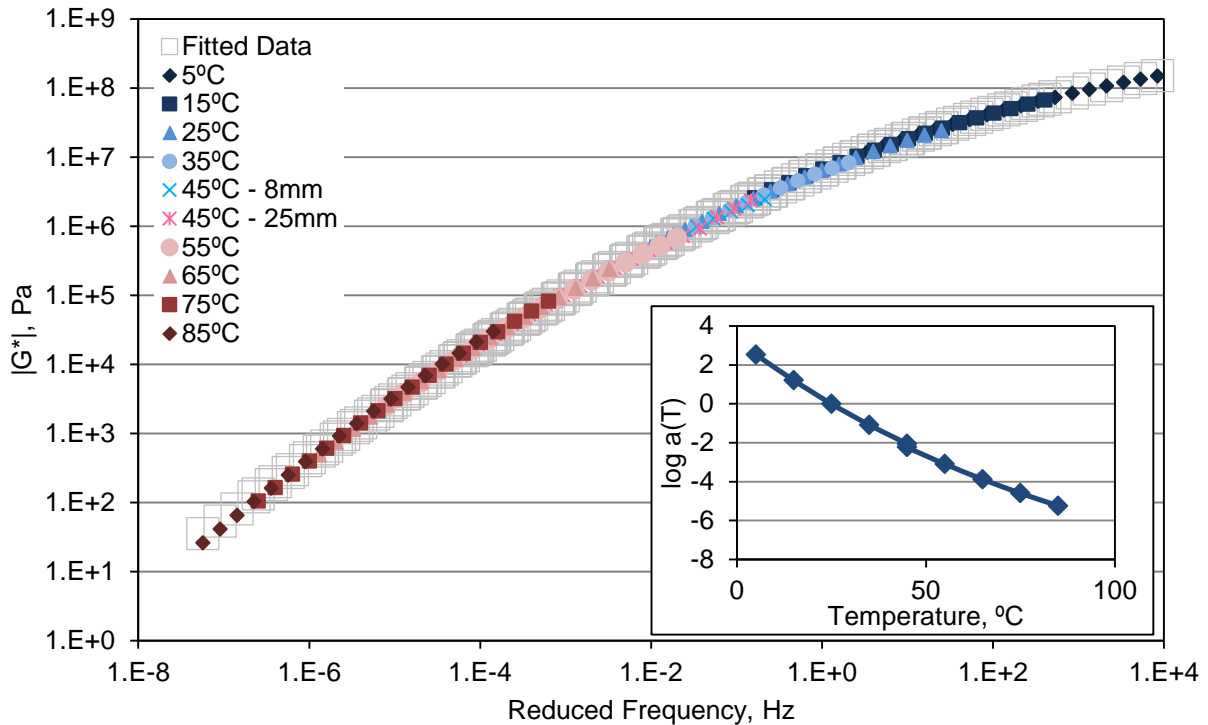


Figure F20. Extracted Binder Mastercurve for Section N, Top Half of Cores

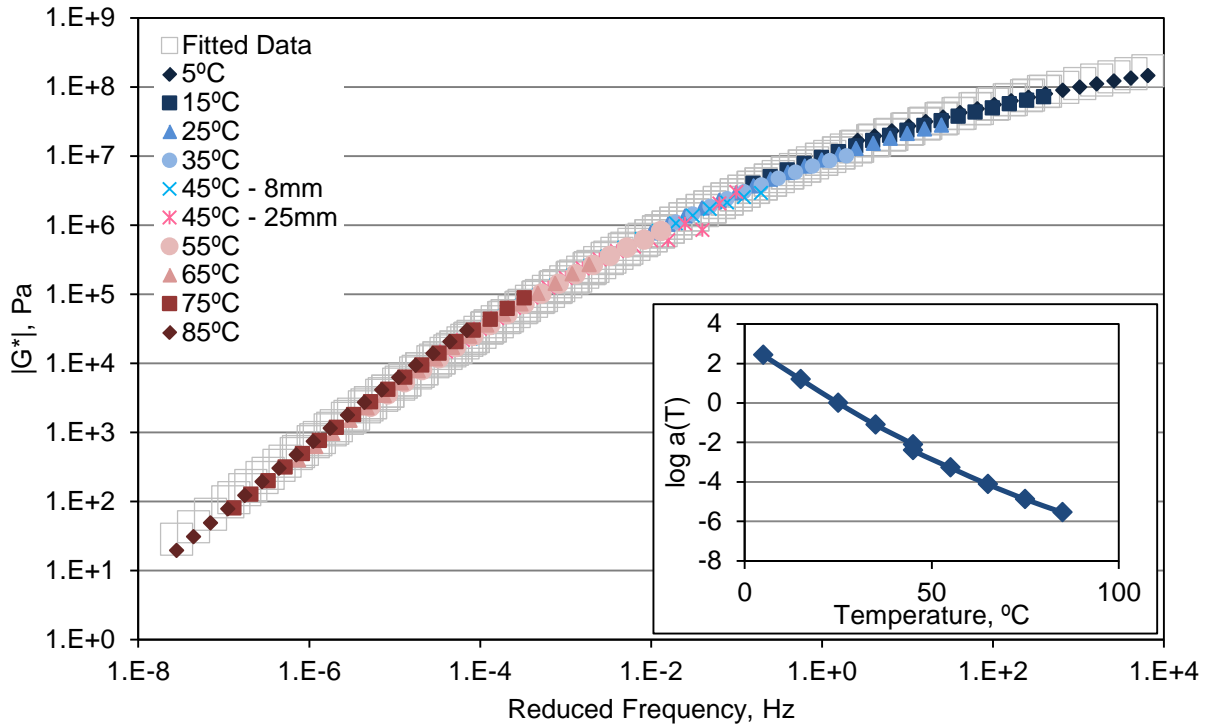


Figure F21. Extracted Binder Mastercurve for Section O, Entire Core

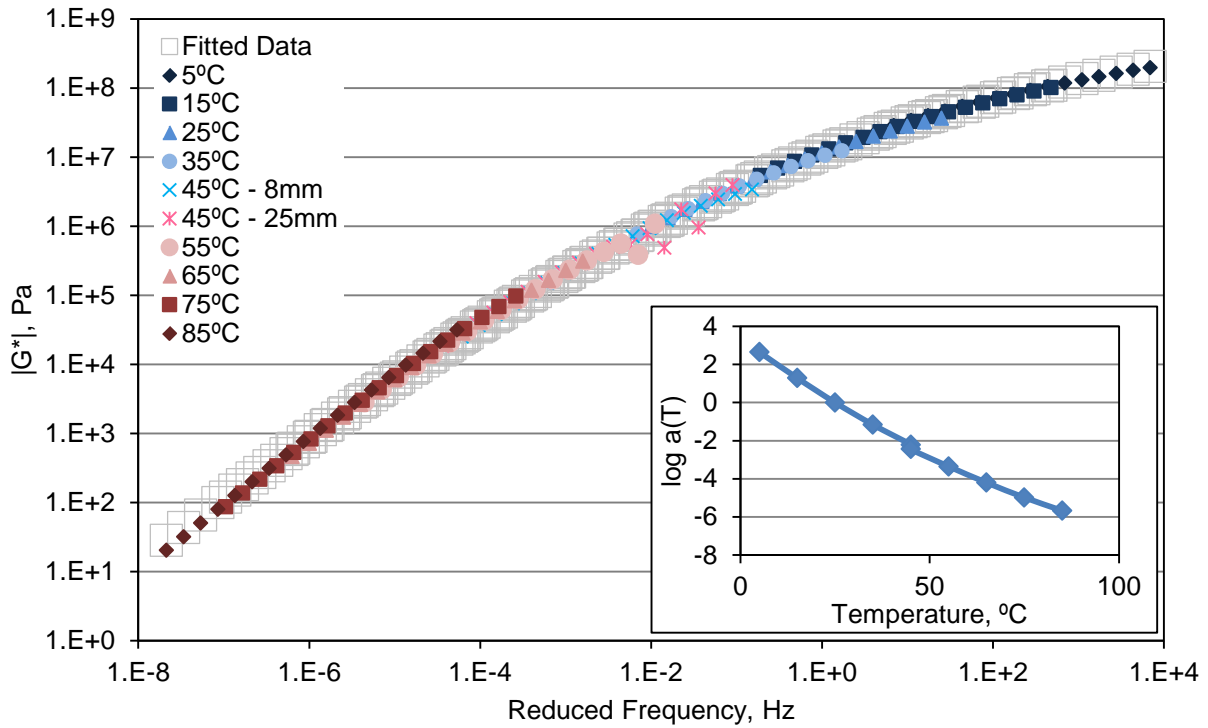


Figure F22. Extracted Binder Mastercurve for Section P, Entire Core

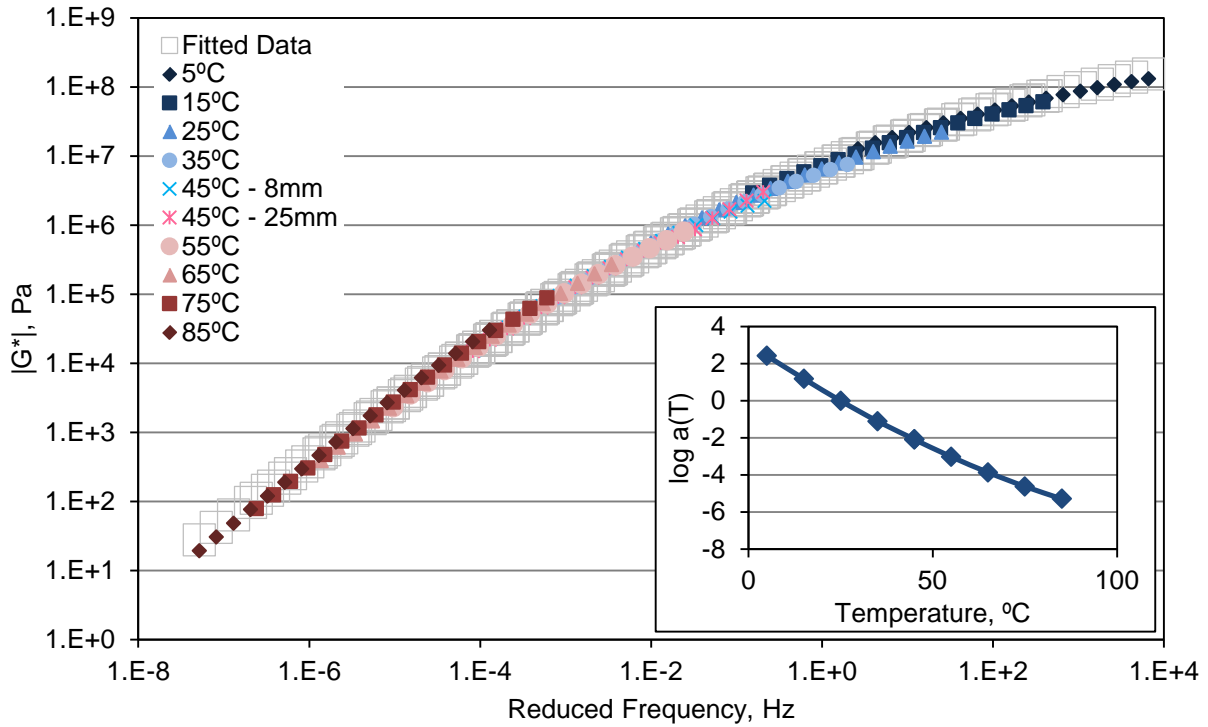


Figure F23. Extracted Binder Mastercurve for Section Q, Bottom Half of Cores

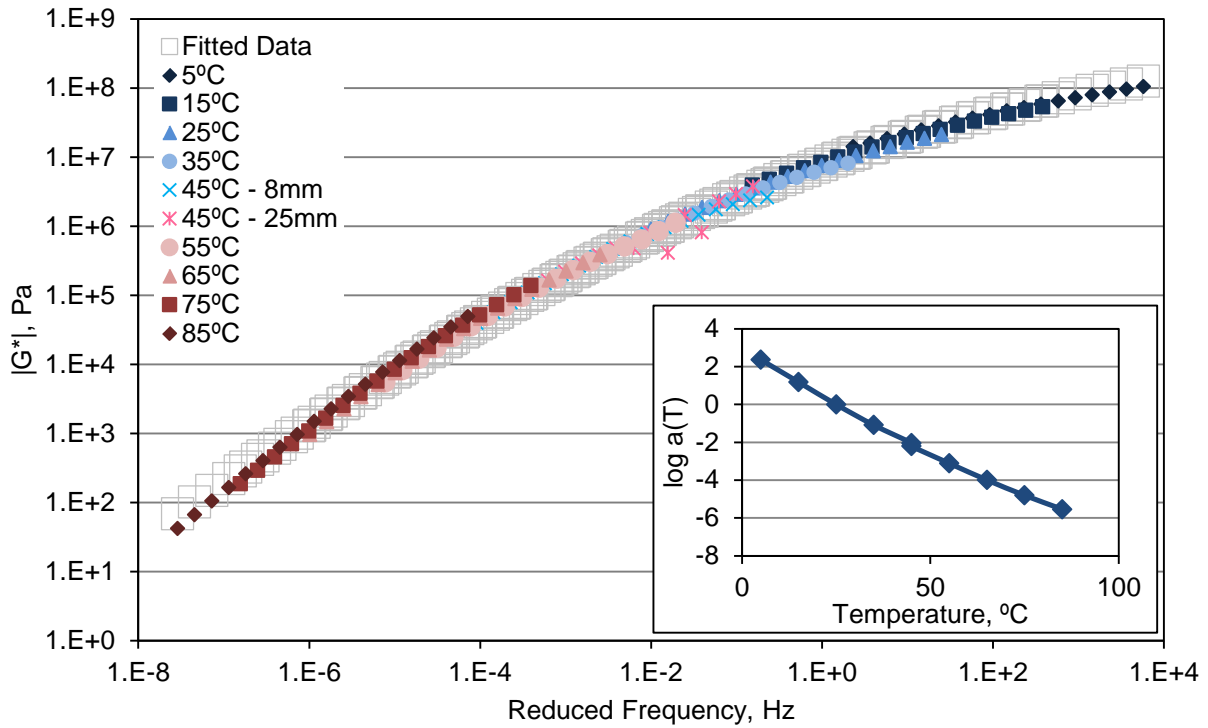


Figure F24. Extracted Binder Mastercurve for Section Q, Top Half of Cores

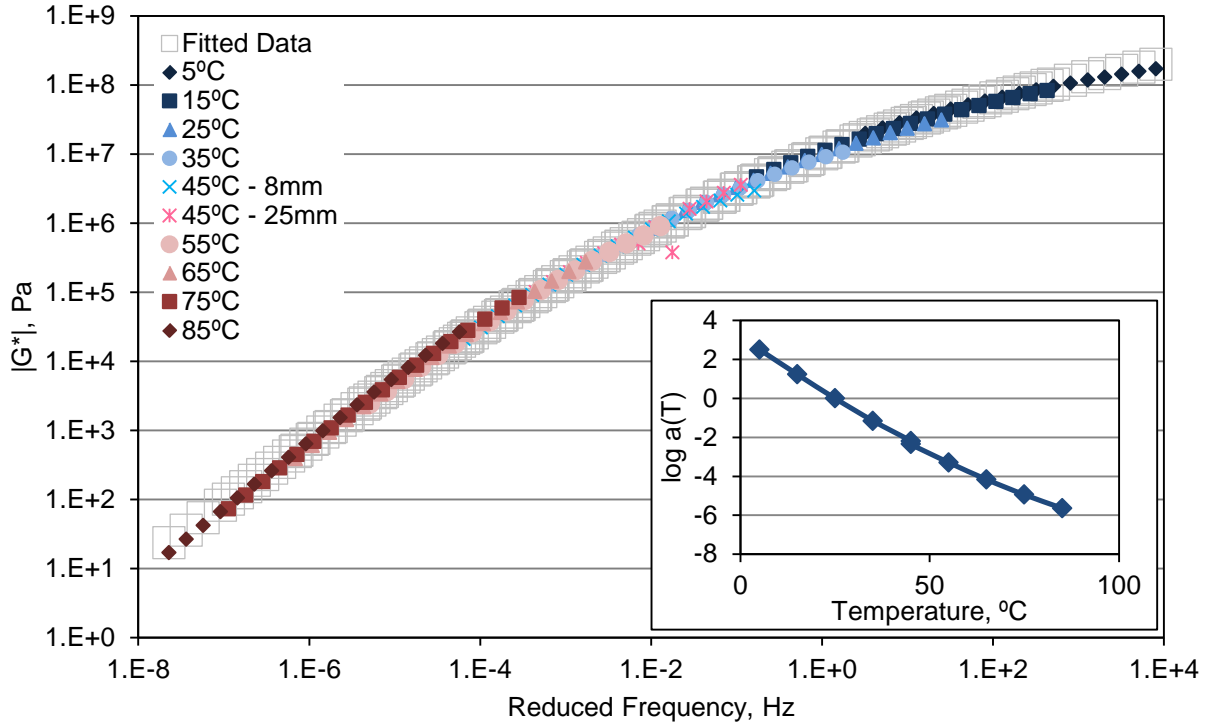


Figure F25. Extracted Binder Mastercurve for Section R, Bottom Half of Cores

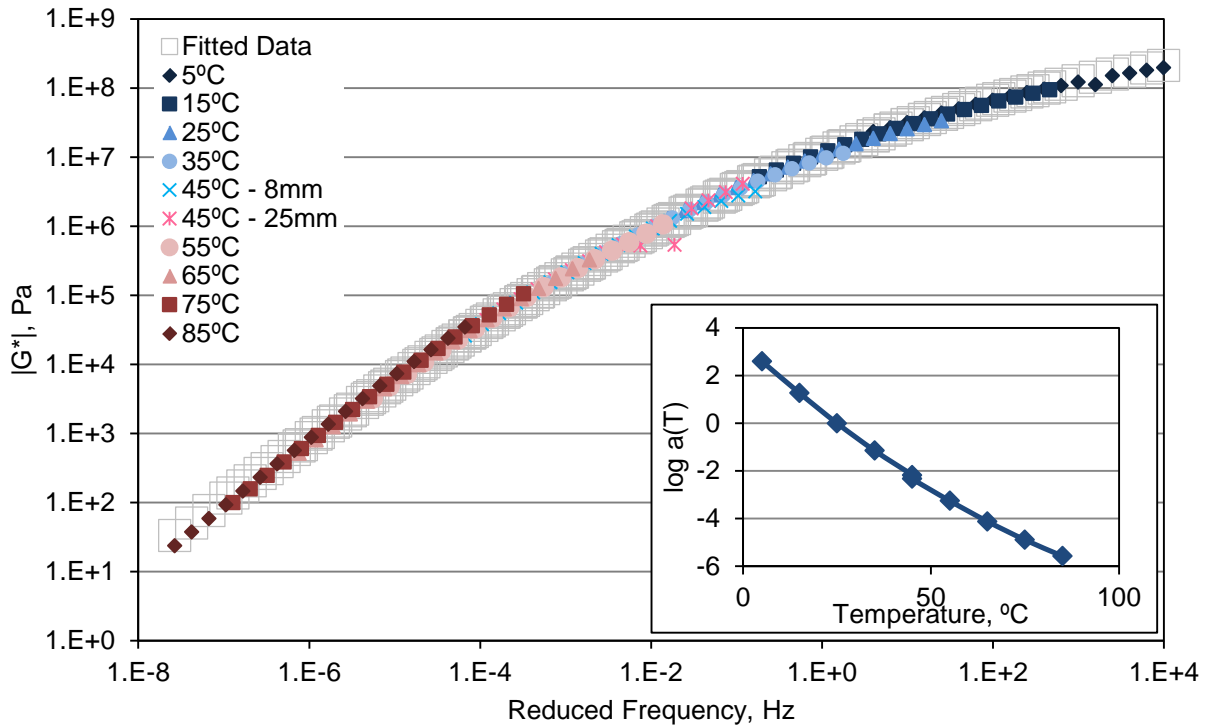


Figure F26. Extracted Binder Mastercurve for Section R, Top Half of Cores

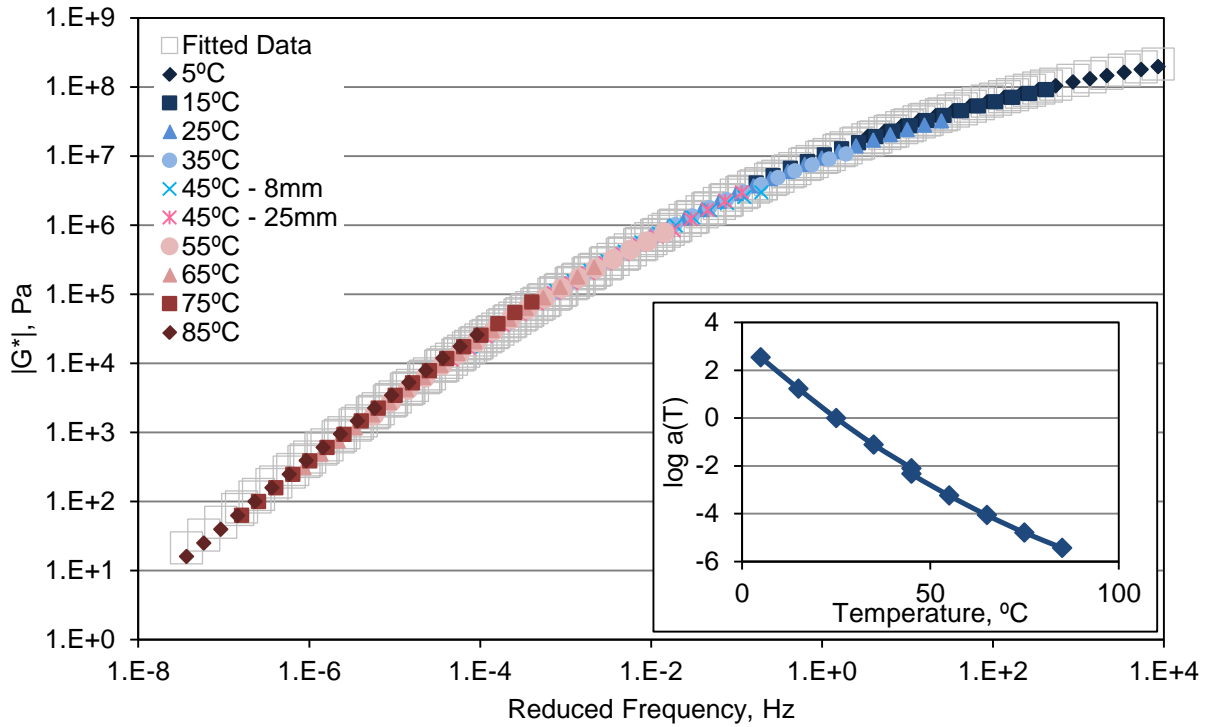


Figure F27. Extracted Binder Mastercurve for Section S, Bottom Half of Cores

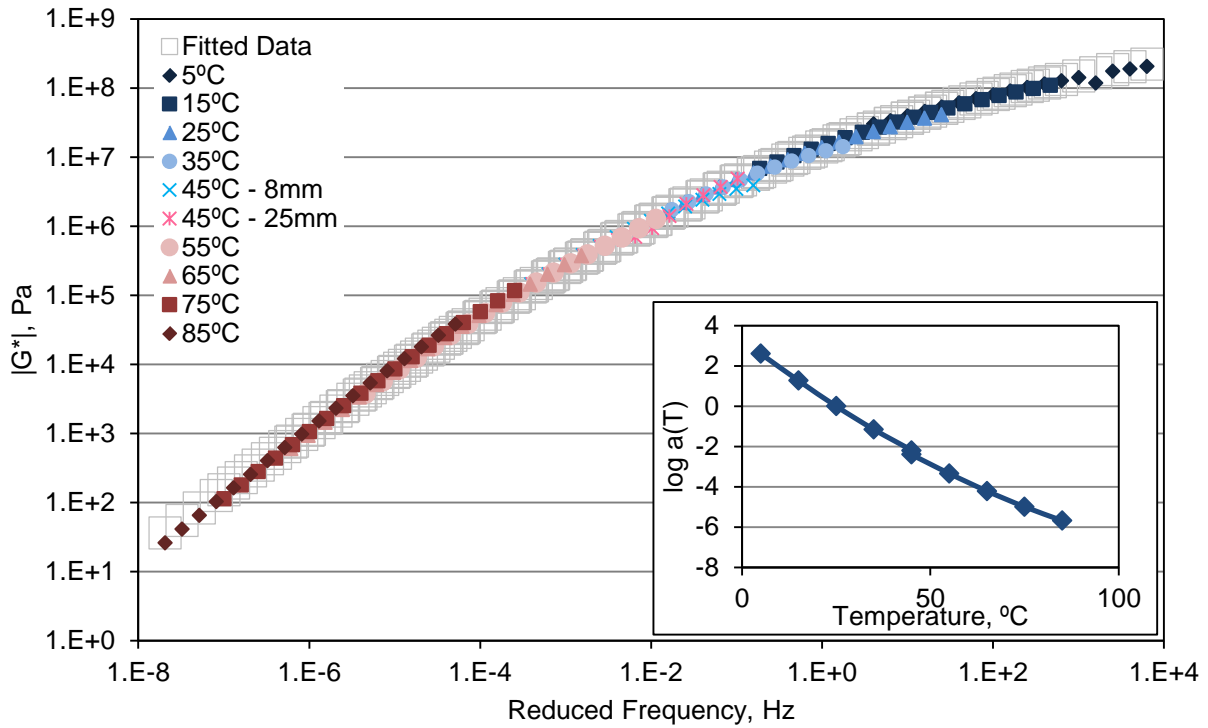


Figure F28. Extracted Binder Mastercurve for Section S, Top Half of Cores

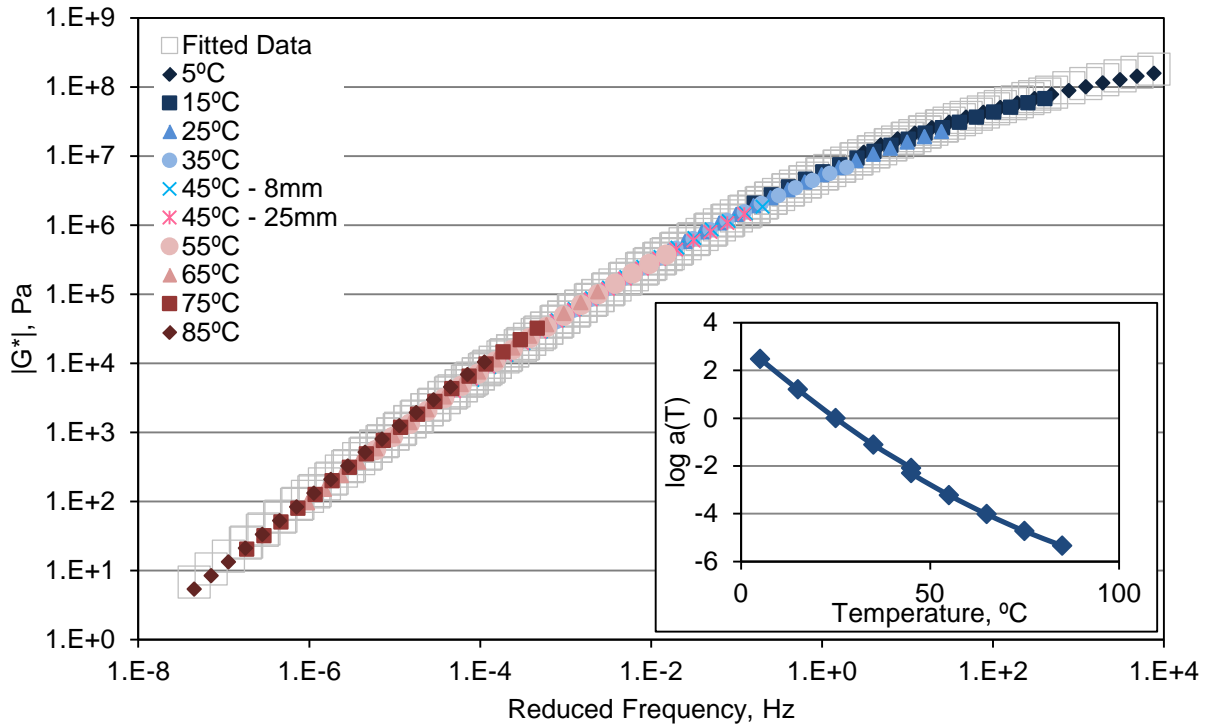


Figure F29. Extracted Binder Mastercurve for Section U, Entire Core

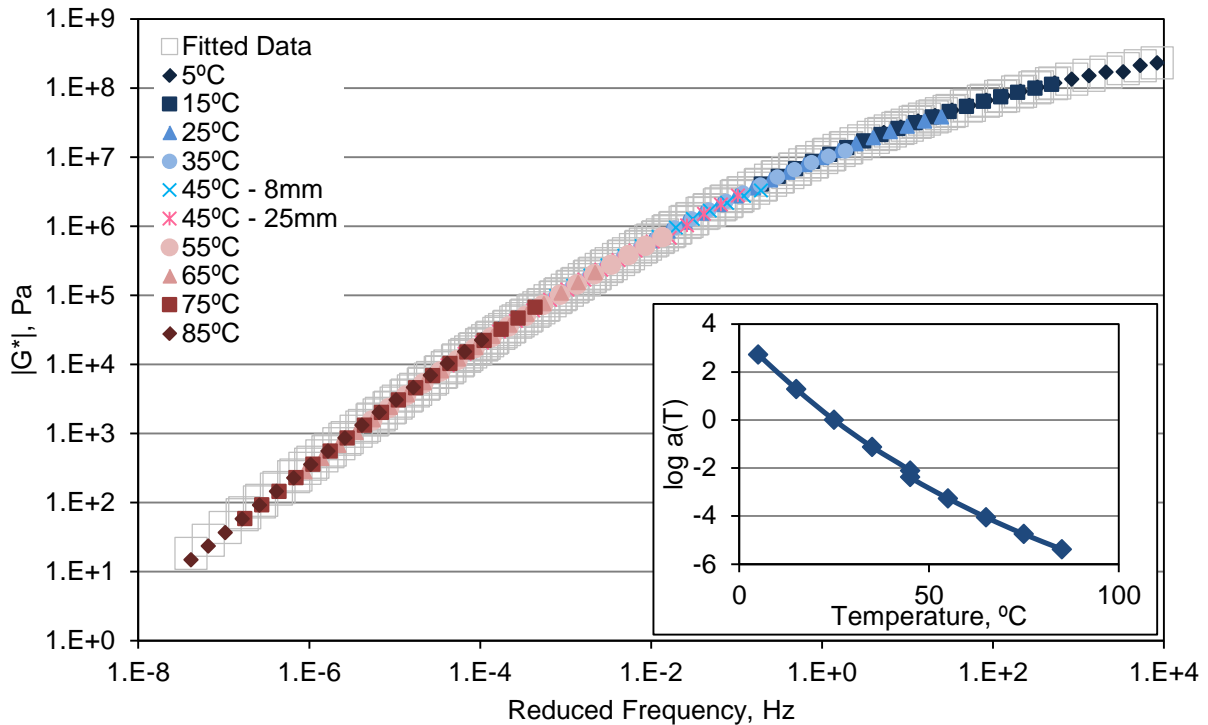


Figure F30. Extracted Binder Mastercurve for Section V, Bottom Half of Cores

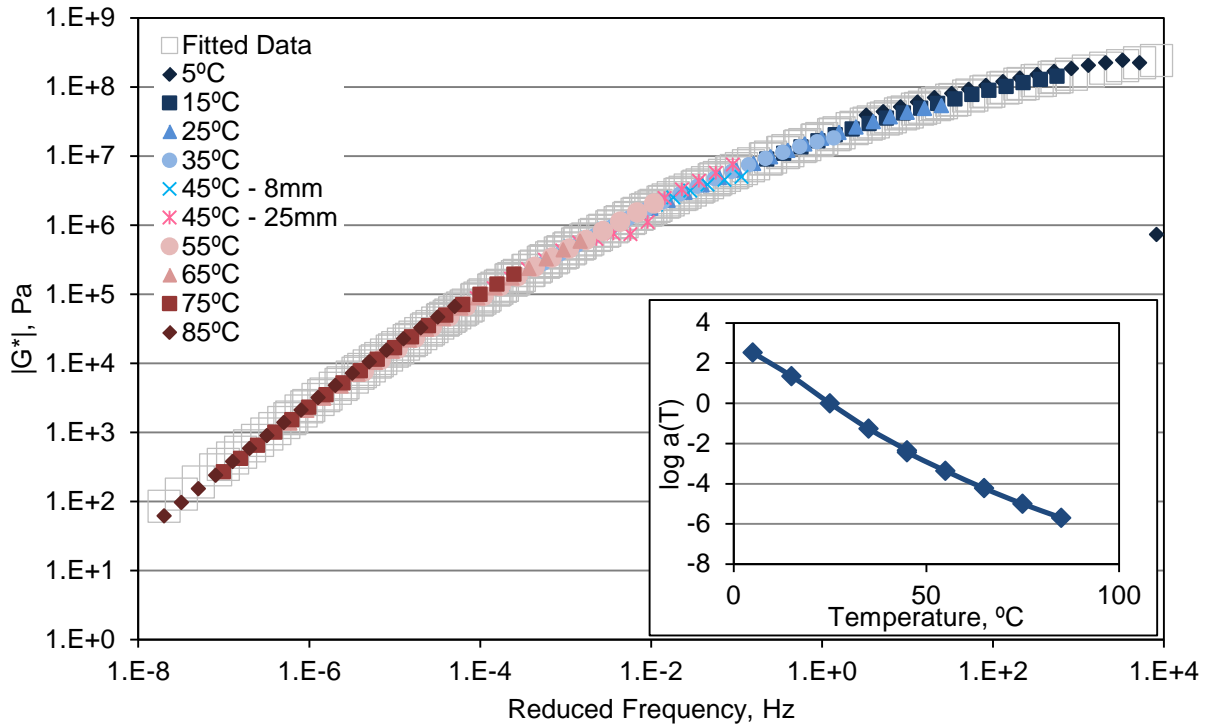


Figure F31. Extracted Binder Mastercurve for Section V, Top Half of Cores

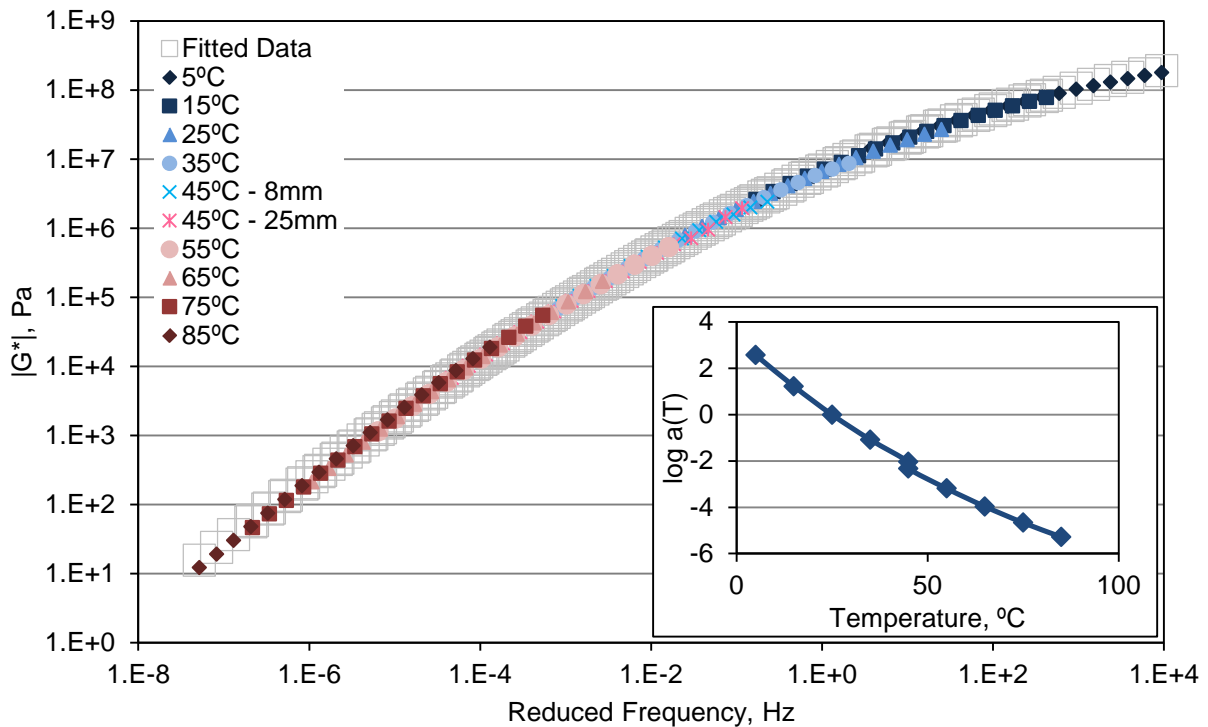


Figure F32. Extracted Binder Mastercurve for Section W, Entire Core

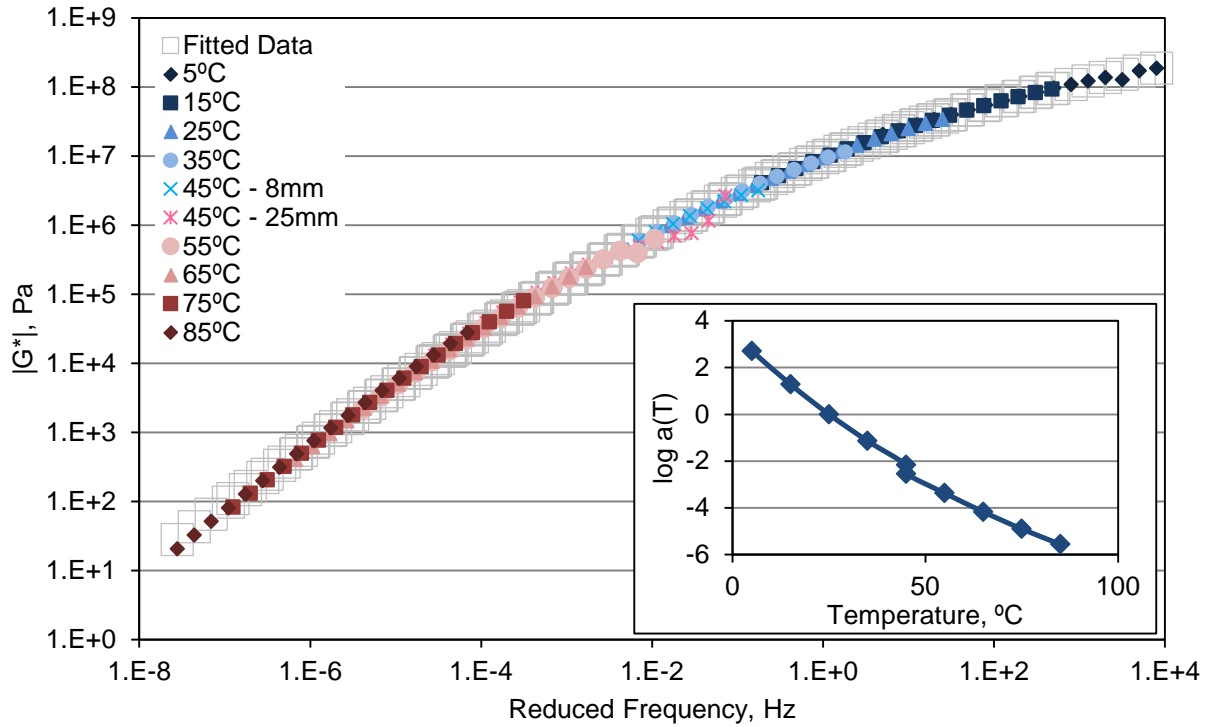


Figure F33. Extracted Binder Mastercurve for Section X, Entire Core

APPENDIX G
SUPPLEMENTARY ANALYSIS

Since the original work on RAP contents was performed in 2007 (Maupin et al., 2008) the specifications for RAP and binder grade contents for dense-graded mixtures have evolved. During the review of this work, it was requested that consideration be given to performing analyses with more recent specifications applied to the evaluated mixtures. These specifications changed the minimum RAP content for binder grade adjustments to dense-graded mixtures from >20% to >25%, as shown in Table G1, excerpted from VDOT specifications (VDOT, 2012).

Applying this specification to the evaluated sites in this study resulted in the deletion of two sites: O and P. These sites do not meet the requirement shown in Table G1 as they do not contain PG 70-22 binder in conjunction with the mixture RAP content of 21%. All remaining sites were considered under their original designation of comparison or RAP sites.

In addition, concerns were raised about the inclusion of three comparison sites paved with WMA. Experience and the data indicated that there were no significant differences between HMA and WMA; however, these three sites (K, H, and M) were also removed from the dataset evaluated in this appendix.

Table G1. Recent Specifications for Binder Grade and Percentage of RAP

Mix Type	Percentage of Reclaimed Asphalt Pavement (RAP) in Mix		
	% RAP ≤ 25%	25.0% < % RAP ≤ 30%	25.0% < % RAP ≤ 35%
SM-4.75A, SM-9.0A, SM-9.5A, SM-12.5A	PG 64-22	PG 64-22	
SM-4.75D, SM-9.0D, SM-9.5D, SM-12.5D	PG 70-22	PG 64-22	
IM-19.0A	PG 64-22	PG 64-22	
IM-19.0D	PG 70-22	PG 64-22	
BM-25.0A	PG 64-22		PG 64-22
BM-25.0D	PG 70-22		PG 64-22

Source: VDOT, 2012.

Visual Survey Data

Visual survey data were compiled and analyzed for the 18 sections addressed in this Appendix. A summary of the data is shown in Table G2.

Table G2. Summary of Visual Distress Surveys

Fatigue Cracking, ft²								
Comparison Site	Low	Medium	High	RAP Site	Low	Medium	High	
E	1240	600	5800	A	3608	1650	249	
I	0	998	0	B	18040	4530	500	
L	0	8	0	C	2017	0	0	
N	0	0	0	D	1736	0	0	
Q	0	988.2	0	F	0	0	0	
T	0	502.2	0	J	112	0	0	
V	0	0	0	R	0	319	0	
W	0	20.9	0	S	0	101.1	0	
				U	0	0	0	
				X	0	0	0	
Tot. Quantity	1240	3117.3	5800	Tot. Quantity	25513	6600.1	749	
No. Sites w/ Distress	1	6	1	No. Sites w/ Distress	5	4	2	
% Sites w/ Distress	13%	75%	13%	% Sites w/ Distress	50%	40%	20%	
Longitudinal Cracking, Wheelpath, ft								
Comparison Site	Low	Medium	High	RAP Site	Low	Medium	High	
E	0	0	0	A	0	0	0	
I	0	3000	0	B	40	0	0	
L	67	72	0	C	22	0	0	
N	0	0	0	D	49	0	0	
Q	0	3.4	0	F	0	0	0	
T	136.3	211.7	0	J	39	232	0	
V	0	0	0	R	0	1208	0	
W	0	450.2	0	S	25.2	8034	0	
				U	6.2	0	0	
				X	0	0	0	
Tot. Quantity	203.3	3737.3	0	Tot. Quantity	181.4	9474	0	
No. Sites w/ Distress	2	5	0	No. Sites w/ Distress	6	3	0	
% Sites w/ Distress	25%	63%	0%	% Sites w/ Distress	60%	30%	0%	
Longitudinal Cracking, Non-wheelpath, ft								
Comparison Site	Low	Medium	High	RAP Site	Low	Medium	High	
E	0	0	44	A	0	1000	1000	
I	0	25	0	B	130	110	250	
L	0	1112	0	C	16	0	0	
N	0	1000	0	D	0	0	0	
Q	0	0	0	F	0	406	0	
T	0	343.3	0	J	184	92	0	
V	0	0	0	R	0	39	0	
W	0	202.3	0	S	115.7	480.8	0	
				U	0	0	0	
				X	0	0	0	
Tot. Quantity	0	2682.6	44	Tot. Quantity	445.7	2127.8	1250	
No. Sites w/ Distress	0	4	1	No. Sites w/ Distress	4	6	2	
% Sites w/ Distress	0%	50%	13%	% Sites w/ Distress	40%	60%	20%	
Transverse Cracking, Unsealed, ft								
Comparison Site	Low	Medium	High	RAP Site	Low	Medium	High	
E	0	33	0	A	0	0	0	
I	0	0	0	B	0	0	0	
L	0	17	0	C	9.5	0	0	
N	168	204	228	D	0	0	0	
Q	0	12	0	F	0	161	0	
T	5	7	0	J	0	0	0	
V	147	36	0	R	0	20	0	
W	0	6	0	S	12	34	0	
				U	31	24	0	
				X	0	0	0	
Tot. Quantity	320	315	228	Tot. Quantity	52.5	239	0	
No. Sites w/ Distress	3	7	1	No. Sites w/ Distress	3	4	0	
% Sites w/ Distress	18%	64%	9%	% Sites w/ Distress	25%	33%	0%	

Raveling, ft²							
Comparison Site	Low	Medium	High	RAP Site	Low	Medium	High
E	0	0	0	A	0	0	0
I	0	0	0	B	720	860	0
L	0	0	0	C	0	0	0
N	0	0	0	D	66	0	0
Q	0	5	0	F	0	0	0
T	0	0	0	J	0	0	0
V	0	0	0	R	0	117	0
W	0	230	0	S	0	0	0
				U	0	0	0
				X	0	0	0
Tot. Quantity	0	235	0	Tot. Quantity	786	977	0
No. Sites w/ Distress	0	2	0	No. Sites w/ Distress	2	2	0
% Sites w/ Distress	0%	18%	0%	% Sites w/ Distress	17%	17%	0%

Statistical analyses were performed to assess the equivalency of the comparison and RAP datasets. Table G3 shows the results of *t*-tests performed to compare the comparison and RAP data for each distress at each severity. A two-sample, two-tailed *t*-test assuming unequal variance at a level of significance of $\alpha = 0.05$ was performed at each severity level for each distress. In addition, the same *t*-test was performed on the results for each distress using data for all severities. The results indicated that there were no significant differences in distresses between the comparison and RAP sites and are consistent with the results determined previously.

Table G3. *p*-Value Results From Two-Sample, Two-Tailed *t*-Tests Performed on Visual Survey Data

Distress	Low Severity	Medium Severity	High Severity	All Severities
Fatigue Cracking	0.2088	0.5887	0.4006	0.3193
Longitudinal Cracking, Wheelpath	0.7097	0.5934	-	0.5980
Longitudinal Cracking, Non-wheelpath	0.0761	0.5382	0.2647	0.8606
Transverse Cracking, Unsealed	0.2207	0.5988	0.3506	0.1003
Raveling	0.3006	0.4646	-	0.2057

p-values less than or equal to 0.05 indicate significant differences between comparison and RAP datasets. - = no test performed as all data points were zero.

Dynamic Modulus

Dynamic modulus values were plotted for the subset of mixtures to investigate if there were apparent differences between the results for mixtures having 20% or less RAP and those having 25% and 30% RAP. Figures G1 through G3 do not show any trends with RAP content for modulus values at frequencies of 0.1 Hz, 1.0 Hz, and 10.0 Hz and all tested temperatures.

An example of two-sample, two-tailed *t*-test results comparing the modulus results for pairs of specimen sets tested at 70°F and 1 Hz (lower left half of table) and 5 Hz (upper right half of table) are presented in Table G4 for the data subset. As previously found for the entire dataset, no trends in significant differences were shown between the subset of sites with mixtures having 20% or less RAP and those with mixtures having 25% to 30% RAP.

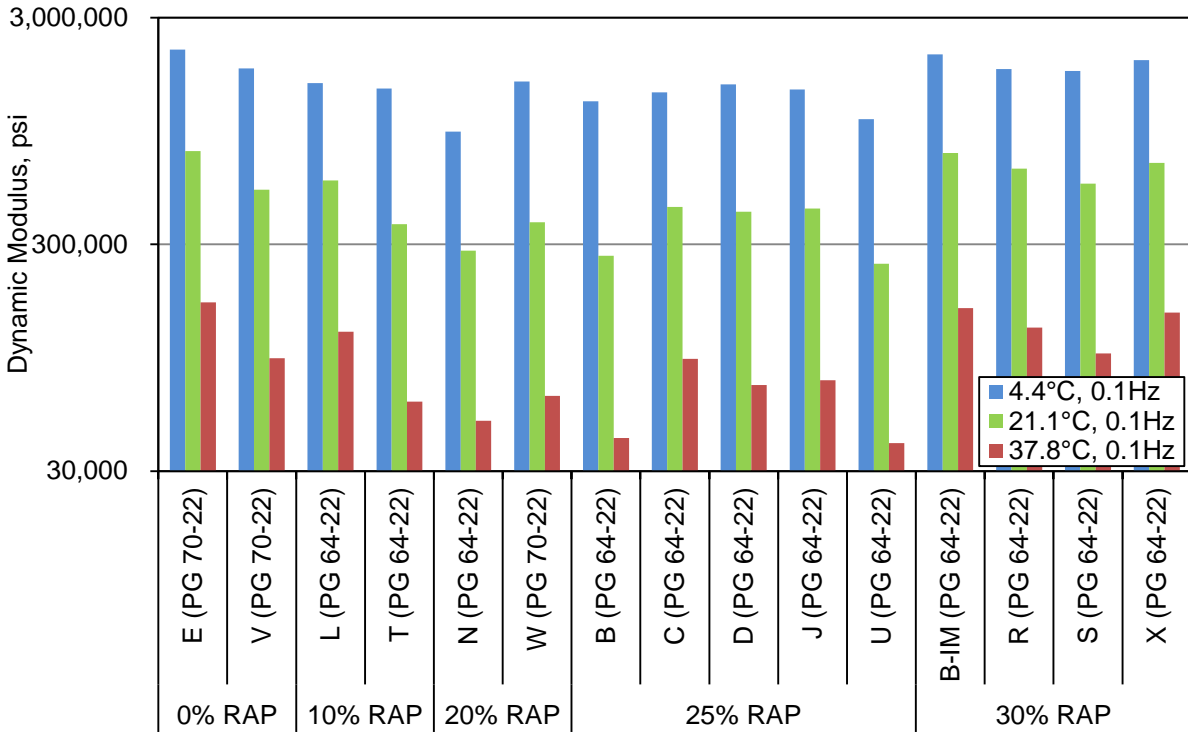


Figure G1. Dynamic Modulus Values at All Test Temperatures and 0.1 Hz Frequency for the Subset of Cores. RAP = reclaimed asphalt pavement.

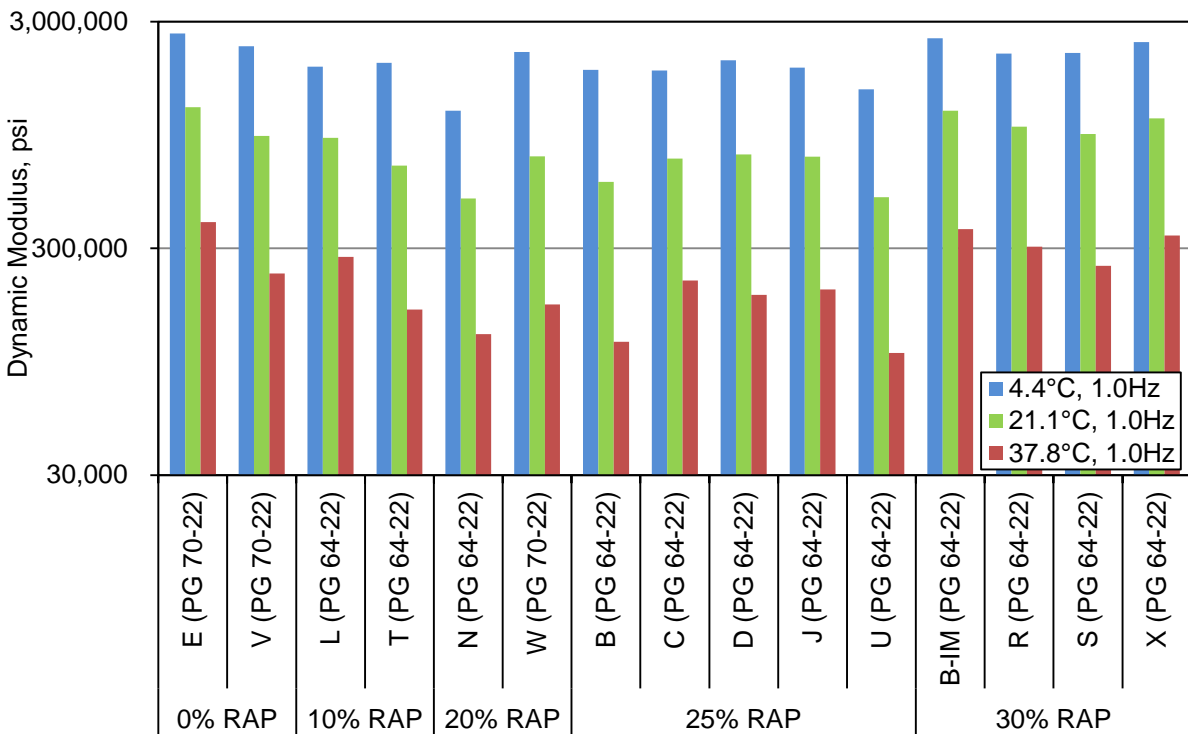


Figure G2. Dynamic Modulus Values at All Test Temperatures and 1.0 Hz Frequency for the Subset of Cores. RAP = reclaimed asphalt pavement.

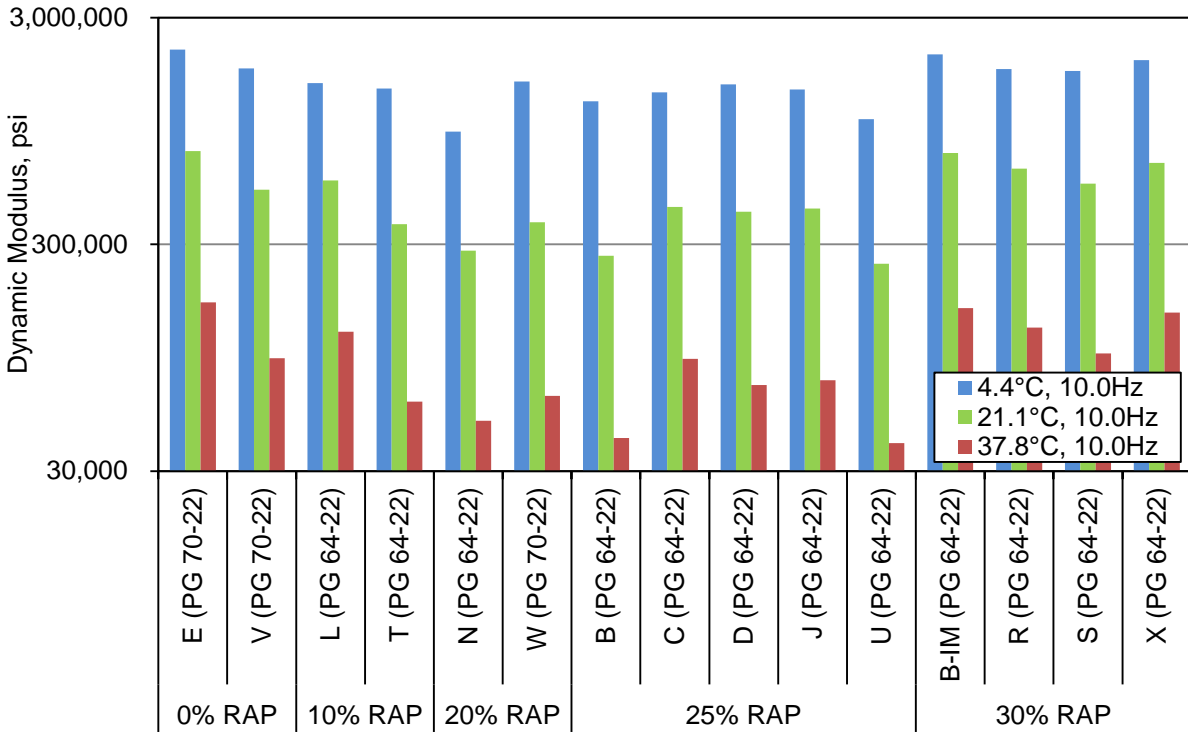


Figure G3. Dynamic Modulus Values at All Test Temperatures and 10.0 Hz Frequency for the Subset of Cores. RAP = reclaimed asphalt pavement.

Table G4. *t*-Test Comparisons of Mixtures at 21.1°C (70°F) and 1 Hz (lower left half of table) and 5 Hz (upper right half of table)

Section (% RAP)	E (0%)	V (0%)	L (10%)	T (10%)	N (20%)	W (20%)	B (25%)	C (25%)	D (25%)	J (25%)	U (25%)	B-IM (30%)	R (30%)	S (30%)	X (30%)
E (0%)		0.0331	0.0259	0.0241	0.0103	0.0081	0.7502	0.0791	0.0087	0.0100	0.0088	0.0035	0.0734	0.0424	0.4695
V (0%)	0.0325		0.8089	0.1668	0.0417	0.1069	0.0976	0.3719	0.1194	0.0210	0.0045	0.0030	0.1336	0.7024	0.3342
L (10%)	0.0179	0.3215		0.1521	0.0883	0.1571	0.0791	0.4140	0.1822	0.0960	0.0187	0.0134	0.2083	0.6248	0.3007
T (10%)	0.0396	0.1854	0.2676		0.6443	0.5803	0.0290	0.7997	0.5082	0.5622	0.2607	0.4061	0.1132	0.1658	0.0846
N (20%)	0.0066	0.0476	0.1729	0.8611		0.8455	0.0310	0.9976	0.7135	0.7909	0.0864	0.0700	0.0172	0.0415	0.1132
W (20%)	0.0123	0.1760	0.6473	0.4006	0.3266		0.0246	0.9361	0.8888	0.9830	0.0634	0.1127	0.0419	0.0909	0.1138
B (25%)	0.5749	0.0459	0.0278	0.0510	0.0080	0.0183		0.0924	0.0271	0.0332	0.0185	0.0138	0.1992	0.1147	0.6320
C (25%)	0.0813	0.2890	0.4745	0.9568	0.9641	0.6154	0.1015		0.8795	0.9410	0.2906	0.4541	0.2332	0.3382	0.1692
D (25%)	0.0079	0.1016	0.4290	0.5335	0.4913	0.7334	0.0113	0.7329		0.8446	0.0542	0.0888	0.0441	0.0993	0.1237
J (25%)	0.0051	0.0109	0.2034	0.7401	0.7678	0.3989	0.0056	0.8897	0.6092		0.0148	0.0340	0.0052	0.0125	0.1219
U (25%)	0.0043	0.0004	0.0272	0.2500	0.0773	0.0382	0.0042	0.3384	0.0413	0.0104		0.1712	0.0030	0.0020	0.0500
B-IM (30%)	0.0027	0.0024	0.0545	0.5503	0.2101	0.0956	0.0028	0.6709	0.1270	0.0936	0.0508		0.0013	0.0029	0.0565
R (30%)	0.0413	0.6614	0.2555	0.1798	0.0519	0.1460	0.0590	0.2657	0.0870	0.0091	0.0001	0.0024		0.1735	0.5962
S (30%)	0.0242	0.6432	0.4370	0.1956	0.0483	0.2318	0.0339	0.3227	0.1305	0.0171	0.0012	0.0033	0.3976		0.3739
X (30%)	0.4275	0.3783	0.2019	0.0817	0.0853	0.1432	0.6191	0.1502	0.1127	0.0949	0.0392	0.0556	0.4280	0.3239	

Shaded bold cells indicate significant differences in modulus values between sites at a level of significance of $\alpha = 0.05$.

Repeated Load Permanent Deformation

RLPD tests were performed on eight mixtures using small-scale specimens. The number of mixtures was limited by the availability of cores of suitable thickness with which to prepare test specimens. Removal of Sites K and M resulted in only six mixtures for consideration, of which two were from comparison sites and four from RAP sites. As the specimens never reached tertiary flow, only average slope and intercept results from the secondary flow portion of the response curve are presented for each mixture. Figure G4 indicates that the slope slightly increases with RAP content for these mixtures. The intercept remains relatively constant. Both trends are similar to those observed with the inclusion of Sites K and M.

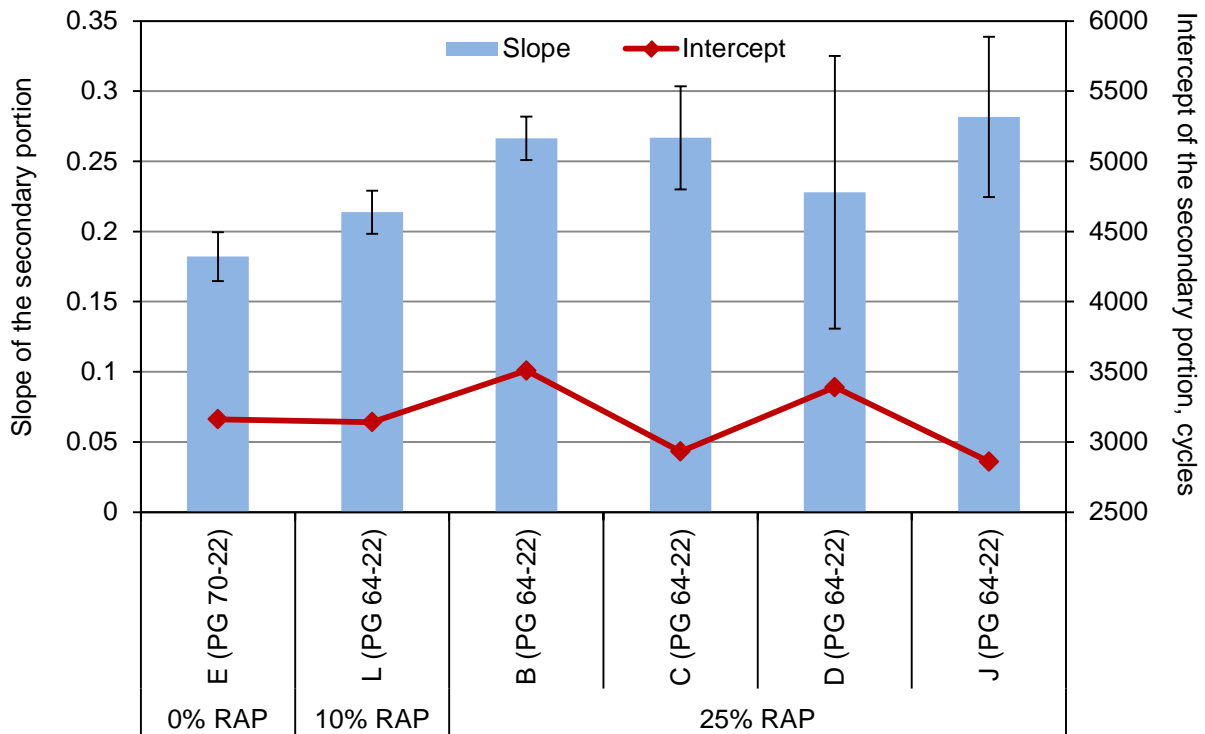


Figure G4. Average Slope and Intercept of Each Mixture, Grouped By RAP Content. Error bars indicate 1 standard deviation. RAP = reclaimed asphalt pavement.

Texas Overlay Test

The Texas overlay test was conducted on 13 mixtures, with at least 4 and as many as 6 replicates tested. Removal of Sites K, M, O, and P from the dataset resulted in 9 sites for further investigation. Figure G5 presents the results of overlay testing for these sites. From Figure G5, it can be seen that Sites E and X, with mixtures containing 0% and 30% RAP, respectively, did not perform as well as the remaining sites, which all averaged more than 1,000 cycles to failure and indicated no significant differences in the results. The COV for Site X was also high, exceeding the 30% target value.

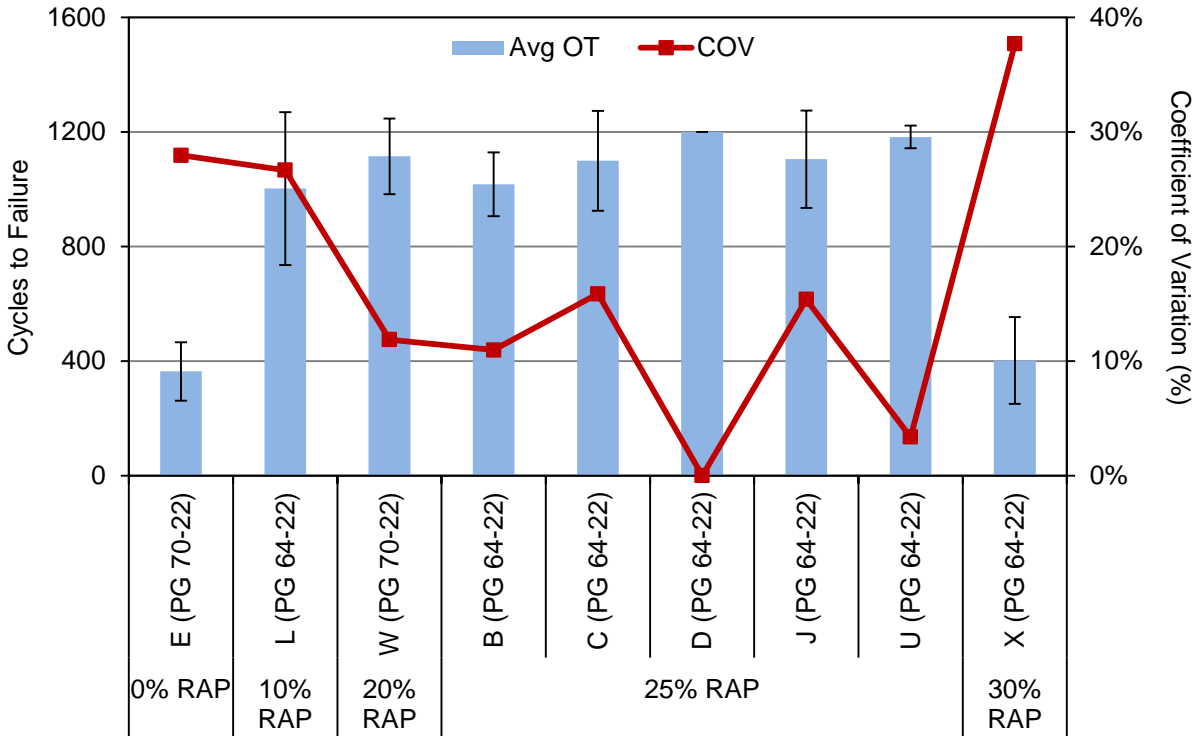


Figure G5. Overlay Test Results After Removal of Outlier Data. Error bars indicate 1 standard deviation. RAP = reclaimed asphalt pavement.

Binder Performance Grading

Analysis of the impact of removing Sites H, K, M, O, and P on binder grading was performed by evaluating the trend in changes in the high and low temperature grade from construction through the in-service period evaluated. Figure G6 shows the trends in high and low failure temperature with increasing RAP content. The trendlines clearly show that the mixtures having less RAP aged over the 6-year period to a greater extent than those having higher RAP contents.

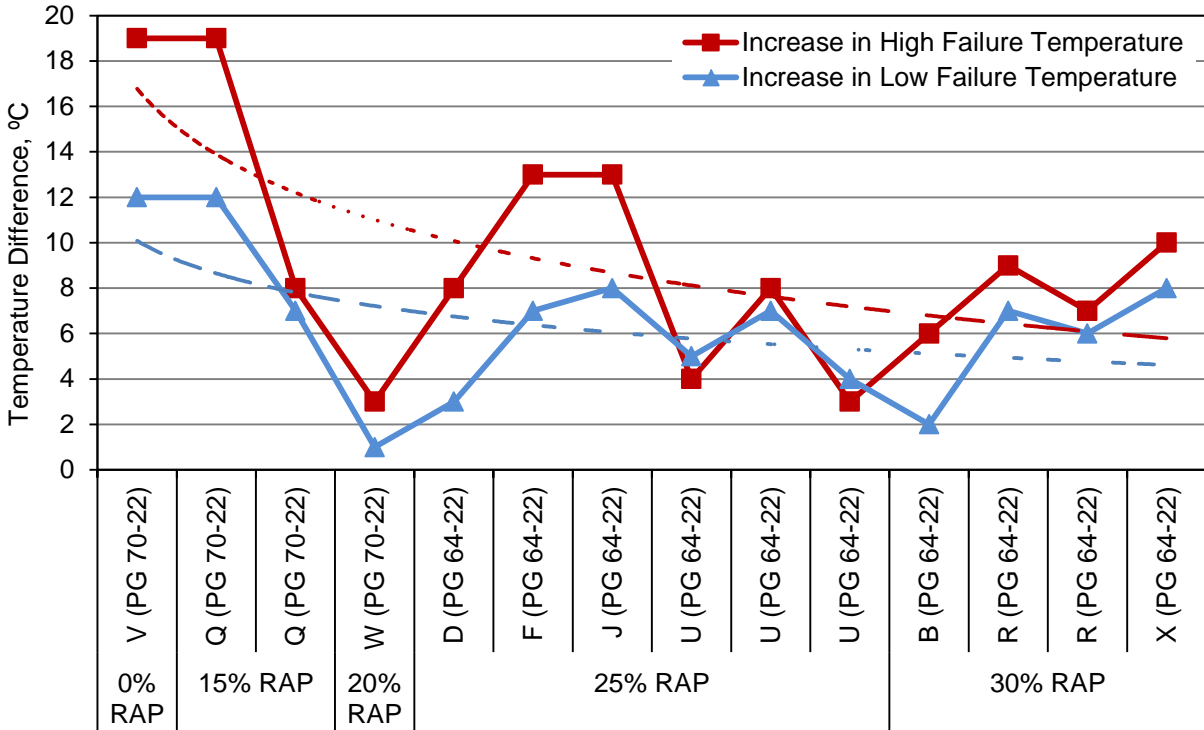


Figure G6. Increase in High and Low Failure Temperatures With RAP Content. RAP = reclaimed asphalt pavement.

Summary

Based on the data analyzed, there does not appear to be any significant impact on the results of this study from the inclusion of either the WMA sites (Sites H, K, and M) or the 21% RAP content sites (Sites O and P).